AD-A068 759 TORONTO UNIV DOWNSVIEW (ONTARIO) INST FOR AEROSPACE --ETC F/G 20/4
NONSTATIONARY OBLIQUE-SHOCK-WAVE REFLECTION IN NITROGEN AND ARG--ETC(U)
NOV 78 G BEN-DOR AFOSR-77-3033

UNCLASSIFIED UTIAS-237 AFOSR-TR-79-0516 NL

| OF
AD
A068759

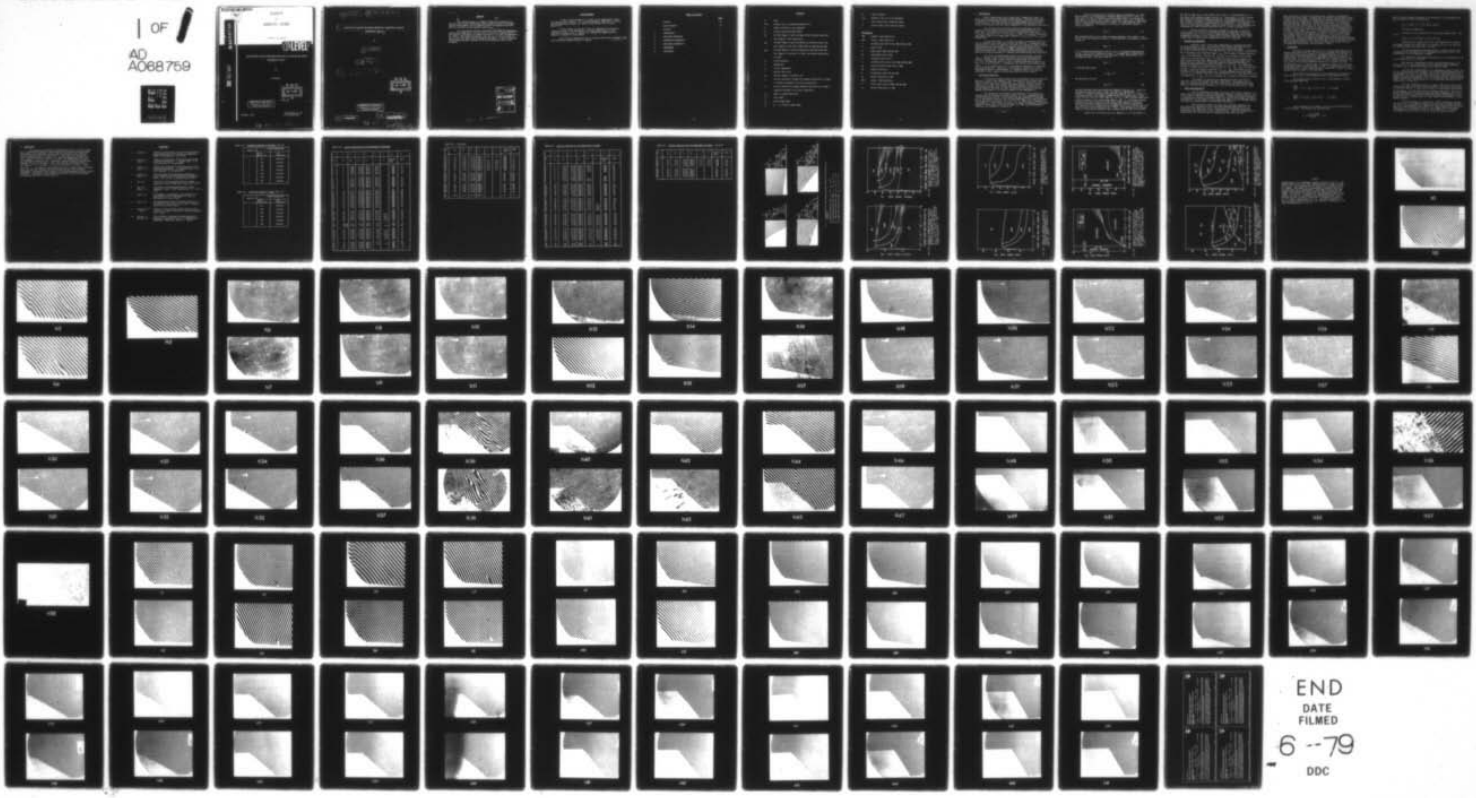

END
DATE FILMED
6 -79
DDC

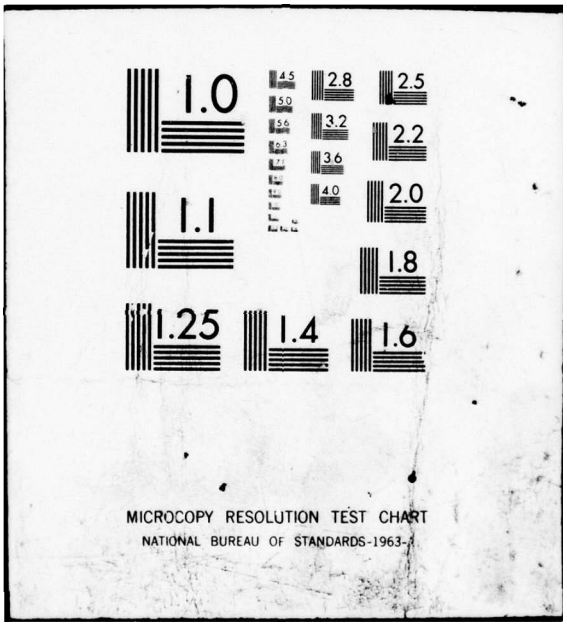
1.0
1.1
1.25
1.4
1.6
1.8
2.0
2.2
2.5
2.8
3.2
3.6
4.0
4.5
5.0
5.6
6.3
MICROCOPY RESOLUTION TEST CHART
NATIONAL BUREAU OF STANDARDS-1963-A

INSTITUTE
FOR
AEROSPACE STUDIES

UNIVERSITY OF TORONTO

(13) LEVEL II

NONSTATIONARY OBLIQUE-SHOCK-WAVE REFLECTIONS IN NITROGEN AND ARGON: EXPERIMENTAL RESULTS

by

G. Ben-Dor

November, 1978

UTIAS Report No. 237
CN ISSN 0082-5255

(18) AFOSR (19) TR-79-0516

(6) NONSTATIONARY OBLIQUE-SHOCK-WAVE REFLECTION IN NITROGEN AND ARGON: EXPERIMENTAL RESULTS,

by

(10) G. Ben-Dor

(12) 81 p.

(15) AFOSR-77-3033

(14) UTIAS [redacted]-237
CN ISSN 0082-5255

(11) November, 1978

Abstract

The interferograms of a detailed study on the reflection of non-stationary oblique shock-waves using a 23 cm dia field of view Mach-Zehnder interferometer and the UTIAS 10 cm x 18 cm Hypervelocity Shock Tube are presented in this separate report.

The investigated incident shock-wave Mach number and compression corner angle ranges were $1 \leq M_s \leq 8$ and $2° \leq \theta_w \leq 60°$, respectively for both argon and nitrogen at an initial pressure $P_o \approx 15$ torr and temperature $T_o \approx 300$ K. The initial conditions, i.e., M_s, θ_w, P_o and T_o as well as the accuracy with which they were measured are given. A brief theoretical review underlying major findings of the above mentioned study is also presented.

Acknowledgement

I wish to thank Professor I.I. Glass for the opportunity to work with him and learn from him. His invaluable guidance, supervision, interest and understanding throughout the course of this project are very much appreciated.

Sincere thanks are due also to Mr. W.L. Buchanan for his help in carrying out some of the experiments, the UTIAS machine shop for their technical assistance, Mrs. L. Quintero for drawing the figures and Ms. B. Waddell for typing this final report.

This work was supported by the U.S.Airforce under Grant AF-AFOSR-77-3033 and the National Research Council of Canada.

Table of Contents

Notation

Ar	argon
E(a)	absolute error in measuring quantity "a"
H	height difference in the manometer
M_s	incident shock wave Mach number
M_o	the Mach number of the flow ahead of the incident shock wave with respect to the triple point
M_{2T}	the Mach number of the flow behind the reflected shock wave with respect to the first triple point of SMR, CMR and DMR
M_{2K}	the Mach number of the flow behind the reflected shock wave with respect to the kink of a CMR or the second triple point of a DMR
P_o	initial pressure
T	temperature
T_o	initial temperature
γ	specific heat ratio
Δa	absolute change in quantity "a"
θ_1	the flow deflection through the incident shock wave in a frame of reference attached to the first triple point
θ_2	the flow deflection through reflected shock wave in a frame of reference attached to the first triple point
θ_m -	angle of maximum deflection
θ_s -	sonic angle
θ_w	actual wedge angle
θ_w'	$\theta_w + \chi$, effective wedge angle

ρ_o	initial density
ρ_{oil}	density of the oil in the manometer
χ	first triple point trajectory angle
χ'	second triple point trajectory angle

Shortenings

CMR	complex - Mach Reflection
DMR	double - Mach Reflection
I	incident shock wave in RR, SMR, CMR and DMR
K	kink in CMR
M	Mach stem in SMR, CMR and DMR
M_1	second Mach stem in DMR
P	reflection point in RR
R	reflected shock wave in RR, SMR, CMR and DMR
R_1	second reflected shock wave in DMR
RR	regular reflection
S	slipstream in SMR, CMR and DMR
S_1	second slipstream in DMR
SMR	single - Mach Reflection
T	first triple point in SMR, CMR and DMR
T_1	second triple point in DMR

1. INTRODUCTION

When a planar shock wave collides with a compression corner in a shock tube, two processes take place simultaneously. The shock wave itself is reflected from the wedge surface and the shock-induced flow is deflected over the corner. The first process is called shock-wave reflection, the second flow deflection and the overall phenomenon is the shock-wave diffraction.

The non-stationary shock-wave-diffraction phenomenon has been intensively investigated recently theoretically and experimentally in the UTIAS 10cm x 18cm Hypervelocity Shock Tube in nitrogen and argon (Refs. 1 & 2) at initial conditions of $P_o \approx 15$ torr and $T_o \approx 300$K. The incident shock wave Mach number range and the wedge angle range were $2 \leq M_s \leq 8$ and $2^o \leq \theta_w \leq 60^o$, respectively.

It was shown (Refs. 1 & 2) that four types of shock-wave reflection and two different flow-deflection processes are possible. Consequently, the superposition of these two phenomena can result in a maximum of eight different shock-wave-diffraction processes. The eight possible diffractions are: regular reflection (RR), single-Mach (SMR), complex-Mach (CMR) and double-Mach (DMR) reflections. The shock-induced-flow negotiates the corner with the aid of either an attached or a detached shock wave during such reflections.

Out of all the experimental studies of this problem, only Smith (Ref. 7) and White (Ref. 8) have published in detail their experimental results. However, their incident shock wave Mach number was limited to $M_s < 2.75$, consequently there is a lack of reported experimental results for $M_s > 2.75$ in the literature. Consequently, the results of the present study (Refs. 1, 2 & 3) should prove to be of considerable assistance to researchers and fluid dynamicists. Therefore, it was decided to publish all of the experimental results (interferograms) in a separate report as an accurate data base of these complex shock-wave-diffraction for their benefit.

2. SHOCK-WAVE REFLECTION

It was quite accepted among various investigators that the reflection process in a shock tube, depends on the combination of the incident shock wave Mach number M_s, and the wedge angle θ_w. However, Ben-Dor and Glass (Refs. 1,2 & 3) have shown recently the significance of real-gas effects on shifting the boundary lines between domains of different reflections by several degrees, and hence, one must conclude that the reflection process depends additionally on the initial pressure P_o and temperature T_o.

The reasons for the formation and termination of the various reflections are all discussed in detail in Refs. 1, 2 & 3, consequently only a brief discussion follows. The criterion for the termination of RR makes use of the boundary condition that the flow downstream of the reflection point must be parallel to the wall, i.e., $\theta_1 + \theta_2 = 0$. When this is violated (i.e., θ_w decreases to a point where it forces θ_1 to exceed in magnitude the maximum deflection value (θ_{2m}) of the flow in state (1), Fig. 1(a), RR terminates. Therefore, the termination criterion is:

$$\theta_1 + \theta_{2m} = 0 \qquad 2\text{-}1$$

When RR terminates three different types of reflection, i.e., SMR, CMR and DMR can occur depending on the Mach number of the flow in state (2), (Fig. 1(b), (c) and (d)) behind the reflected shock wave R. As long as the flow behind R is subsonic with respect to the first triple point T, SMR occurs. When this flow becomes supersonic with respect to T, SMR terminates and a CMR forms. Consequently, the termination criterion of SMR and the formation criterion of CMR is,

$$M_{2T} = 1 \qquad 2\text{-}2$$

CMR terminates when the flow behind R becomes supersonic with respect to the kink K, thus the termination criterion of CMR and hence, the formation criterion of DMR is,

$$M_{2K} = 1 \qquad 2\text{-}3$$

It is worthwhile mentioning that the line $M_{2K} = 1$ corresponds approximately to $M_{2T} = 1.30$ in both nitrogen and argon. Alternatively, one may use the following empirical criteria for the existance of SMR, CMR and DMR in both nitrogen and argon. SMR occurs only if:

$$M_{2T} < 1 \qquad 2\text{-}4$$

A CMR takes place when:

$$1 < M_{2T} < 1.3 \qquad 2\text{-}5$$

and DMR results for all

$$M_{2T} > 1.3 \qquad 2\text{-}6$$

The non-stationary shock wave reflection domains in the (M_s, θ_w') - plane for nitrogen and argon are shown in Figs. 2(a) and (b), respectively. In addition to the above mentioned four reflection domains, there is a domain of no reflection (NR). This domain disappears when the vertical axis is transformed from the effective wedge angle θ_w' ($\theta_w' = \theta_w + \chi$ and χ is the triple point trajectory angle) to the actual wedge angle θ_w (Ref. 1). The dashed boundary lines are for a perfect gas, while the solid lines account for real-gas effects (dissociation equilibrium for nitrogen and ionization equilibrium for argon) with four different initial pressures (P_o = 1, 10, 100 and 1000 torr) and a constant initial temperature (T_o = 300K). The significance of real-gas effects in shifting the boundary lines is clearly seen in Figs. 2(a) and (b).

Recall that the vertical axis, θ_w' equals $\theta_w + \chi$ in the domains of

SMR, CMR and DMR, and θ_w in the domain of RR, where $\chi = 0$ by definition (χ is the triple point trajectory angle, see Fig. 1). Consequently, in order to obtain the domains of different reflection processes in a more physical plane, i.e., (M_s, θ_w)-plane, χ should be subtracted from the corresponding curves Law and Glass (Ref. 5 and 6) developed a graphical method for predicting χ. An analytical version of their graphical method, which was found to be in a better agreement with experiments was later developed by Ben-Dor (Ref. 1) to get a prediction of χ.

The non-stationary shock-wave reflection in the (M_s, θ_w)-plane is shown in Figs. 3(a) and (b) for nitrogen and argon, respectively. Only lines corresponding to P_o = 15 torr and T_o = 300K are drawn. Note that the NR domain disappeared, and hence one can conclude that an incident shock wave will always reflect when it collides with a compression corner in a shock-tube.

3. INDUCED-FLOW DEFLECTION

Consider a planar shock wave propagating in a shock-tube and denote the state behind it as (2'). For any given set of initial conditions (P_o, T_o) and incident shock-wave Mach number, M_s, the induced flow Mach number $M_{2'}$, as well as its pressure $P_{2'}$, and temperature $T_{2'}$, can be calculated. Consequently, the corresponding sonic deflection angle, $\theta_{s2'}$, and the angle of maximum deflection, $\theta_{m2'}$, can be determined. Thus the (M_s, θ_w)-plane is now divided into two main regions, one corresponding to $M_{2'} < 1$, where the induced flow is subsonic and hence, turns over the corner subsonically, and the other corresponding to $M_{2'} > 1$, where the flow is supersonic. The latter region is subdivided into three regions of different flow deflection processes: $0 < \theta_w < \theta_{s2'}$, for deflection through a straight and attached oblique shock wave, $\theta_{s2'} < \theta_w < \theta_{m2'}$, for deflection through a curved and attached shock wave, and $\theta_w > \theta_{m2'}$, where the deflection is through a curved and detached shock wave. Since the maximum separation between $\theta_{m2'}$ and $\theta_{s2'}$ is usually very small, only two regions, $0 < \theta_w < \theta_{m2'}$, where the shock is attached and $\theta_w > \theta_{m2'}$, where it is detached are considered for practical purposes.

The domains of different flow deflection processes are shown in Figs. 4(a) and (b) for nitrogen and argon, respectively. The dashed lines are again for a perfect gas whereas, the solid lines are for the imperfect gas model with four different initial pressures, P_o = 1,10,100 and 1000 torr and T_o = 300K.

4. SHOCK-WAVE DIFFRACTION

The two independent phenomena discussed in the previous chapters, i.e., shock reflection (Chapter 2) and flow deflection (Chapter 3) interact and give rise to the overall shock-wave diffraction phenomenon. To show this process the figures corresponding to shock wave reflection [Figs. 3(a) and (b) for nitrogen and argon, respectively] and the figures for flow deflection [Figs. 4(a) for nitrogen and 4(b) for argon] were superimposed to results Figs. 5(a) and (b).

The interaction between the shock-wave reflection phenomenon and the induced-flow deflection process causes the reflected shock wave R to curl back towards the compression corner. Consequently, the reflected shock-wave terminates at the wedge corner or the shock tube wall. Since the configuration is growing with time, the point where R terminates at the shock tube-wall

moves towards the on-coming shock-induced flow, therefore increasing the on-coming flow Mach number. Consequently, the subsonic turning regions shown in Figs. 4(a) and (b) cannot be established in non-stationary flows. At the limiting case of a degenerated incident shock wave ($M_s = 1$) the reflected shock wave becomes a Mach wave. Therefore, as there are four reflection processes (RR, SMR, CMR and DMR) and two deflection processes (an attached or detached shock wave) a maximum of eight different shock-diffractions are possible. However, only seven diffractions are possible in nitrogen and six in argon (in the range $1 \leq M_s \leq 10$). The domains of different diffractions for both nitrogen and argon are given in Fig. 5(a) and (b), respectively. The boundary lines are for imperfect gas with $P_o = 15$ torr and $T_o = 300K$. The different types of diffraction are summarized in Talbes 1(a) and (b), respectively. A detailed comparison between the various diffraction processes was done and discussed by Ben-Dor and Glass (Refs. 2,3 & 4) and Ben-Dor (Ref.1), where the density field of each diffraction process was deduced from the corresponding interferograms, and discussed in detail.

5. EXPERIMENTS

The above mentioned analyses for the non-stationary reflection of oblique shock waves in the (M_s, θ_w') and (M_s, θ_w)-planes, the prediction of χ and the non-stationary diffraction of oblique shock waves in the (M_s, θ_w)-plane have all been substantiated by experimental results from various sources (Refs. 5 to 9) as well as 58 experiments in nitrogen and 48 in argon that have been performed by Ben-Dor (Ref. 1). The initial conditions θ_w, M_s, P_o and T_o of all these experiments are given in columns 2,3,4 and 5 of Tables 2(a) and (b), respectively. The measured values of the first and second triple points trajectory angles (χ and χ', respectively) are given in columns 6 and 7, and the observed type of reflection is listed in column 8. Column 9 gives the number of the experiment.

The accuracy in measuring the various parameters is discussed in detail in Refs. 1 and 10 and consequently only a brief summary follows.

The maximum possible relative error in calculating the incident shock wave Mach number was:

$$\frac{E(M_s)}{M_s} = (1.15 \times M_s + 10.18) \times 10^{-3} \quad \text{for nitrogen}$$

$$\frac{E(M_s)}{M_s} = (1.05 \, M_s + 10.18) \times 10^{-3} \quad \text{for argon}$$

Inital pressures in the range $5 \leq P_o \leq 40$ torr were measured with an oil manometer. The pressure was calcuated from:

$$P_o = \frac{\rho_{oil} \times H \text{ (mm)}}{13.5951} \quad \text{torr}$$

where H is the oil-hight difference in mm (as measured in the manometer) and ρ_{oil} the density of the oil is given by:

$$\rho_{oil} = [1.069 + 9.5 \times 10^{-4} (25-T)] \text{ g/cm}^3$$

T is the oil temperature.

The absolute error associated with the initial pressure (Ref. 1 and 10) is:

$$E(P_o) = 1.4 \times 10^{-5} H(\text{mm}) + 7.86 \times 10^{-2} \text{ torr}$$

Pressures in the range $P_o \gtrsim 40$ torr, were measured with a Wallace and Tiernan, type FA 160 (0-200 torr) to an accuracy of $\pm$ 0.2 torr and hence the maximum possible error was $E(P_o) = 0.4$ torr.

The initial temperature was measured with a standard mercury bulb thermometer to an accuracy of $\pm 0.1^\circ$, consequently, an error of $E(T) = 0.2^\circ$ is associated with all temperature readings.

The compression wedge models were machined in the UTIAS machine shop to an accuracy of $\pm$ 1' or $\pm 0.0167^\circ$.

The value of χ was measured from the interferograms within $\pm 0.5^\circ$. In the case of χ_t the accuracy was $\pm 0.5^\circ$ for DMR and $\pm 1^\circ$ for CMR where the kink is not so clear as the second triple point of a DMR.

All but three interferograms of the experiments listed in Tables 2(a) and (b) are presented in the following. The excluded interferograms are those of experiments 7, 9 and 10 in nitrogen (Table 2(a)), lines No.41, 38 and 39, respectively which were recorded after the incident shock wave passed the test section and hence the diffraction is out of the field of view. The interested reader can see these interferograms and the corresponding discussion in Ref. 1 [(Figs. 66(b), (c) and (d)].

Note that experiments 76 and 77 in argon (Table 2(b), lines 5 and 6, respectively) does not show any reflection owing to the low initial pressure P_o, and hence density ρ_o, that did not result in a sufficiently large change in the density, $\Delta\rho$, that would produce a visible fringe shift. Note that in similar experiments with almost the same Mach number (experiment 78, line 4) and also with stronger and weaker incident shock waves [experiments 75 (line 3) and 81 (line 8), respectively] but a much higher initial pressure, a clear SMR was obtained.

Each interferogram is labelled with a letter followed by a number. The letter N or A, corresponds to nitrogen or argon and the number indicates the line in the appropriate table [Table 2(a) for nitrogen and 2(b) for argon], where the initial conditions are listed. For example, interferogram No.9 corresponds to the experiment listed in line 9, Table 2(a), i.e., a SMR in nitrogen with $M_s = 7.77$, $\theta_w = 2^\circ$, $P_o = 9.80$ torr and $T_o = 297.6$K.

6. CONCLUSIONS

The foregoing interferometric experimental results, fill up a large gap of experimental information concerning non-stationary oblique-shock-wave diffractions over compression corners, that have existed in the literature since the pioneering work of Smith (Ref. 7). More than three decades ago, Smith (1945) published the results of his detailed experimental study in air in the ranges $1 \leq M_s \leq 2.75$ and $5^\circ \leq \theta_w \leq 85^\circ$. The present report extends the experimental information to a much wider range of incident shock-wave Mach numbers $2 \leq M_s \leq 8$ in nitrogen. In the case of argon the present data in the range of $2^\circ \leq \theta_w \leq 60^\circ$, $2 \leq M_s \leq 8$ is the first of its kind. Unlike Smith (Ref. 7) who measured various quantities such as angles between different shock wave and then reported them while presenting only a few Schlieren photographs, the present report contains all the interferograms and their initial conditions. Consequently, investigators can benefit from the interferograms by measuring quantities of their interest.

REFERENCES

1. Ben-Dor, G. "Regions and Transitions of Non-stationary Oblique Shock-Wave Reflections in Perfect and Imperfect Gases", UTIAS Report No. 232 (1978).

2. Ben-Dor, G.
   Glass, I. I. "Domains and Boundaries of Non-stationary Oblique Shock-Wave Reflections: I. Diatomic Gas", J. of Fluid Mechanics (to be published).

3. Ben-Dor, G.
   Glass, I. I. "Domains and Boundaries of Non-stationary Oblique Shock-Wave Reflections: II. Monatomic Gas", J. of Fluid Mechanics (to be published).

4. Ben-Dor, G.
   Glass, I. I. "Non-stationary Oblique Shock-Wave Reflection - Actual Isopyonics and Some Numerical Experiments", AIAA J., Vol. 16, No. 11, pp.1146-1158, (1978).

5. Law, C.K. "Diffraction of Strong Shock Waves by a Sharp Compressive Corner", UTIAS Tech. Note No.150 (1970).

6. Law, C.K.
   Glass, I. I. "Diffraction of Strong Shock Waves by a Sharp Compressive Corner", CASI Transactions, Vol. 4, No. 1, (1971).

7. Smith, L.G. "Photographic Investigation of the Reflection of Plane Shocks in Air", OSRD Report No. 6271, or NDRC Report No. A-350, (1945).

8. White, D.R. "An Experimental Survey of the Mach Reflection of Shock Waves", Tech. Report II-10, Dept. of Physics, Princeton University, (1951).

9. Bazhenova, T.V. et al. "Regions of Various Forms of Mach Reflection and Transition to Regular Reflection", Acta Astronautica, Vol.3, (1976).

10. Ben-Dor, G.
    Whitten, B.T. "Interferometric Techniques and Data Evaluation Methods for the UTIAS 10 cm x 18 cm Hypervelocity Shock Tube", UTIAS Tech. Note No. (1979).

TABLE 1(a): Diffraction Regions in Nitrogen (Fig. 5a)

REGION NO.	SHOCK DIFFRACTION	
	Shock Reflection	Flow Deflection
1	RR	Detached
2	SMR	Detached
3	SMR	Attached
4	CMR	Detached
5	CMR	Attached
6	DMR	Detached
7	DMR	Attached

TABLE 1(b): Diffraction Regions in Argon (Fig. 5b)

REGION NO.	SHOCK DIFFRACTION	
	Shock Reflection	Flow Deflection
1	RR	Detached
2	SMR	Detached
3	SMR	Attached
4	CMR	Detached
5	CMR	Attached
6	DMR	Detached

TABLE 2(a): Initial Conditions for the Experiments in Nitrogen

1	2	3	4	5	6	7	8	9
No.	θ_w	M_s	P_o	T_o	χ	χ'	Reflec-tion	Exp.
1	2	1.95	52.50	297.2	26.0		SMR	70
2	2	1.89	53.50	297.3	26.5		SMR	71
3	2	1.85	52.50	297.4	26.5		SMR	72
4	2	3.84	15.19	297.4	23.5		SMR	73
5	2	4.15	15.17	297.3	23.0		SMR	74
6	5	3.75	15.25	295.9	20.5		SMR	37
7	5	4.71	15.81	295.2	20.0		SMR	31
8	5	5.85	15.18	297.0	19.5		SMR	33
9	5	6.01	15.19	295.8	18.5		SMR	34
10	5	6.86	10.00	295.6	18.0		SMR	35
11	5	7.51	5.17	296.0	17.5		SMR	36
12	10	2.01	50.00	295.8	19.0		SMR	39
13	10	2.37	35.44	297.7	18.5		SMR	88
14	10	2.61	37.00	297.8	18.0		SMR	90
15	10	2.82	30.34	297.6	18.0		SMR	89
16	10	3.62	15.23	295.4	16.5		SMR	40
17	10	4.59	15.16	298.5	16.2		SMR	20
18	10	4.72	15.00	295.0	16.0		SMR	41
19	10	5.92	15.27	295.0	15.5		SMR	42
20	10	6.79	10.21	295.2	15.0		SMR	43
21	10	7.58	5.13	294.8	14.5		SMR	44
22	20	1.93	51.00	297.2	12.5		SMR	50
23	20	3.74	15.31	297.4	12.0		CMR	49
24	20	4.81	15.29	296.6	11.5	15.5	CMR	48
25	20	6.27	15.33	296.0	11.2	14.5	CMR	47
26	20	6.87	10.12	295.8	11.0	14.0	CMR	46
27	20	7.71	5.06	296.0	10.0	11.5	CMR	45
28	26.56	2.01	50.00	296.6	9.2		SMR	26
29	26.56	8.06	5.10	298.2	9.0	9.9	DMR	102
30	30	1.97	51.00	297.4	8.5		SMR	51
31	30	3.68	15.27	297.3	8.0	10.0	CMR	52
32	30	4.68	15.28	297.4	7.8	9.5	DMR	53
33	30	5.93	15.22	297.4	7.7	10.0	DMR	54
34	30	6.96	10.11	297.4	7.6	9.8	DMR	55
35	30	7.97	4.99	297.4	7.4	9.0	DMR	56
36	40	2.02	50.00	297.3	4.0		CMR	63
37	40	3.69	15.34	297.4	4.8	7.0	DMR	62
38	40	4.59	15.64	298.2			DMR	9
39	40	4.60	15.15	298.4			DMR	10

TABLE 2(a) - continued:

No.	θ_w	M_s	P_o	T_o	χ	χ'	Reflection	Exp.
40	40	4.64	15.29	297.2	5.0	6.2	DMR	6
41	40	4.72	15.31	296.4			DMR	7
42	40	4.75	15.30	297.4	5.2	6.2	DMR	61
43	40	4.98	5.13	296.9	5.2	6.8	DMR	5
44	40	6.17	15.34	297.4	4.2	6.0	DMR	60
45	40	6.97	10.28	297.3	3.8	5.5	DMR	59
46	40	7.78	5.00	297.3	3.5	4.0	DMR	57
47	40	7.95	5.01	298.5	3.8	4.0	DMR	58
48	50	2.07	50.00	299.6			RR	127
49	50	3.69	15.27	298.9			RR	126
50	50	4.78	15.24	298.4			RR	125
51	50	6.22	15.29	299.6			RR	124
52	50	7.29	10.22	299.1			RR	123
53	60	1.96	65.00	299.0			RR	130
54	60	2.03	59.00	299.2			RR	128
55	60	3.84	17.18	299.0			RR	129
56	60	4.68	15.31	298.1			RR	18
57	60	4.76	15.26	298.4			RR	131
58	63.43	2.01	50.00	296.8			RR	25

TABLE 2(b): Initial Conditions for the Experiments in Argon

1	2	3	4	5	6	7	8	9
No.	θ_w	M_s	P_o	T_o	χ	χ'	Reflec-tion	Exp.
1	2	2.03	50.00	297.4	28.5		SMR	84
2	2	3.02	20.29	297.8	28.0		SMR	83
3	2	4.39	15.00	297.4	27.5		SMR	75
4	2	5.19	15.30	297.2	27.0		SMR	78
5	2	5.33	5.04	297.3				76
6	2	5.42	5.08	297.3				77
7	2	6.13	15.33	296.0			SMR	80
8	2	6.47	15.32	295.4	26.0		SMR	81
9	2	7.77	9.80	297.6	25.0		SMR	82
10	10	2.01	50.00	298.6	21.0		SMR	85
11	10	2.96	20.28	299.0	20.0		SMR	86
12	10	4.39	15.32	297.0	19.5		SMR	87
13	10	5.22	15.22	298.4	19.2		SMR	91
14	10	6.06	15.24	299.0	18.5		SMR	92
15	10	6.47	15.27	299.0	18.5		SMR	93
16	10	7.88	9.96	298.6	17.5		SMR	94
17	20	2.00	50.00	298.4	15.0		SMR	101
18	20	2.82	20.32	299.0	14.5		SMR	100
19	20	4.40	15.26	299.0	14.0		CMR	99
20	20	5.20	15.22	299.0	14.0	17.0	CMR	98
21	20	6.04	15.27	297.2	13.7	17.5	CMR	97
22	20	6.84	15.22	298.4	14.0	18.0	CMR	96
23	20	7.76	9.84	299.0	14.0	17.5	CMR	95
24	30	2.03	50.00	299.6	9.5		SMR	103
25	30	2.89	20.24	299.2	9.5	12.0	CMR	104
26	30	4.51	15.25	299.0	10.0	13.0	CMR	105
27	30	5.29	15.21	299.4	10.0	12.5	CMR	106
28	30	6.36	15.27	299.4	10.2	13.0	CMR	107
29	30	6.96	15.00	295.4	10.0	13.0	CMR	109
30	30	8.01	9.80	299.5	10.0	13.0	CMR	108
31	40	2.05	50.00	297.8	6.0	11.0	CMR	116
32	40	3.11	20.34	299.8	5.5	10.0	CMR	115
33	40	4.44	15.00	299.1	5.5	10.0	DMR	114
34	40	5.28	15.29	297.9	5.5	10.0	DMR	113
35	40	6.12	15.32	297.6	5.7	10.0	DMR	112
36	40	6.81	15.23	298.8	5.7	9.5	DMR	111
37	40	7.53	9.87	297.0	5.5	9.5	DMR	110
38	50	2.04	50.00	298.2	1.0		CMR	117
39	50	2.96	20.50	298.4	1.5	4.0	DMR	118

TABLE 2(b): Initial Conditions for the Experiments in Argon - continued

No.	θ_w	M_s	P_o	T_o	χ	χ'	Reflection	Exp.
40	50	4.40	15.30	299.2	2.0	4.0	DMR	119
41	50	5.27	15.32	298.2	1.5	4.0	DMR	120
42	50	6.27	15.34	299.4	1.4	4.0	DMR	121
43	50	7.03	15.29	299.4	1.3	3.5	DMR	122
44	60	2.03	50.00	301.0			RR	132
45	60	2.03	50.00	299.2			RR	134
46	60	3.03	20.00	299.5			RR	133
47	60	4.50	16.16	299.8			RR	135
48	60	5.24	15.30	299.2			RR	136

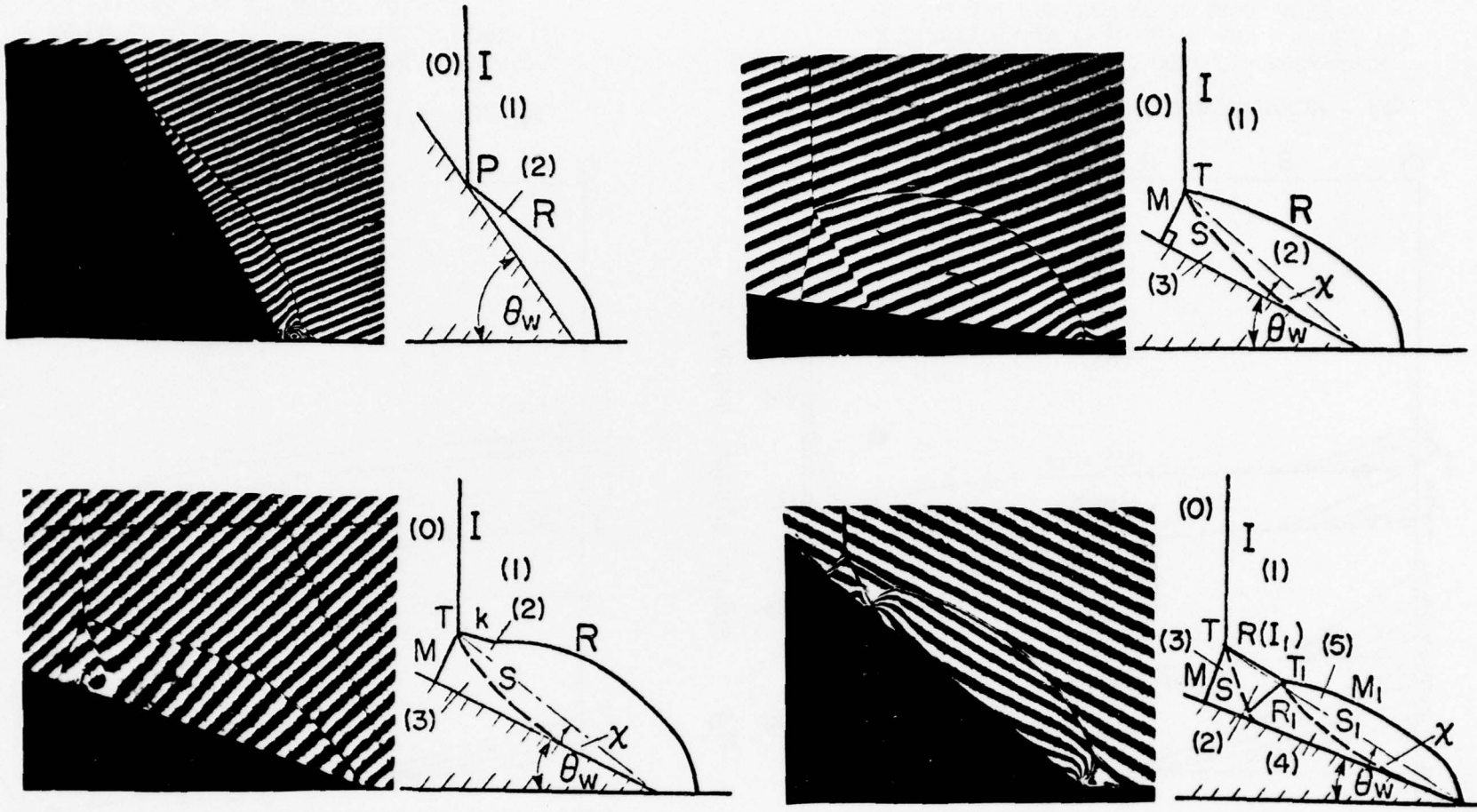

FIG. 1 ILLUSTRATION OF FOUR POSSIBLE OBLIQUE SHOCK-WAVE REFLECTIONS IN NITROGEN

(a) REGULAR REFLECTION (RR), $\Theta_w = 60°$, $M_s = 4.68$.

(b) SINGLE-MACH REFLECTION (SMR), $\Theta_w = 10°$, $M_s = 2.61$.

(c) COMPLEX-MACH REFLECTION (CMR), $\Theta_w = 20°$, $M_s = 6.90$.

(d) DOUBLE-MACH REFLECTION (DMR), $\Theta_w = 40°$, $M_s = 3.76$.

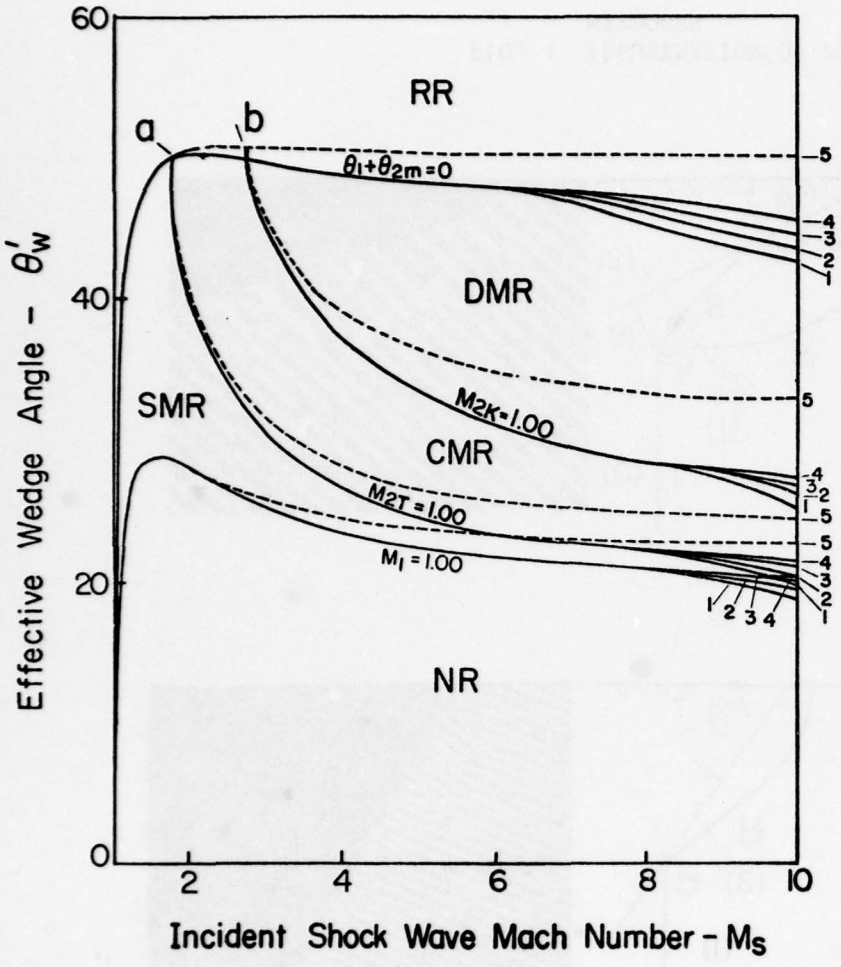

FIG. 2(a) REGIONS OF DIFFERENT OBLIQUE-SHOCK-WAVE REFLECTION IN (M_s, θ_w')-PLANE. LINES (1) TO (4) ARE FOR IMPERFECT NITROGEN WITH P_o = 1, 10, 100 and 1000 TORR, RESPECTIVELY AND T_o = 300 K. LINE (5), DASHED, IS FOR A PERFECT DIATOMIC GAS γ = 7/5.

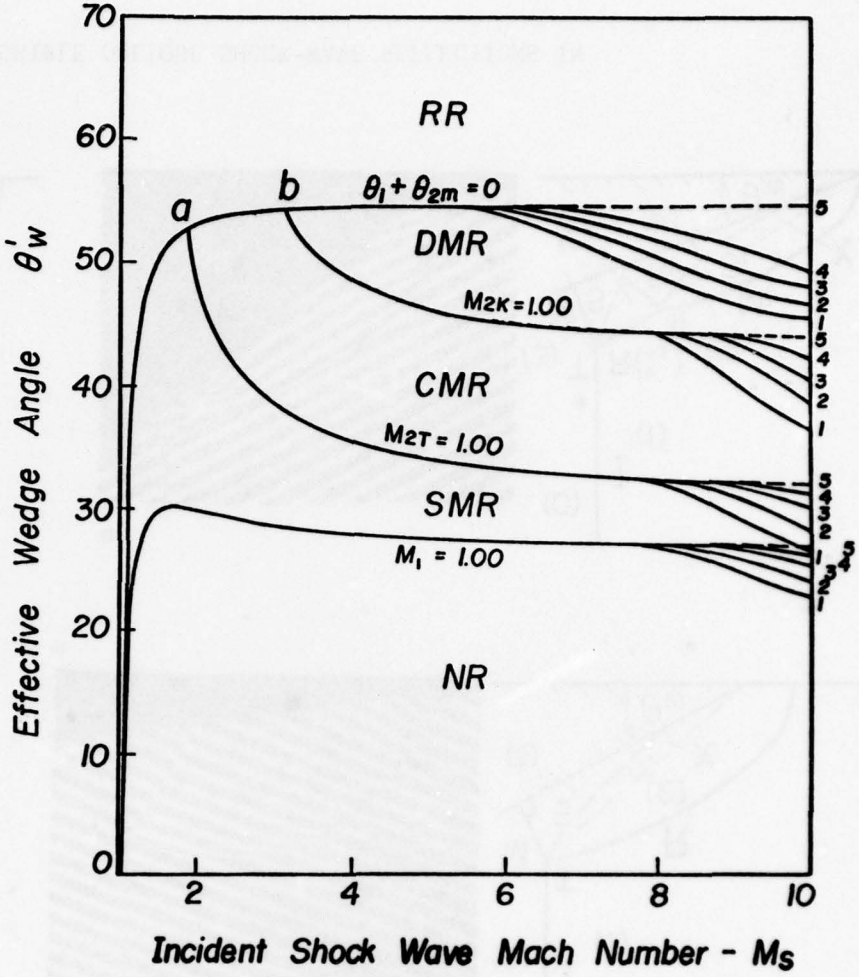

FIG. 2(b) REGIONS OF DIFFERENT OBLIQUE-SHOCK-WAVE REFLECTIONS IN (M_s, θ_w')-PLANE. LINES (1) TO (4) ARE FOR IMPERFECT ARGON WITH P_o = 1, 10, 100 and 1000 TORR, RESPECTIVELY, AND T_o = 300 K. LINE (5), DASHED, IS FOR A PERFECT MONATOMIC GAS γ = 5/3.

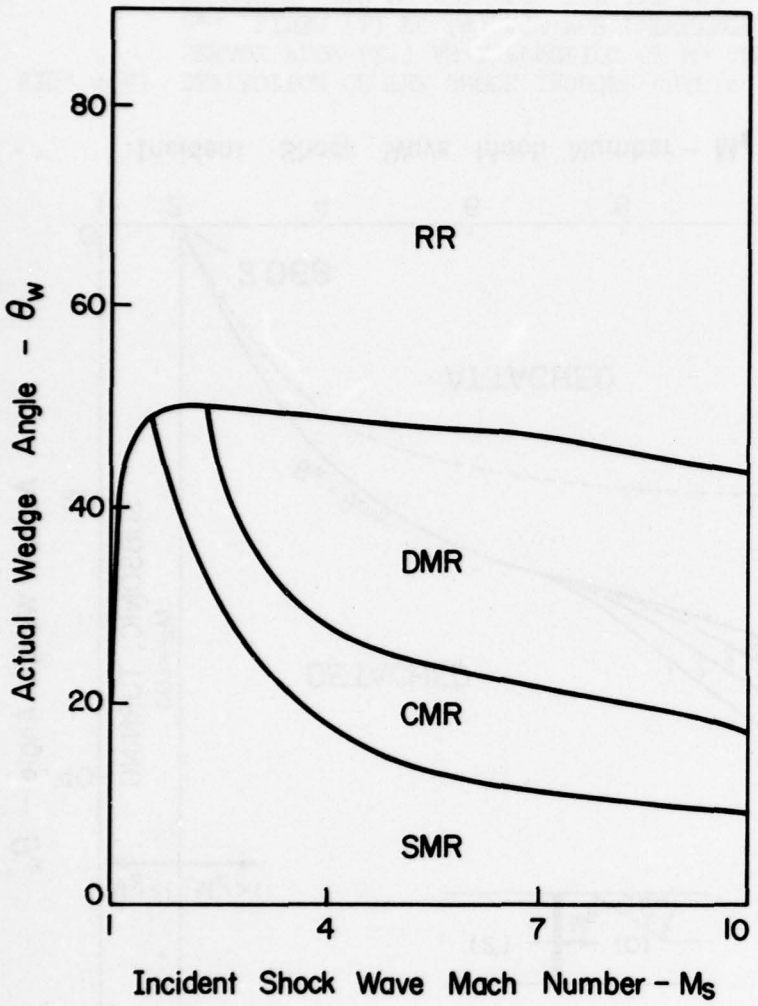

FIG. 3(a) DOMAINS AND BOUNDARIES OF NONSTATIONARY OBLIQUE SHOCK WAVE REFLECTIONS IN (M_s, θ_w)-PLANE. IMPERFECT NITROGEN P_o = 15 TORR, T_o = 300 K.

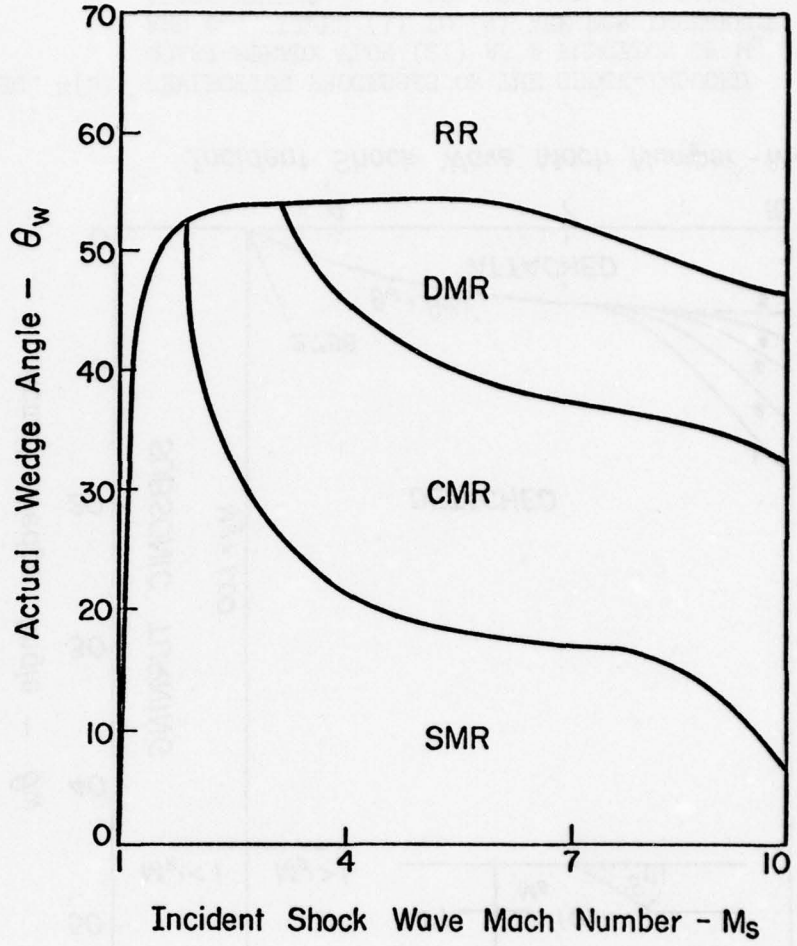

FIG. 3(b) DOMAINS AND BOUNDARIES OF NONSTATIONARY OBLIQUE SHOCK WAVE REFLECTIONS IN (M_s, θ_w)-PLANE. IMPERFECT ARGON P_o = 15 TORR, T_o = 300 K.

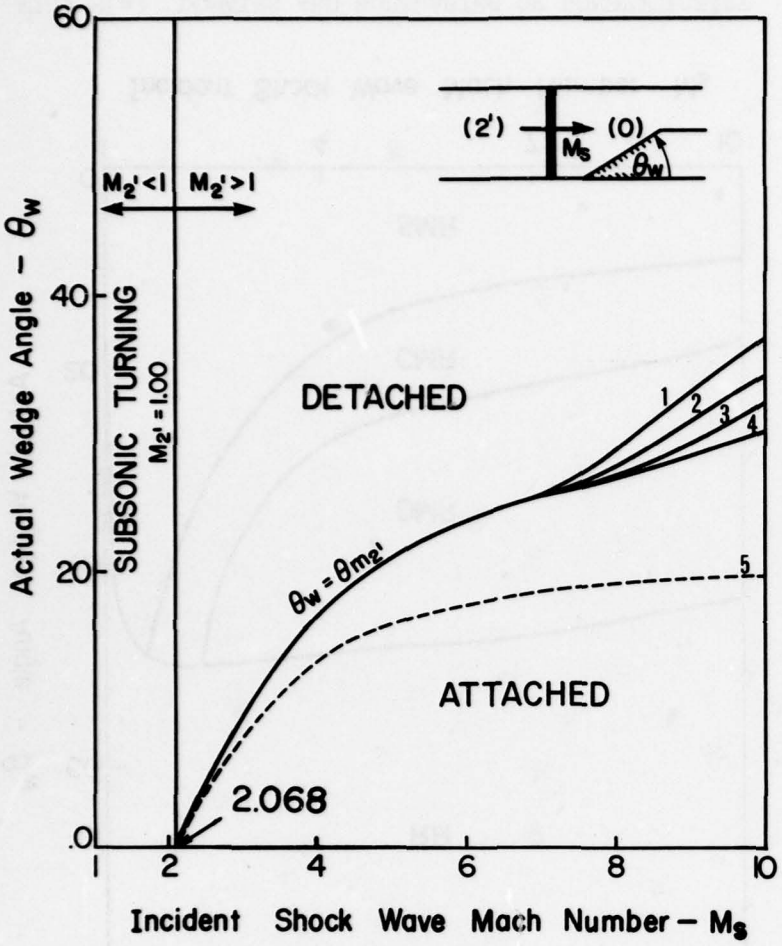

FIG. 4(a) DEFLECTION OF THE SHOCK-INDUCED QUASI-STEADY FLOW (2') AS A FUNCTION OF M_s AND θ_w. LINES (1) TO (4) ARE FOR IMPERFECT NITROGEN WITH P_o = 1, 10, 100 AND 1000 TORR, RESPECTIVELY, AND T_o = 300 K. LINE (5), DASHED, IS FOR A PERFECT DIATOMIC GAS γ = 7/5.

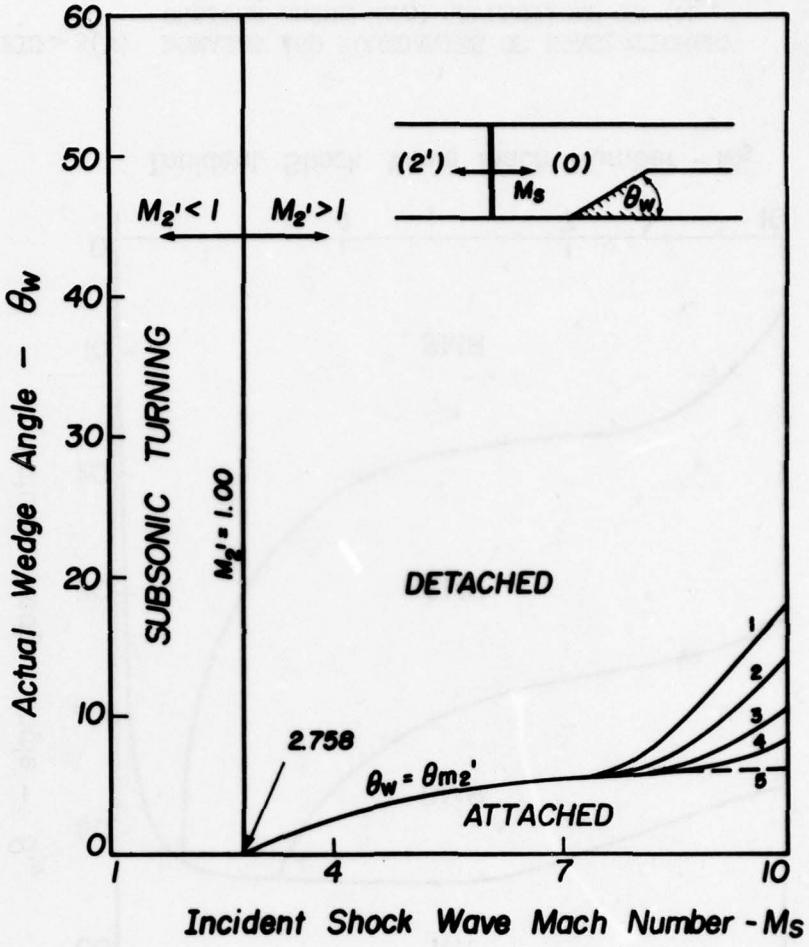

FIG. 4(b) DEFLECTION PROCESSES OF THE SHOCK-INDUCED QUASI-STEADY FLOW (2') AS A FUNCTION OF M_s AND θ_w. LINES (1) TO (4) ARE FOR IMPERFECT ARGON WITH P_o = 1, 10, 100 AND 1000 TORR, RESPECTIVELY, AND T_o = 300 K. LINE (5), DASHED, IS FOR A PERFECT MONATOMIC GAS γ = 5/3.

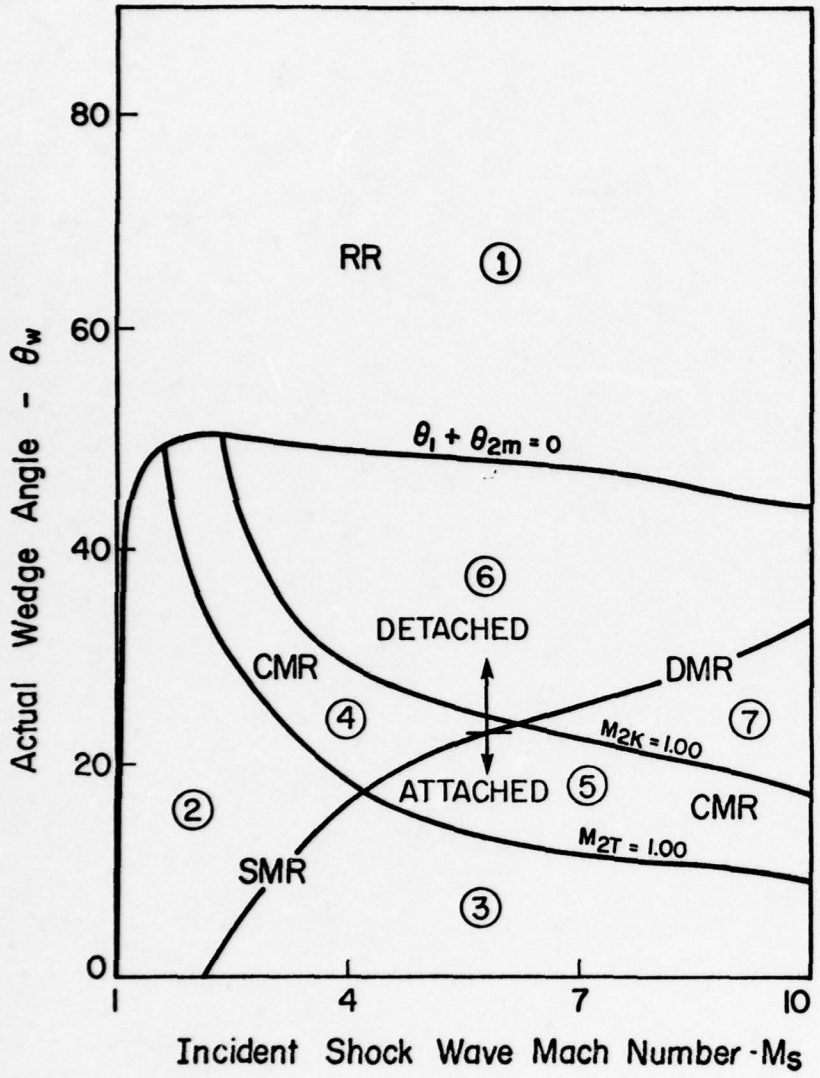

FIG. 5(a) SEVEN DOMAINS AND THEIR TRANSITION BOUNDARIES OF NONSTATIONARY SHOCK-WAVE DIFFRACTIONS IN (M_S, θ_W)-PLANE. IMPERFECT NITROGEN P_O = 15 TORR, T_O = 300 K (SEE TABLE 1).

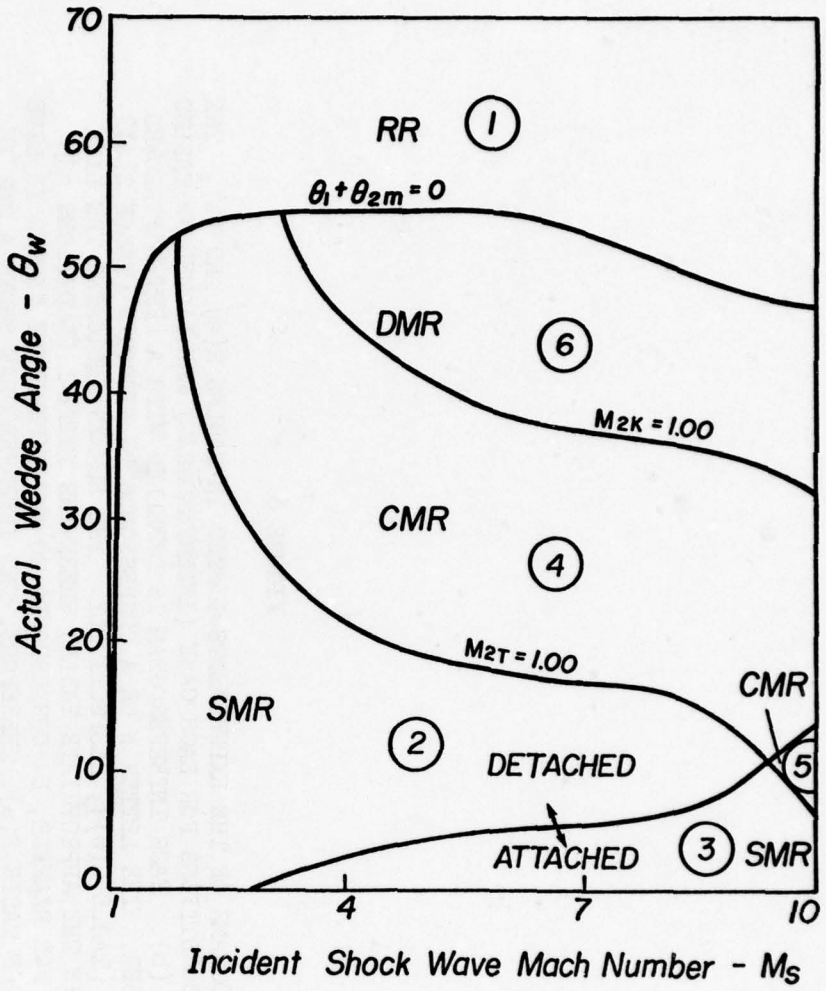

FIG. 5(b) SIX DOMAINS AND THEIR TRANSITION BOUNDARIES OF NONSTATIONARY SHOCK-WAVE DIFFRACTION IN (M_S, θ_W)-PLANE. IMPERFECT ARGON P_O = 15 TORR, T_O = 300 K (SEE TABLE 2).

FIGURE 6

INTERFEROGRAMS OF THE EXPERIMENTS LISTED IN TABLES 2(a) AND (b). THE INITIAL CONDITIONS FOR EACH CASE (INTERFEROGRAM) ARE LISTED IN TABLES 2(a) AND (b). EACH INTERFEROGRAM IS LABELLED WITH A LETTER FOLLOWED BY A NUMBER. THE LETTER N OR A CORRESPONDS TO NITROGEN [TABLE 2(a)] OR ARGON [TABLE 2(b)], RESPECTIVELY. THE NUMBER INDICATES THE LINE NUMBER (IN THE APPROPRIATE TABLE) WHERE THE INITIAL CONDITIONS ARE LISTED. FOR EXAMPLE, N9 CORRESPONDS TO THE EXPERIMENT LISTED IN LINE NUMBER 9 OF TABLE 2(a), THEREFORE, THE INTERFEROGRAM SHOWS A SMR IN NITROGEN THAT WAS OBTAINED BY REFLECTING AN INCIDENT SHOCK WAVE OF $M_s = 7.77$ FROM A WEDGE ANGLE OF $\theta_w = 2°$. THE INITIAL CONDITIONS OF THE GAS AHEAD OF THE SHOCK WAVE FOR THIS CASE ARE: PRESSURE $P_o = 9.80$ TORR AND TEMPERATURE $T_o = 297.6$ K.

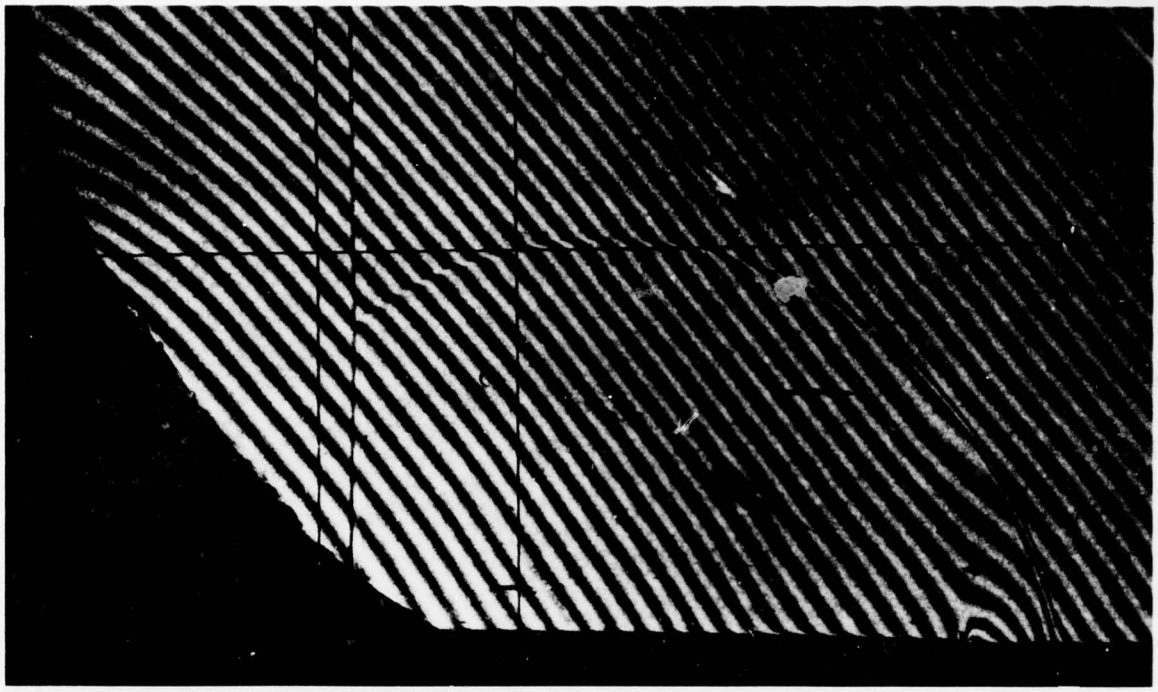

N1

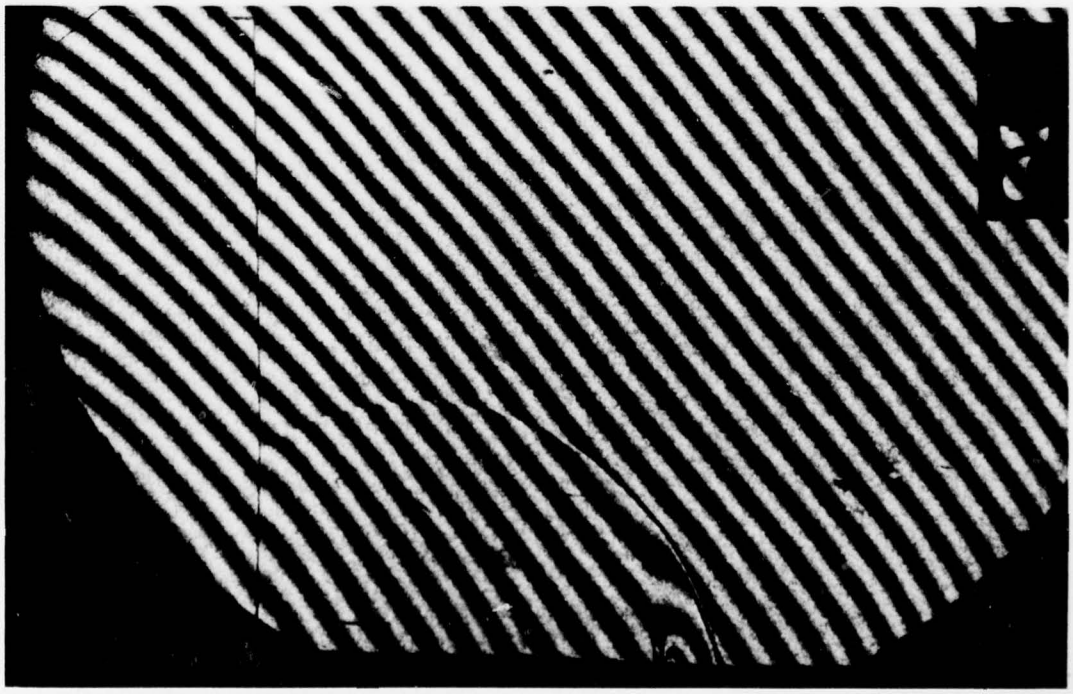

N2

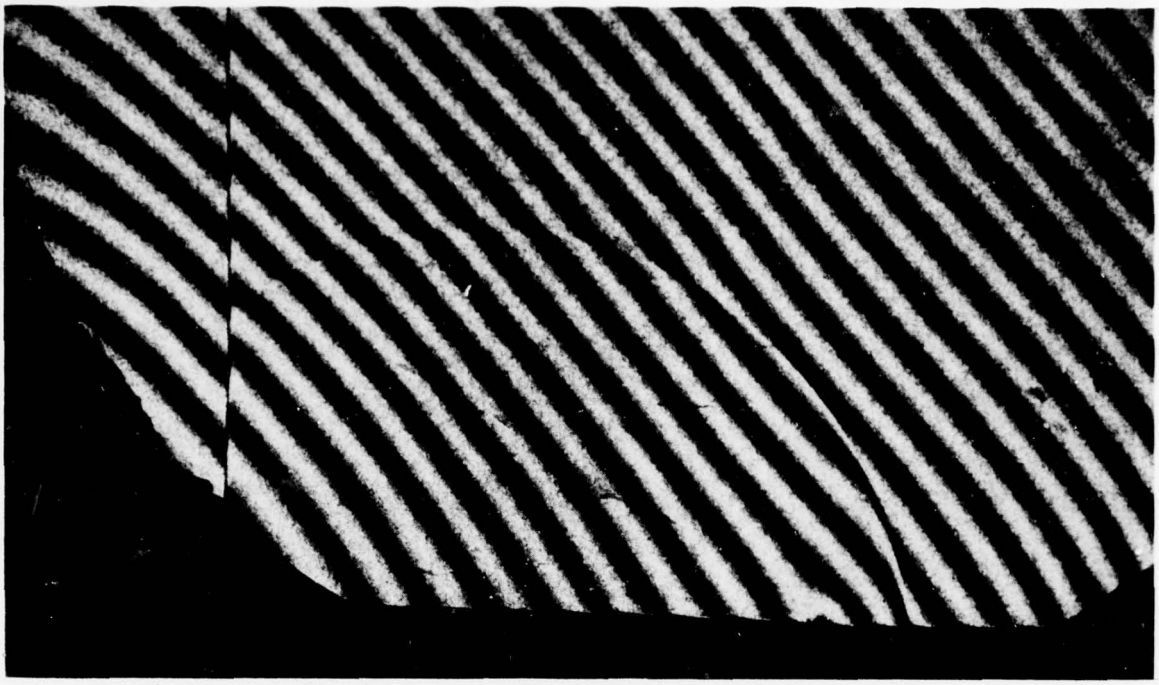

N3

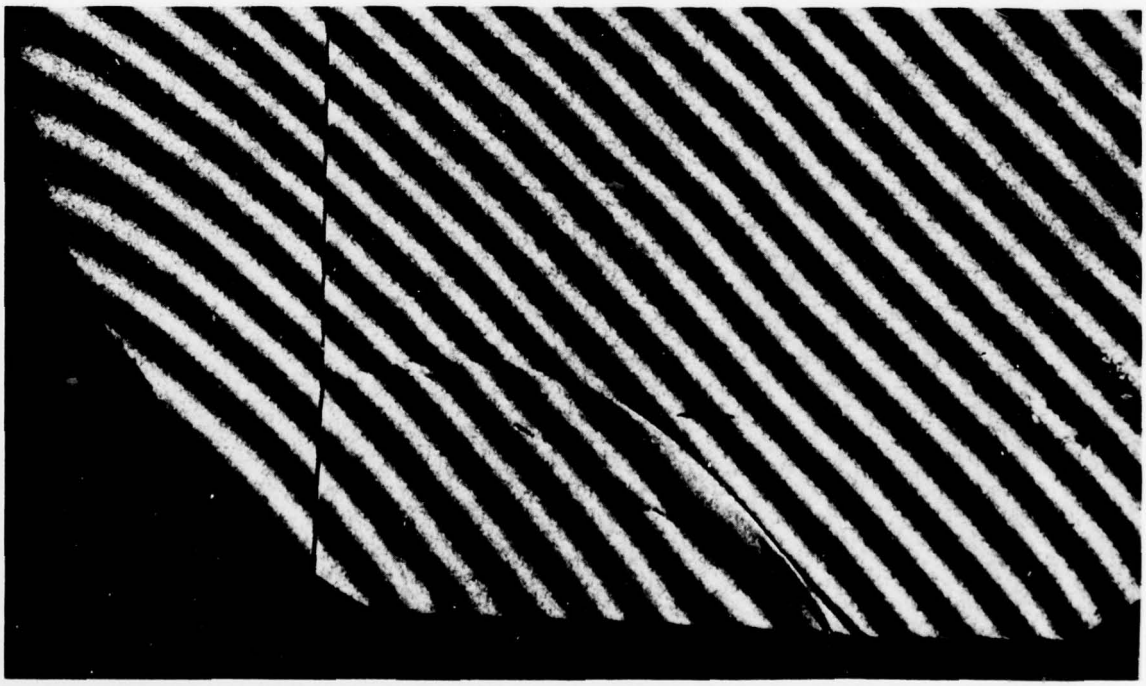

N4

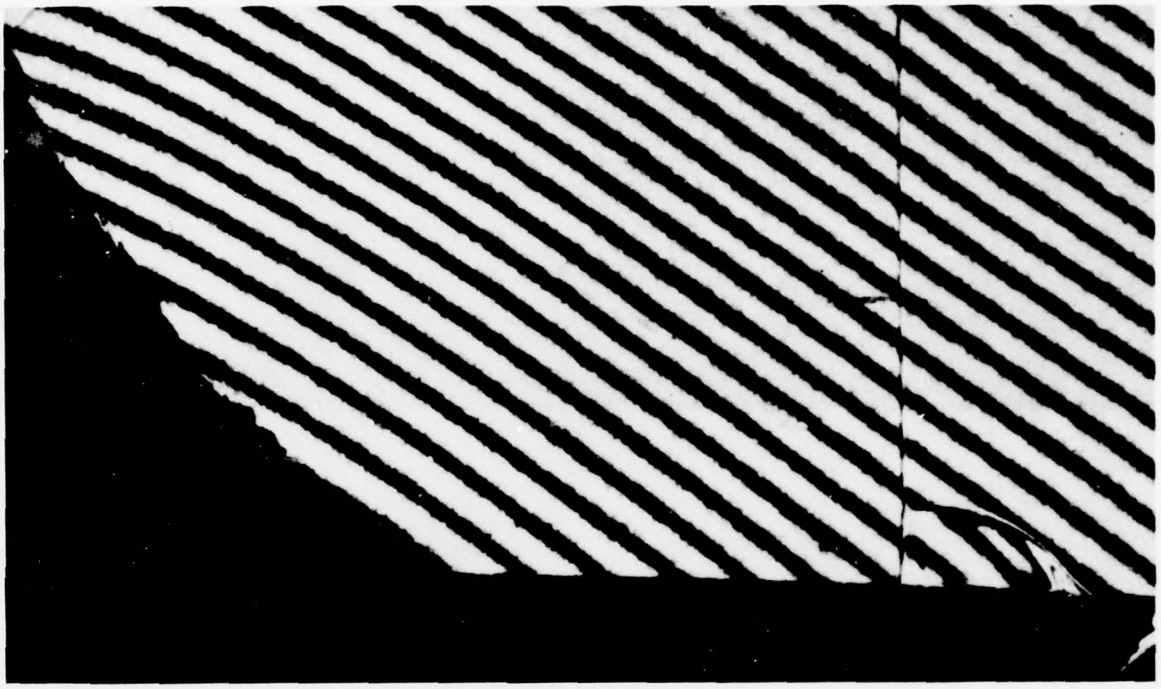

N5

N6

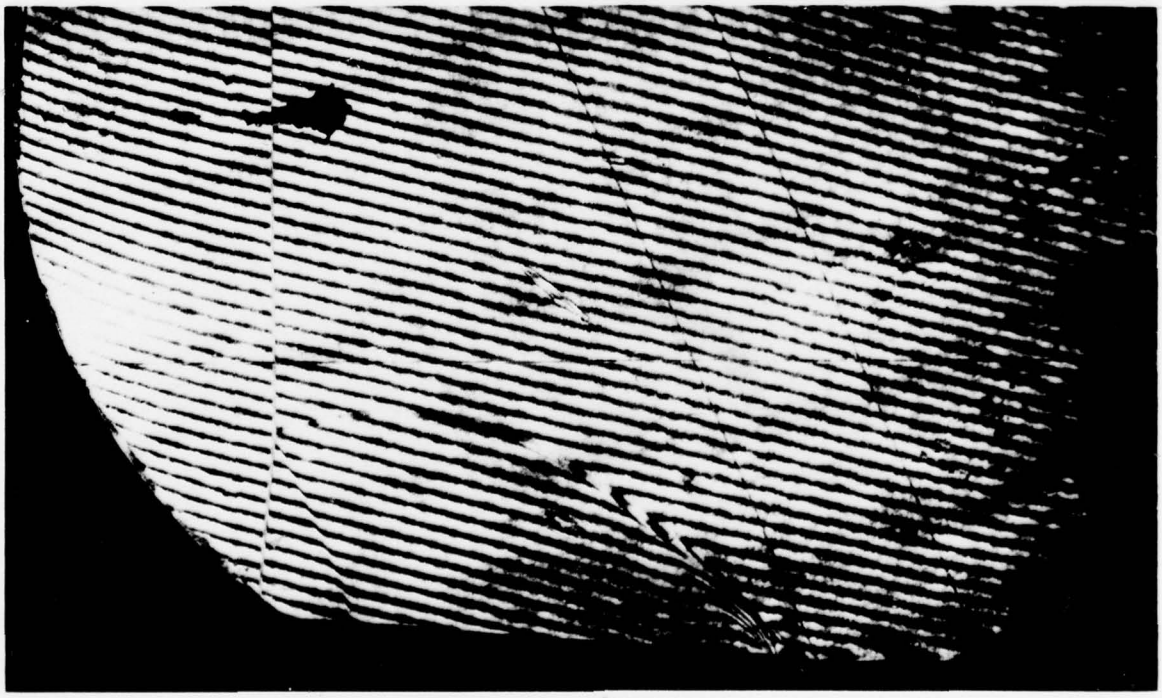

N7

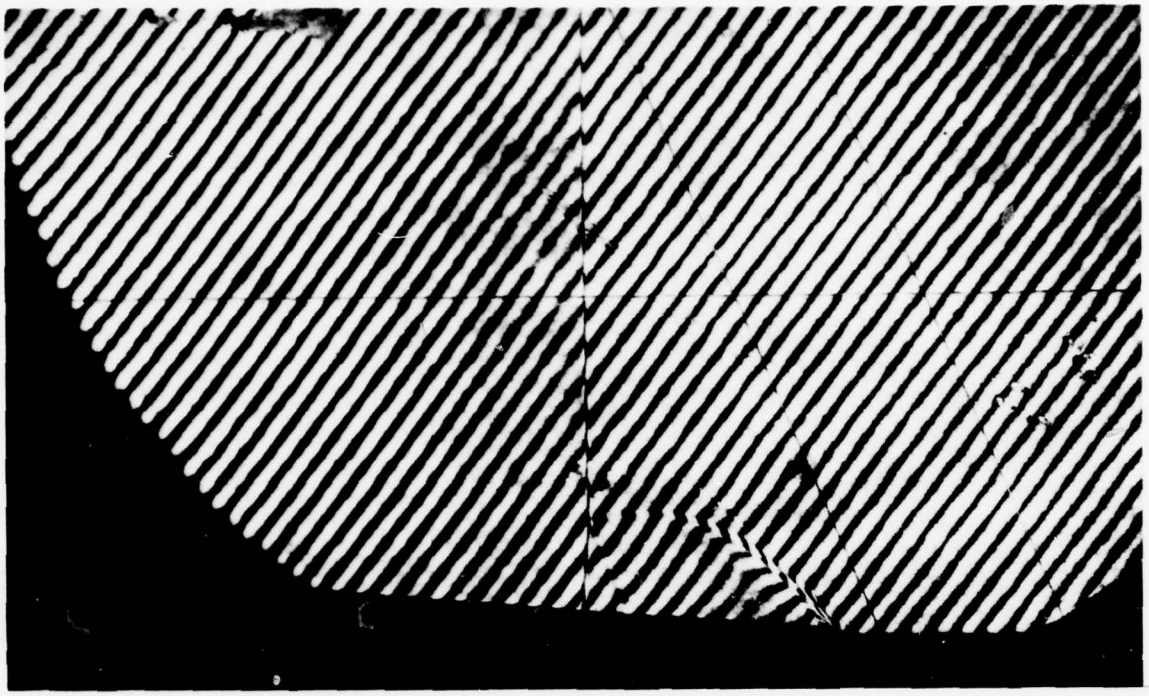

N8

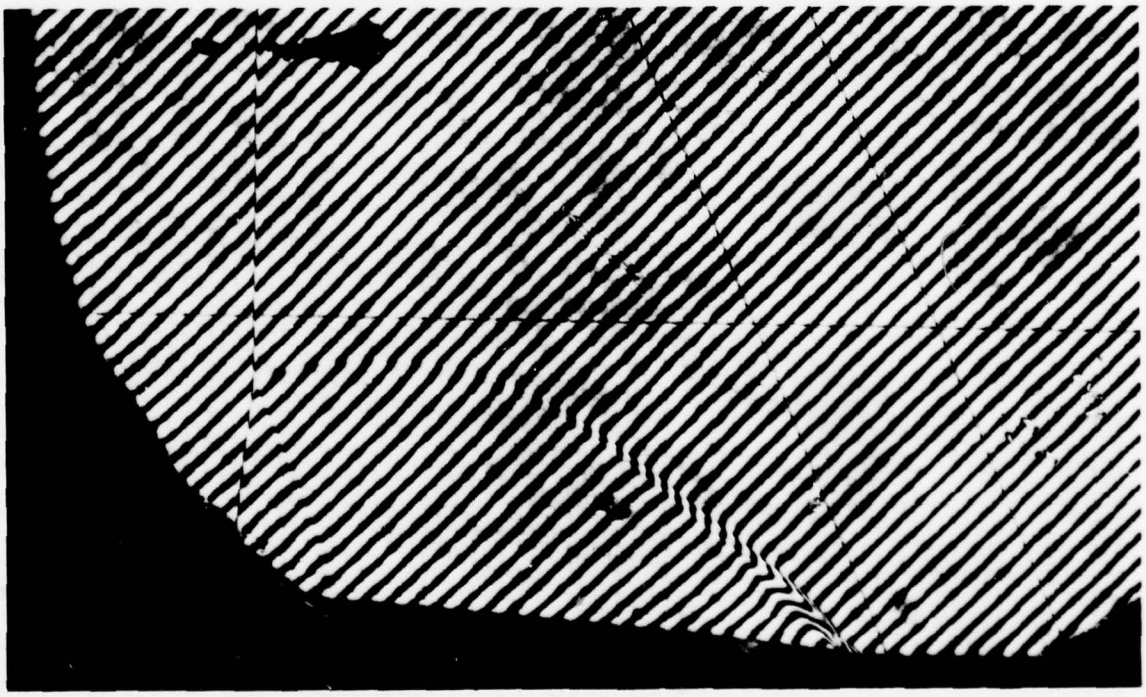

N9

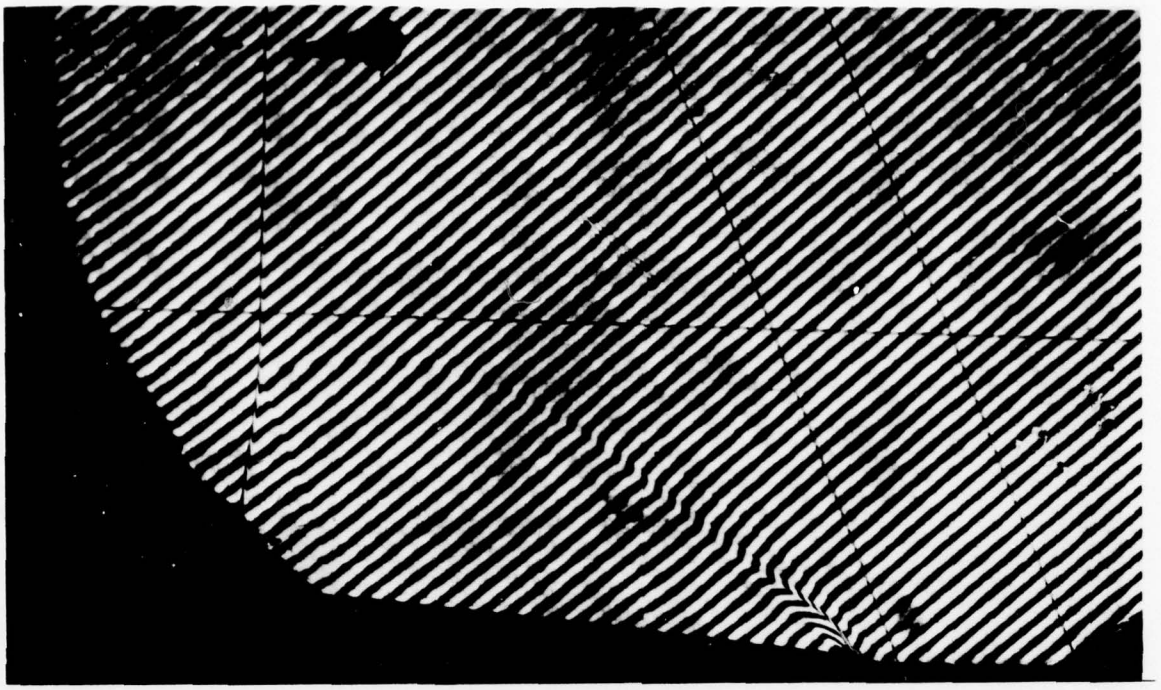

N10

N11

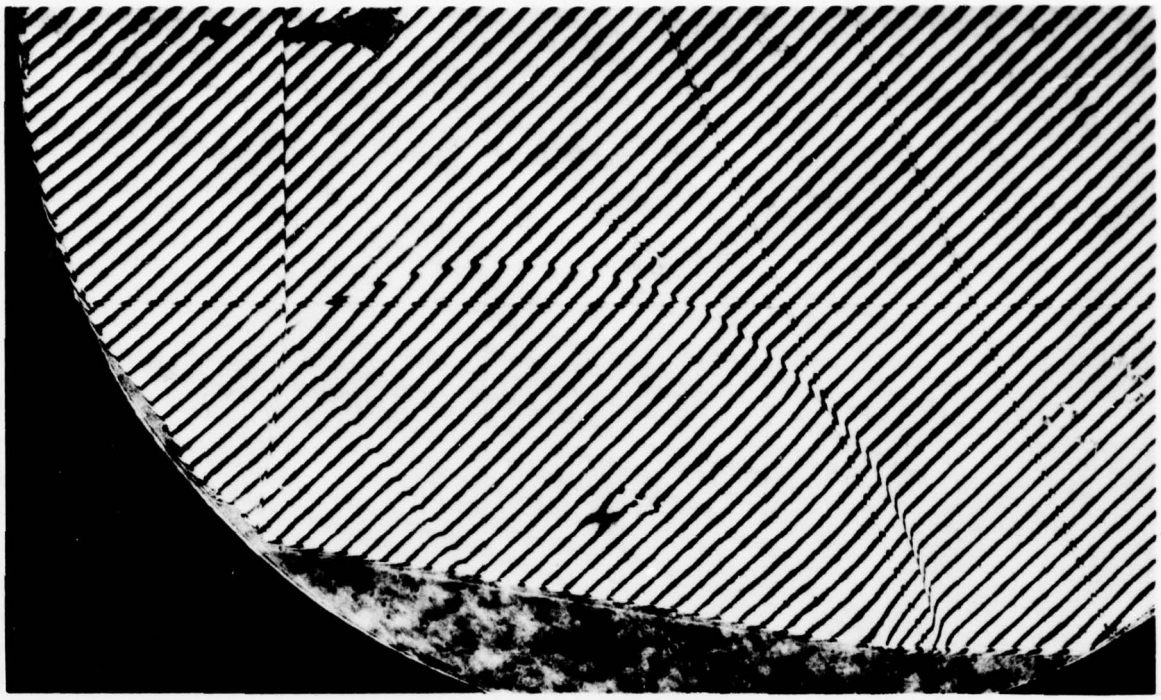

N12

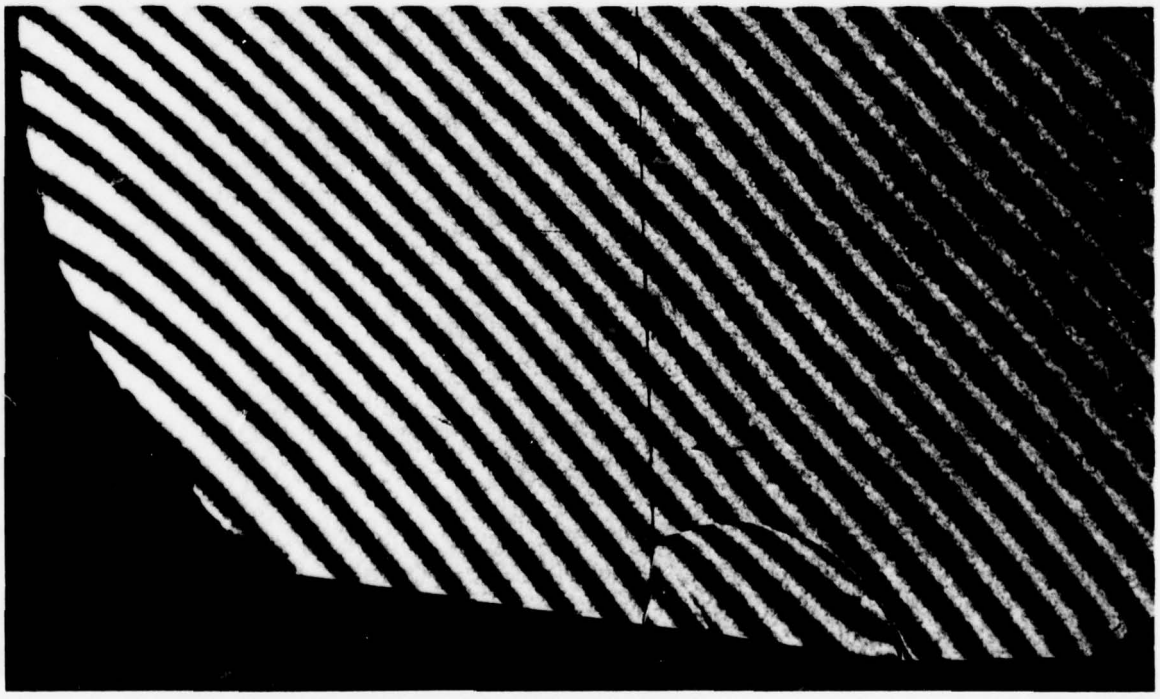

N13

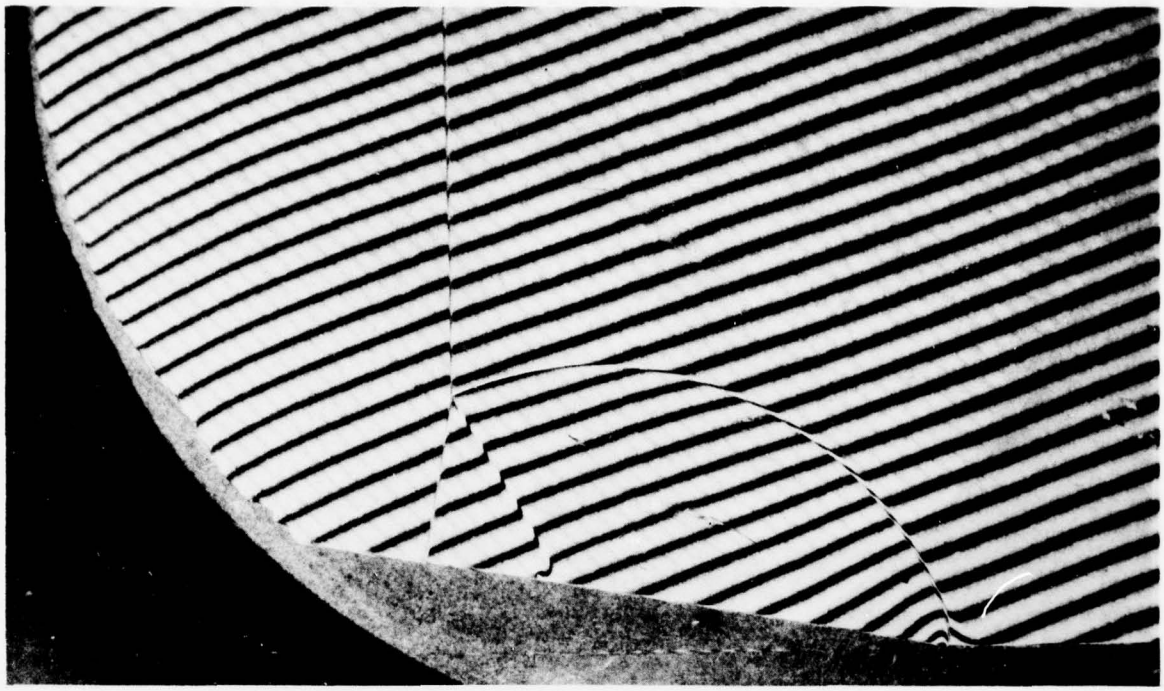

N14

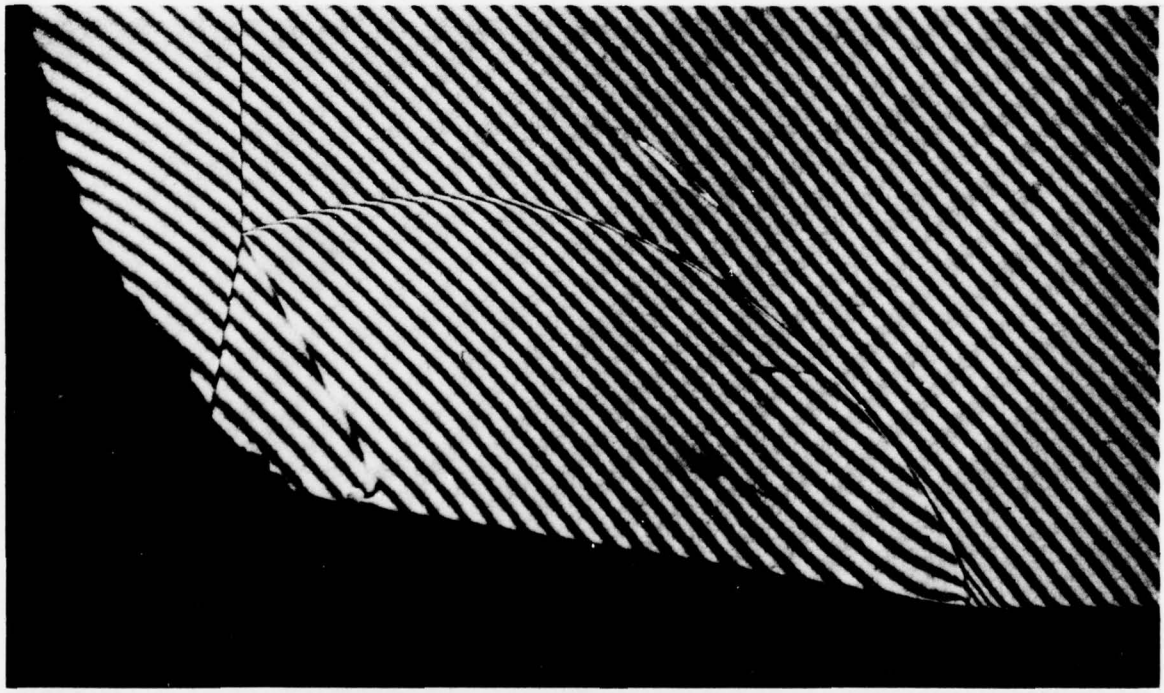

N15

N16

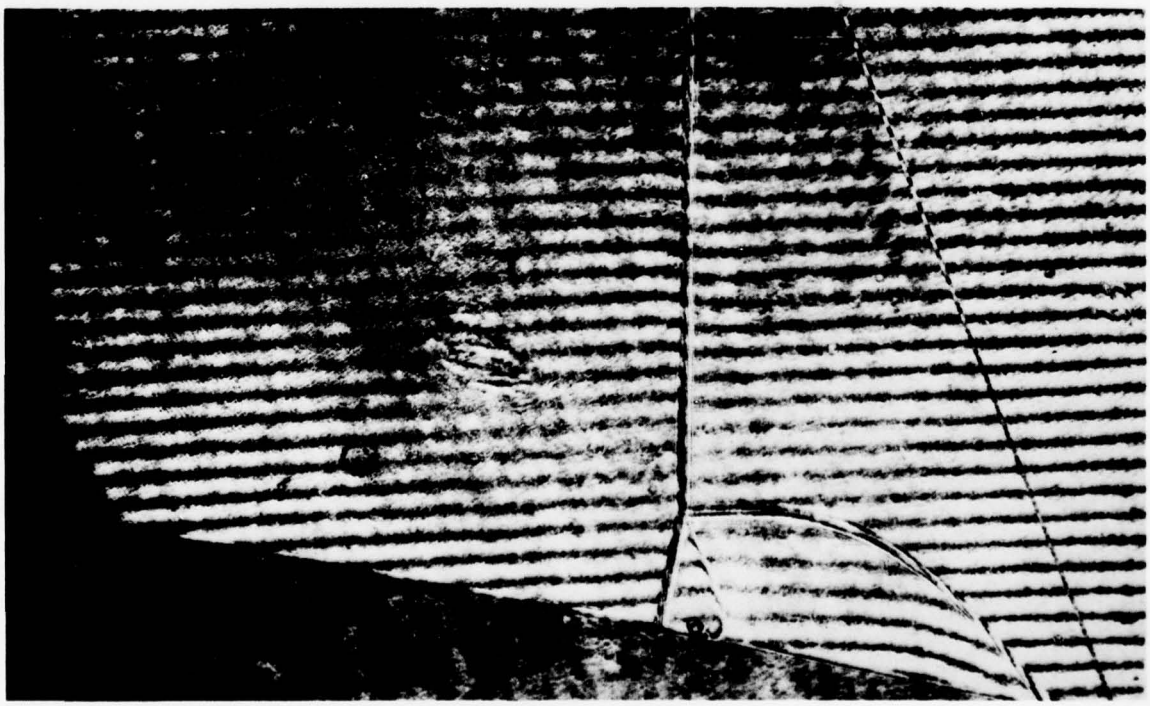

N17

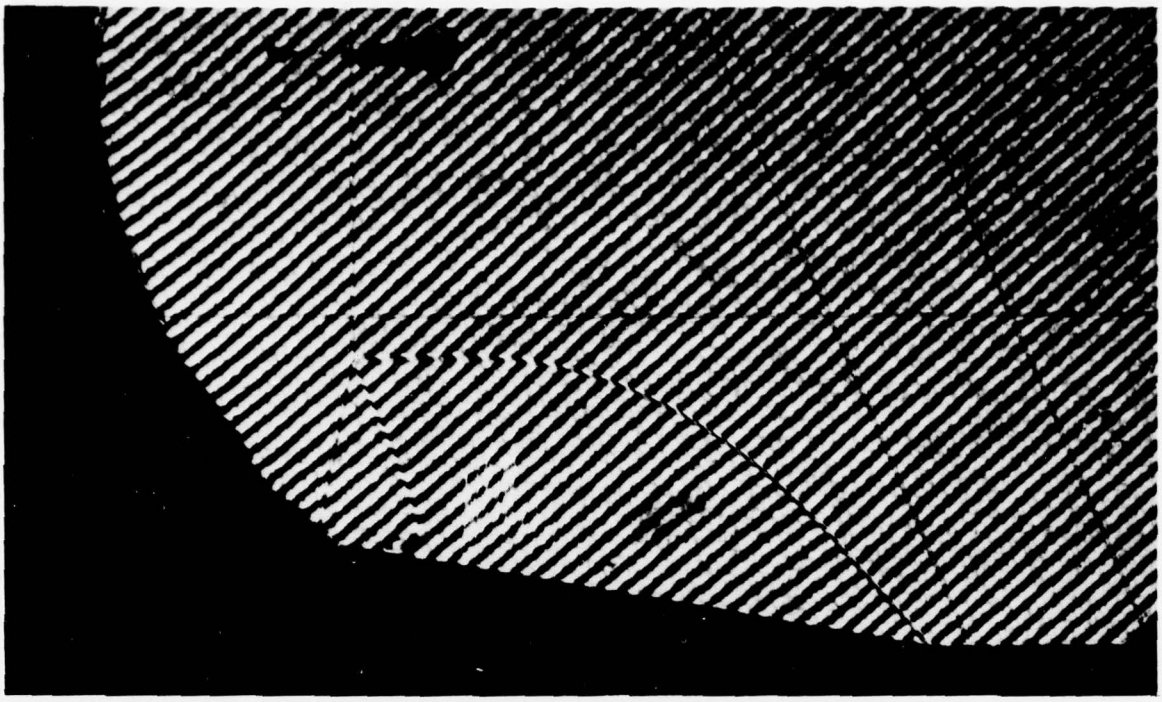

N18

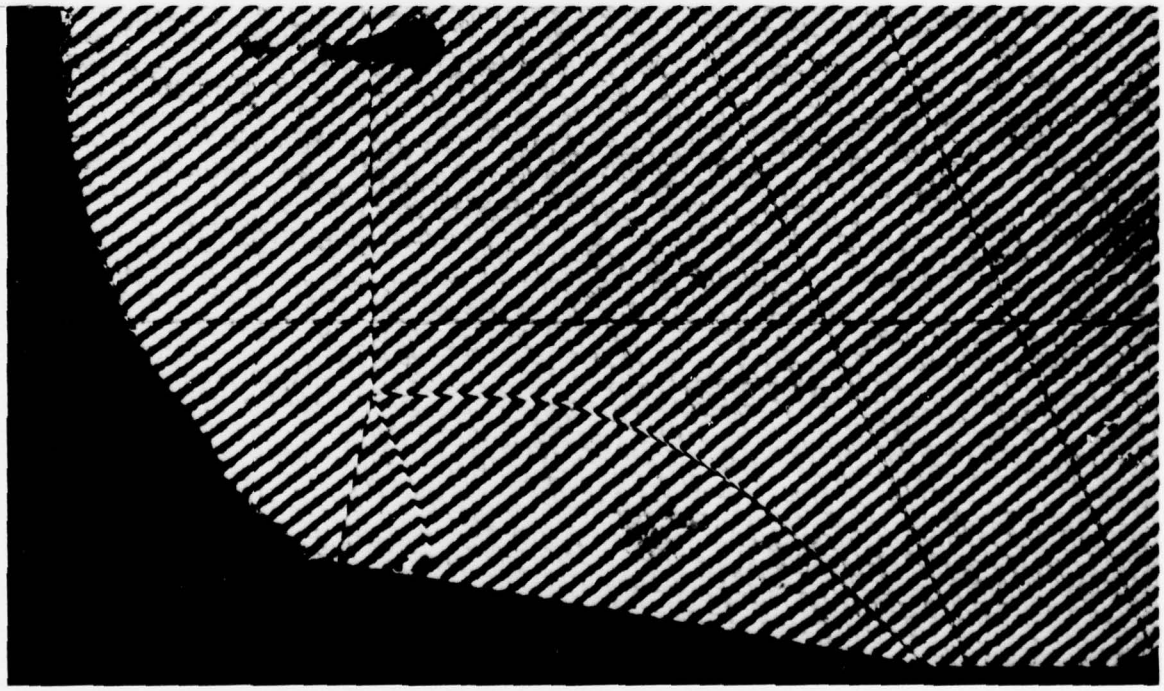

N19

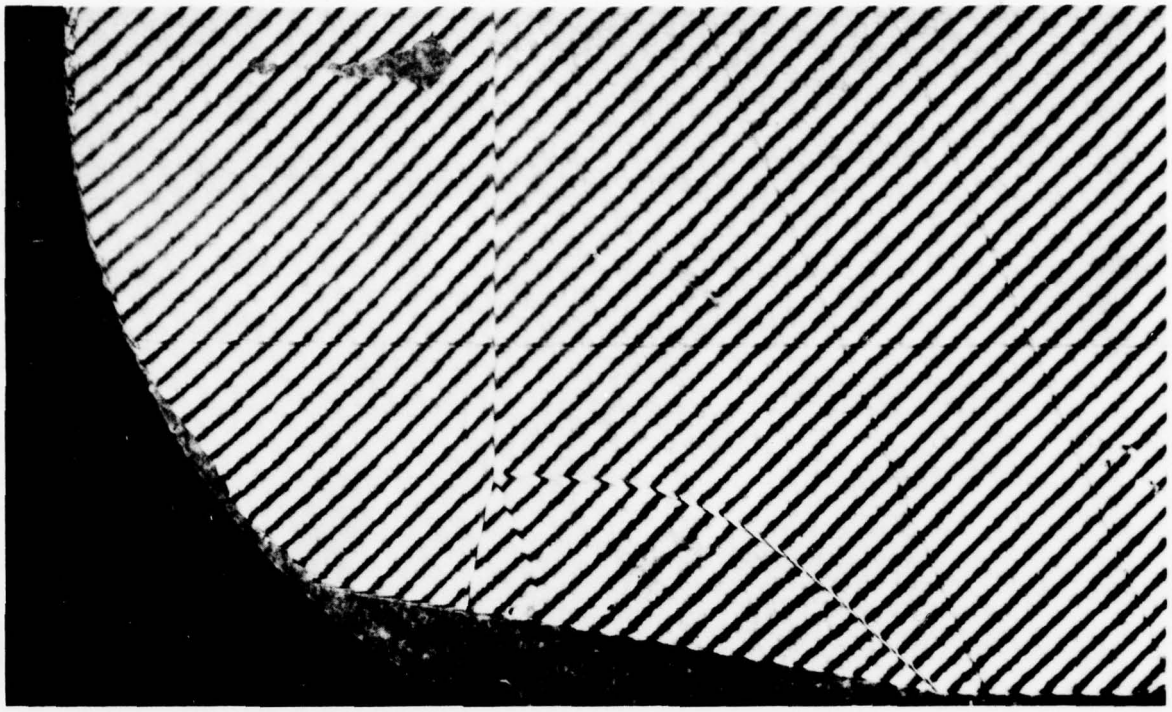

N20

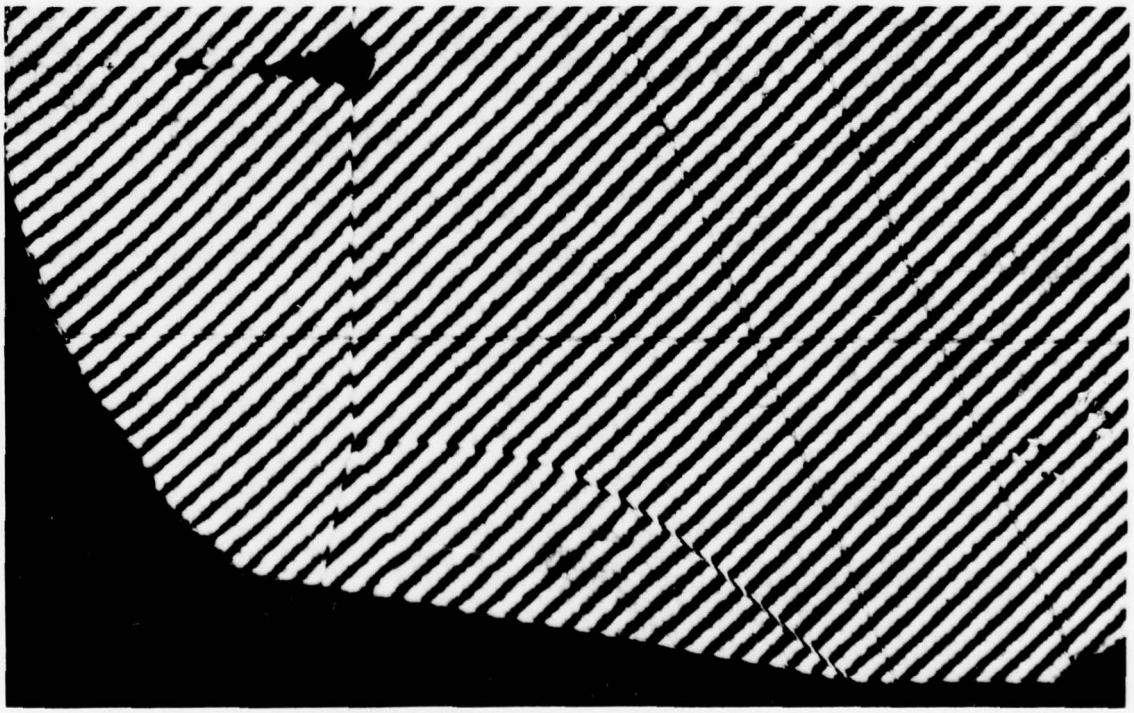

N21

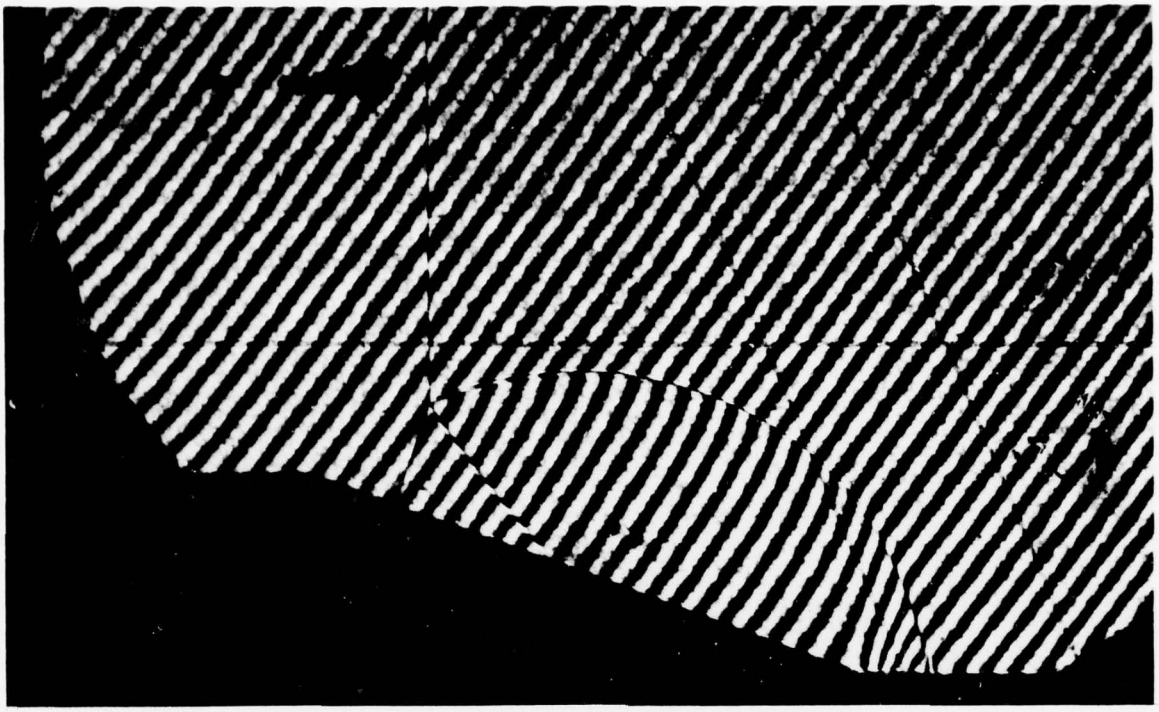

N22

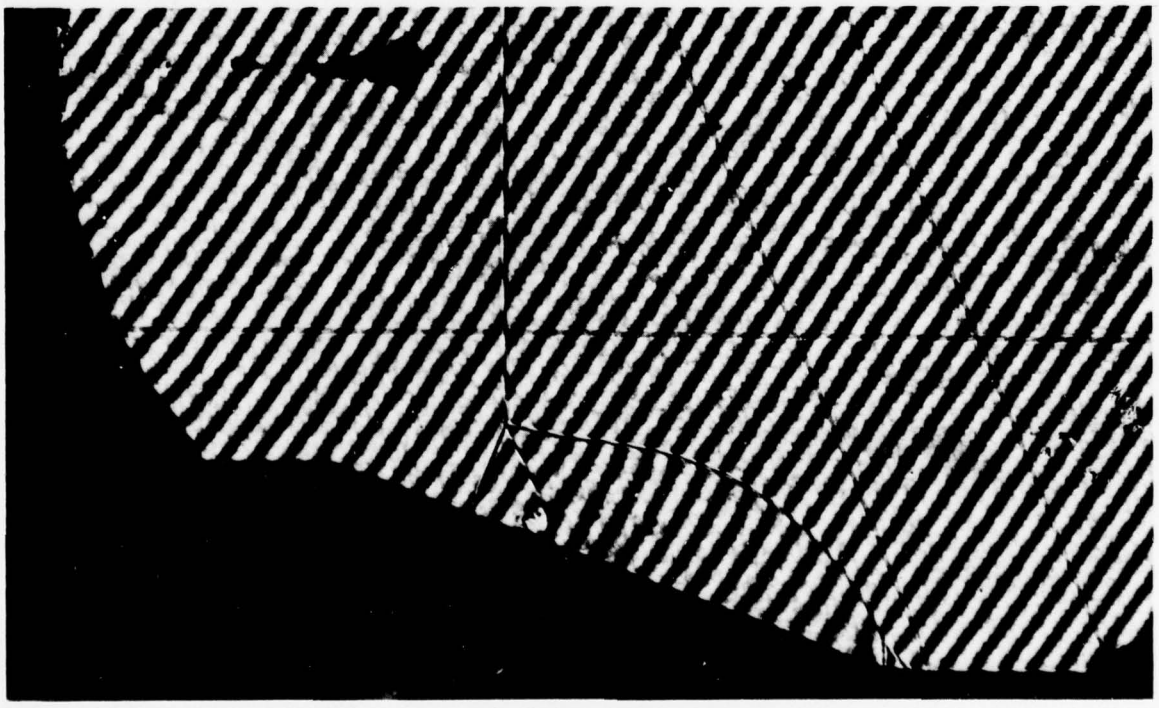

N23

N24

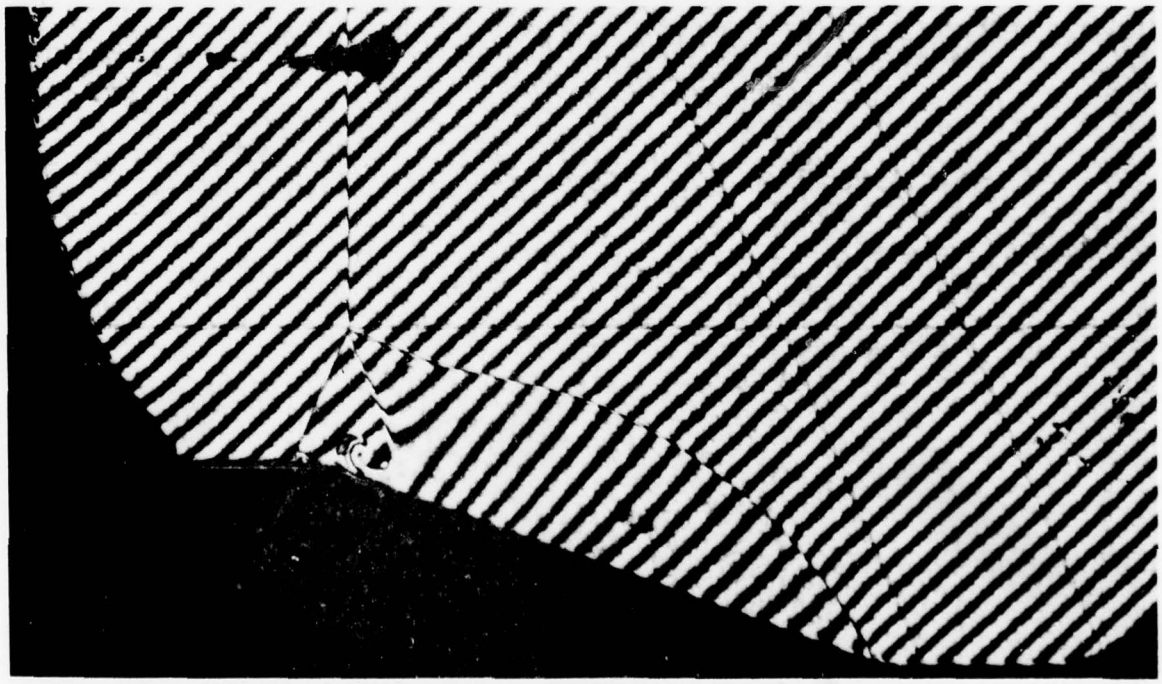

N25

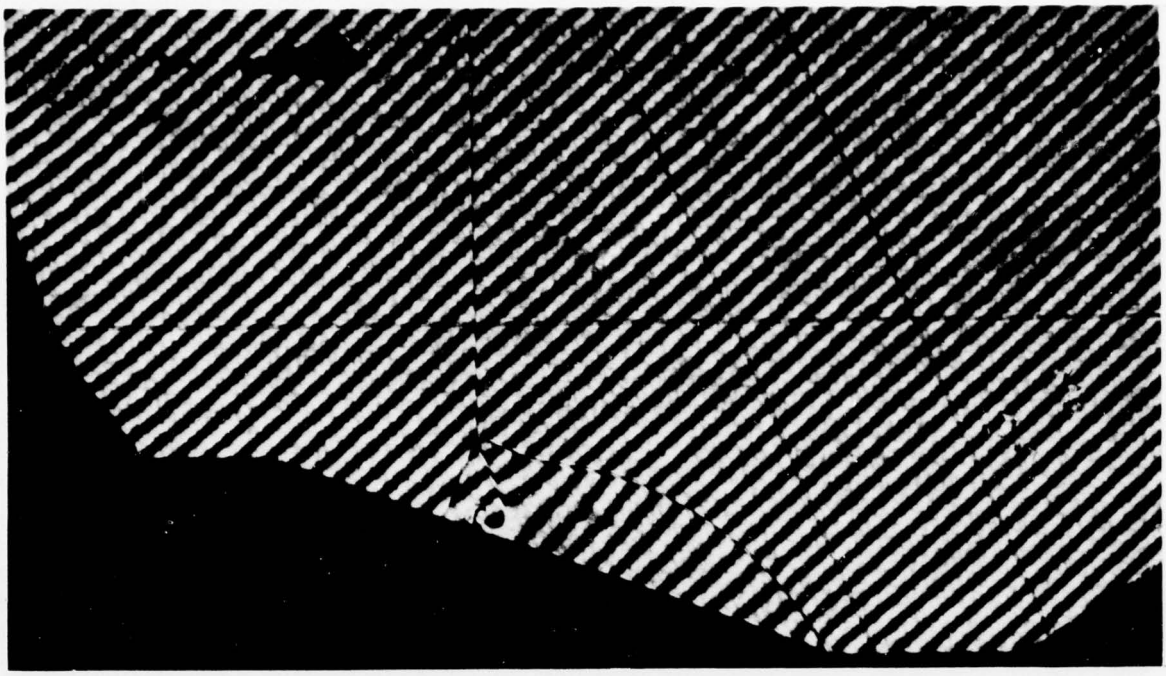

N26

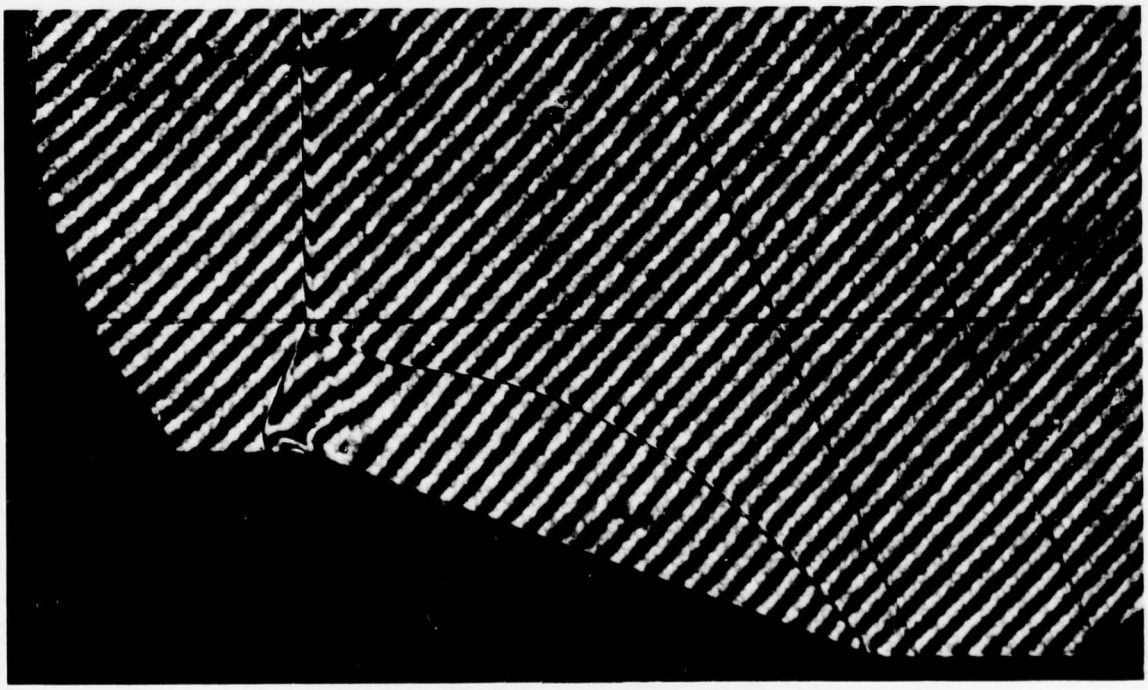

N27

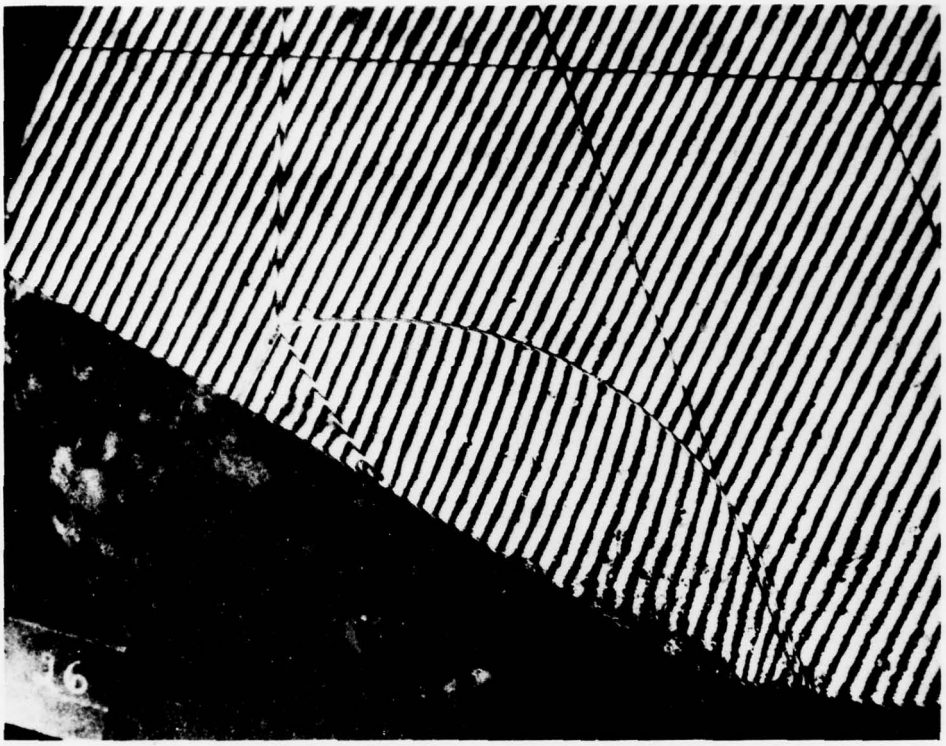

N28

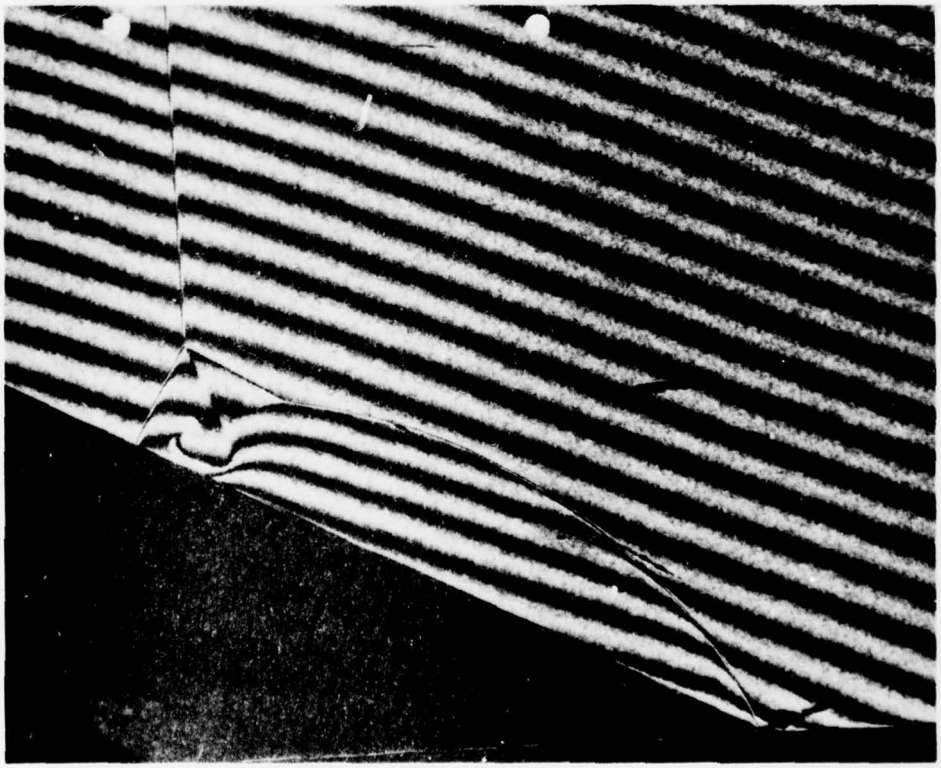

N29

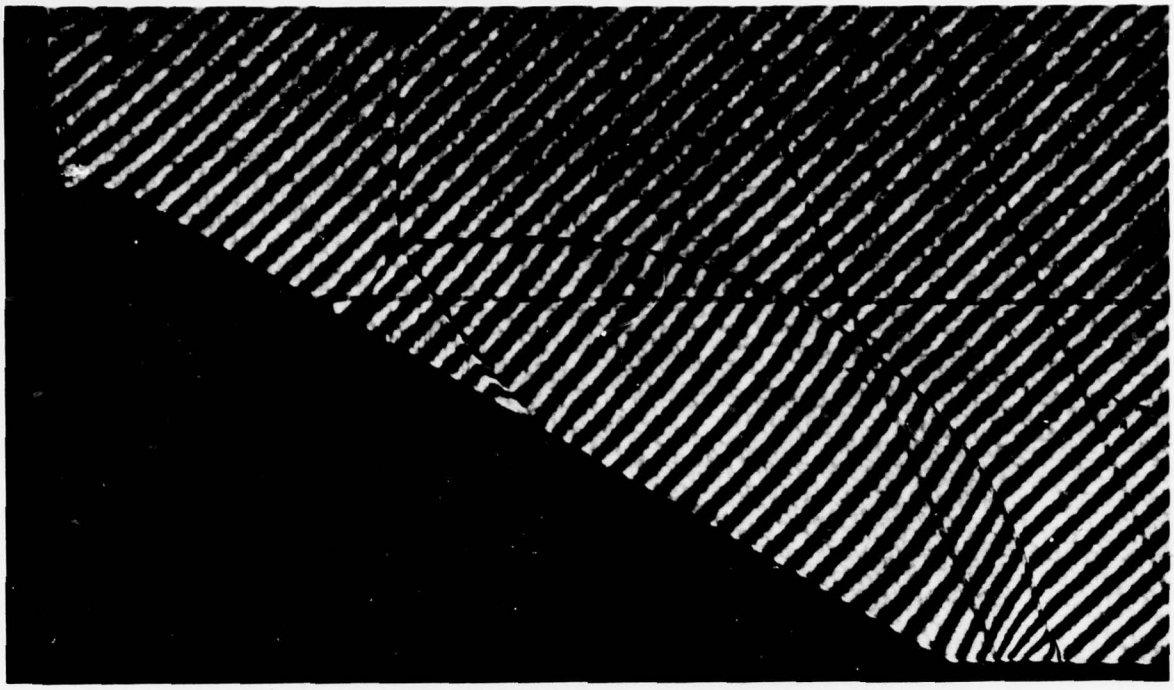

N30

N31

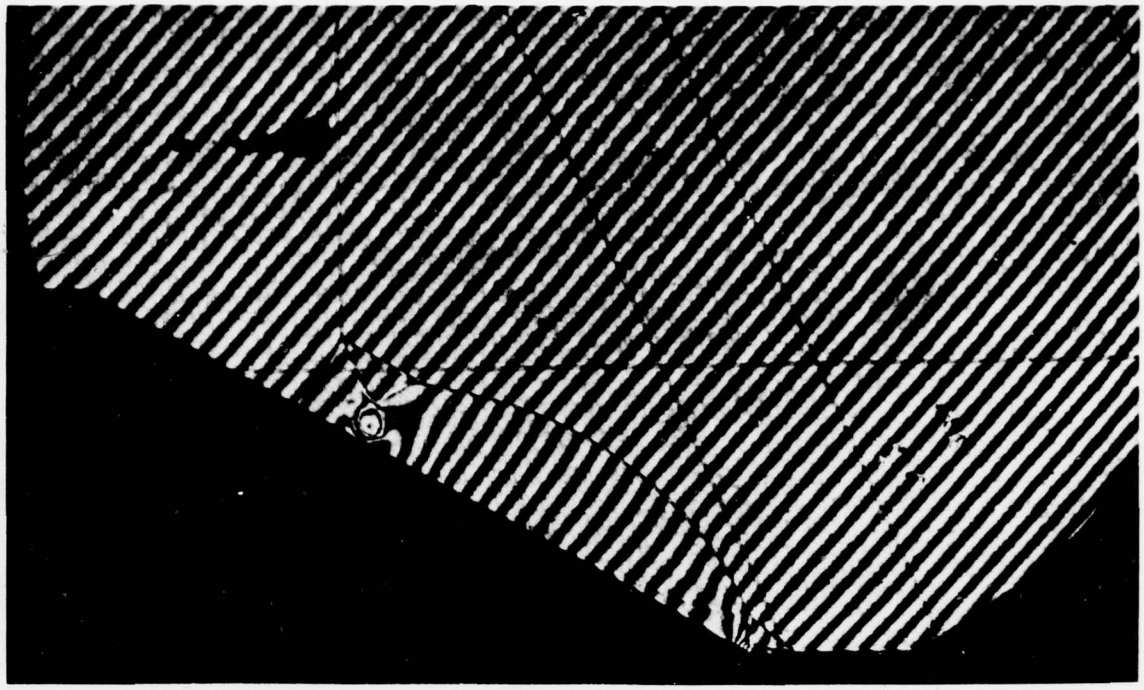

N32

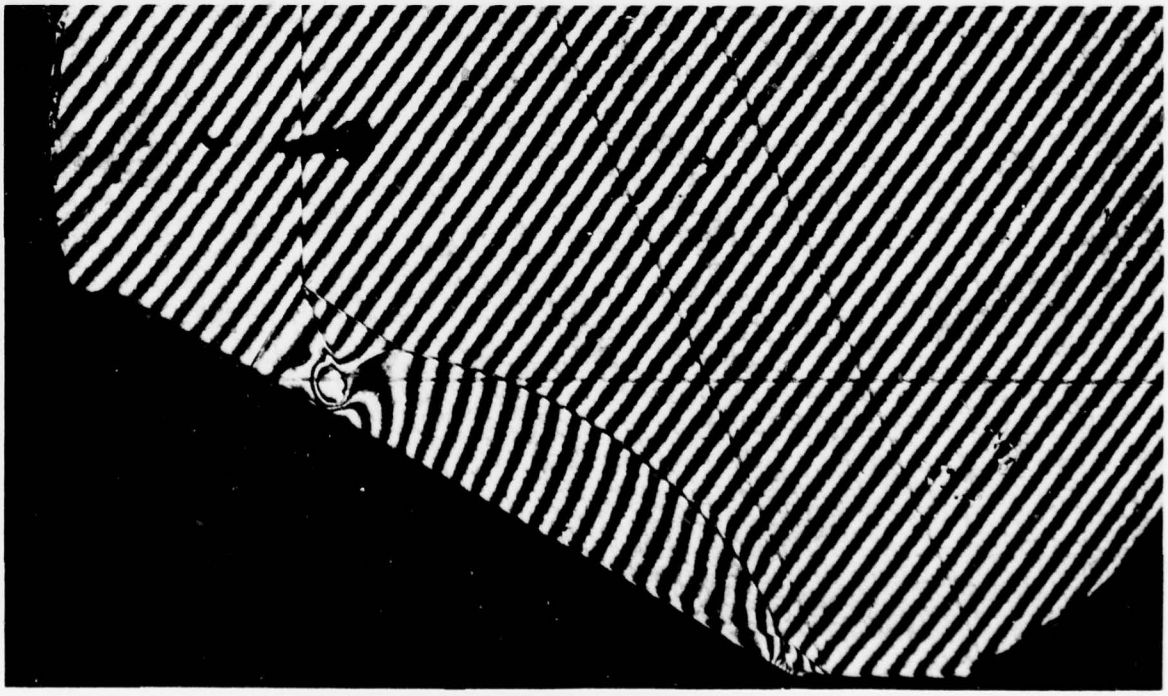

N33

N34

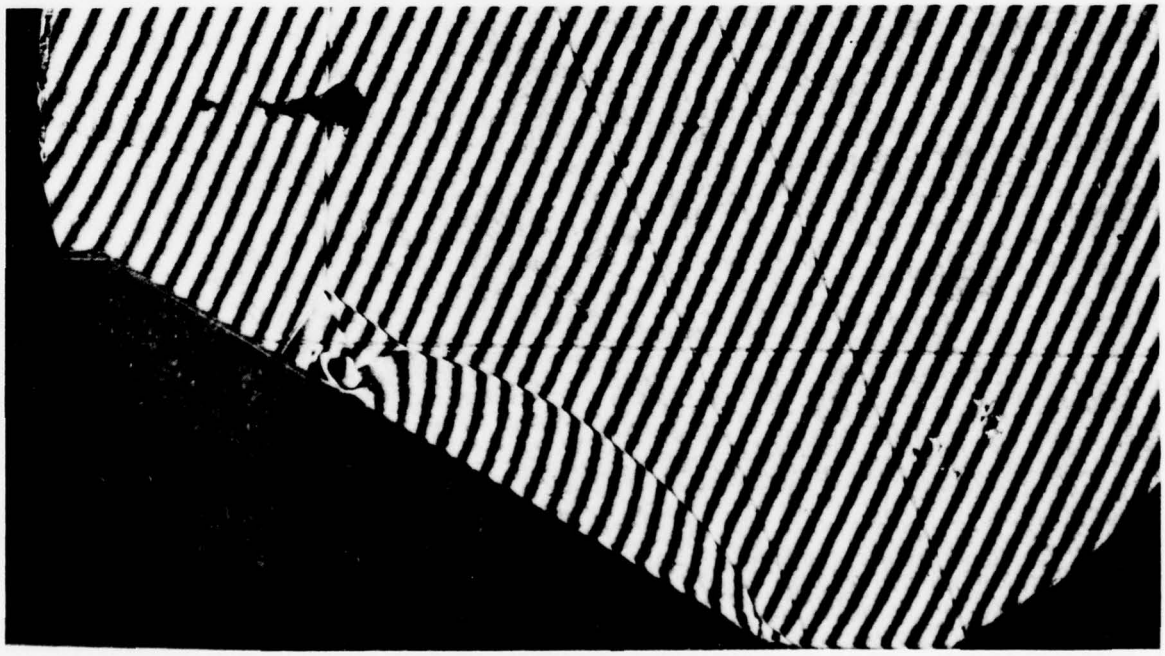

N35

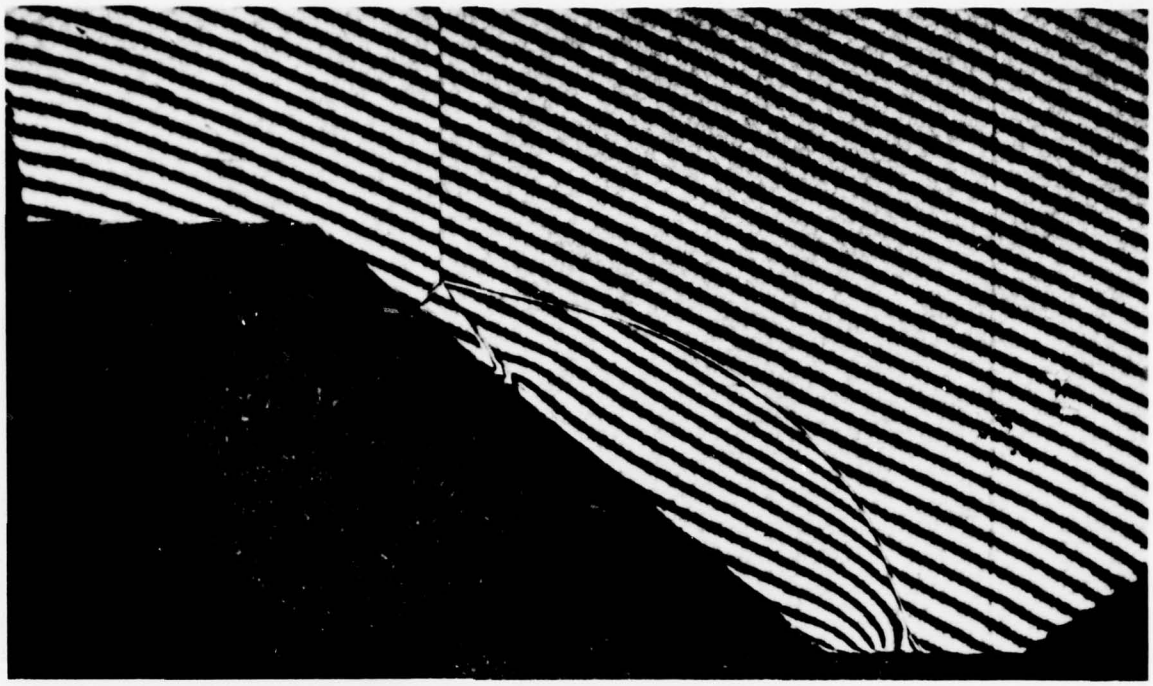

N36

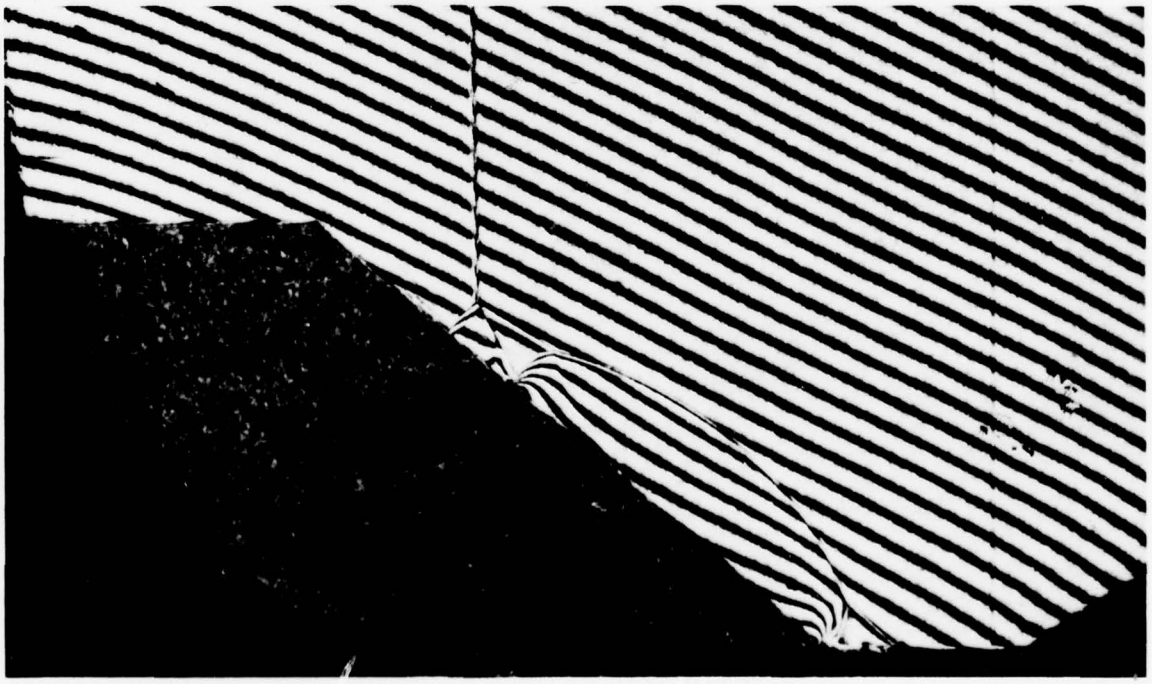

N37

N 38

N 39

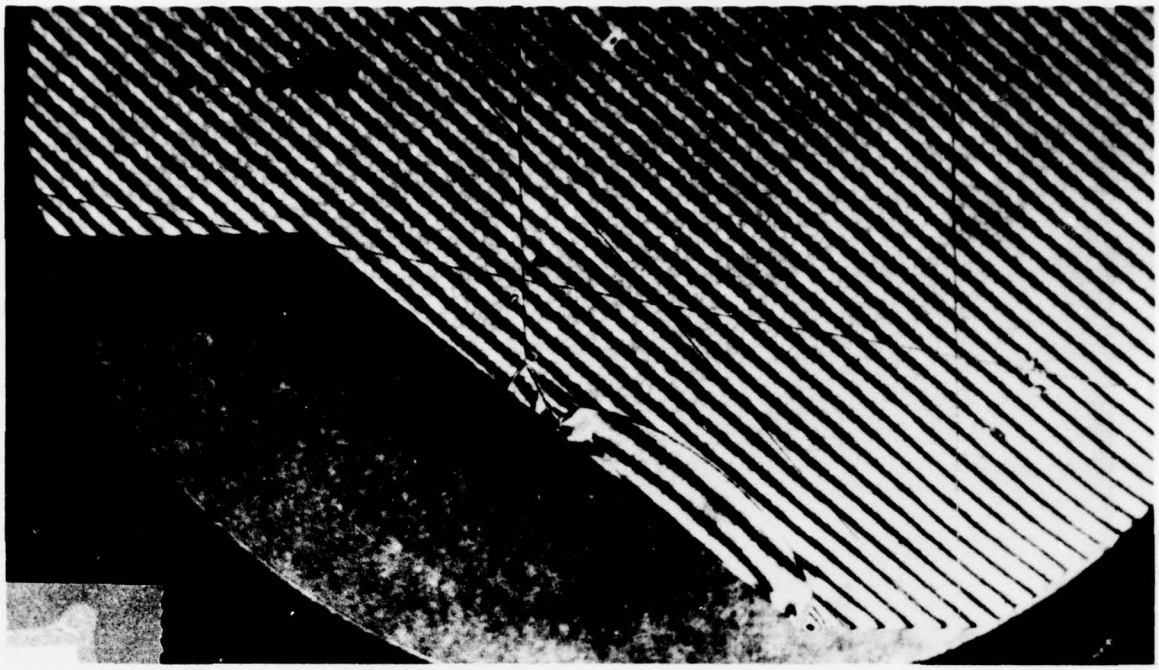

N40

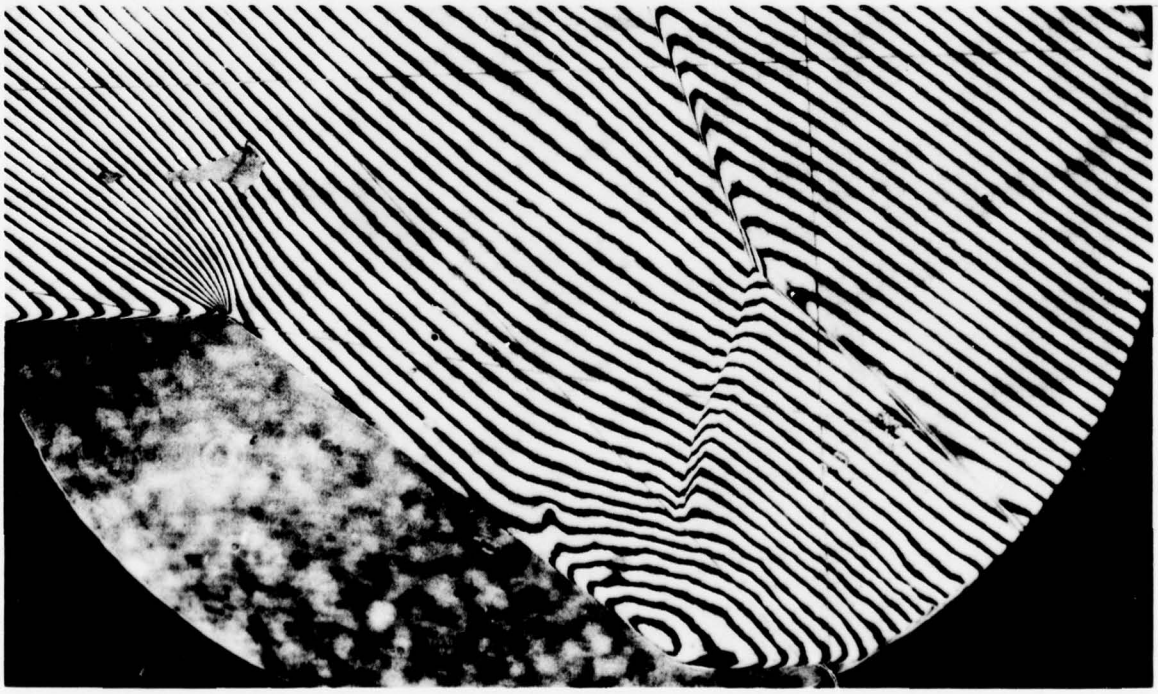

N41

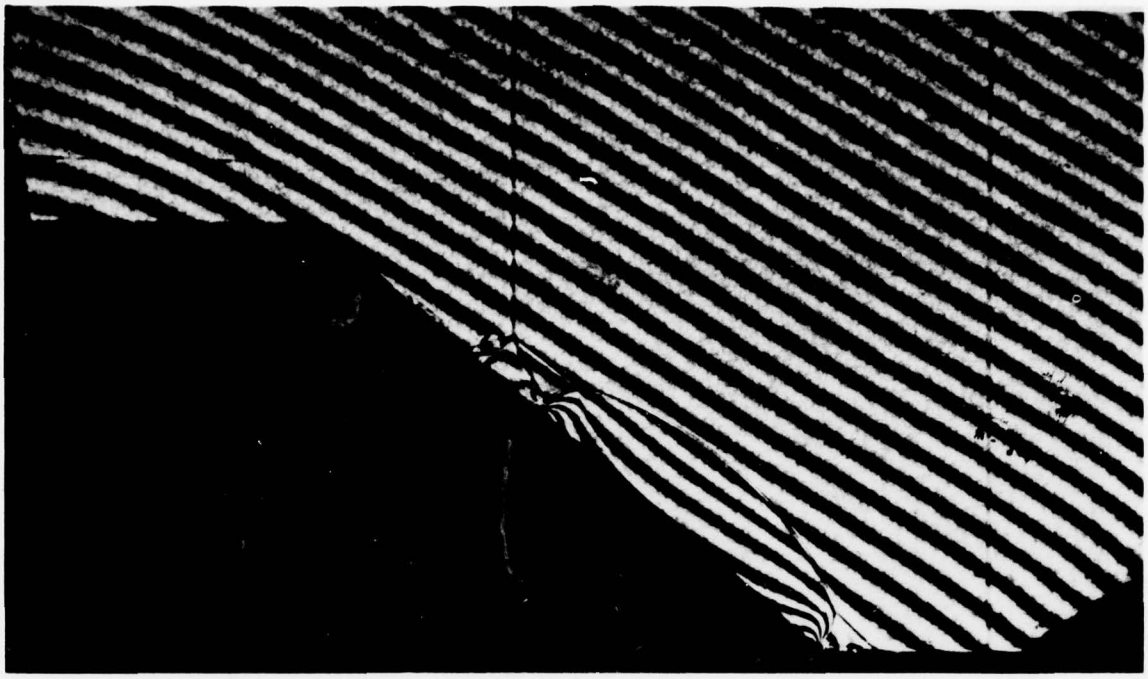

N42

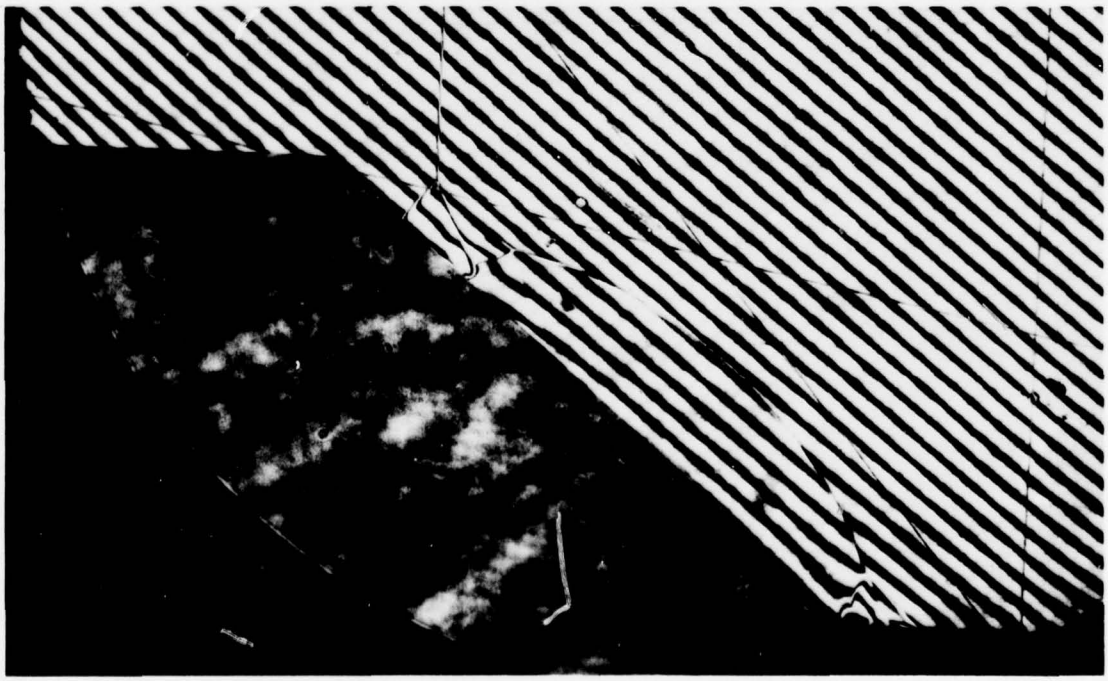

N43

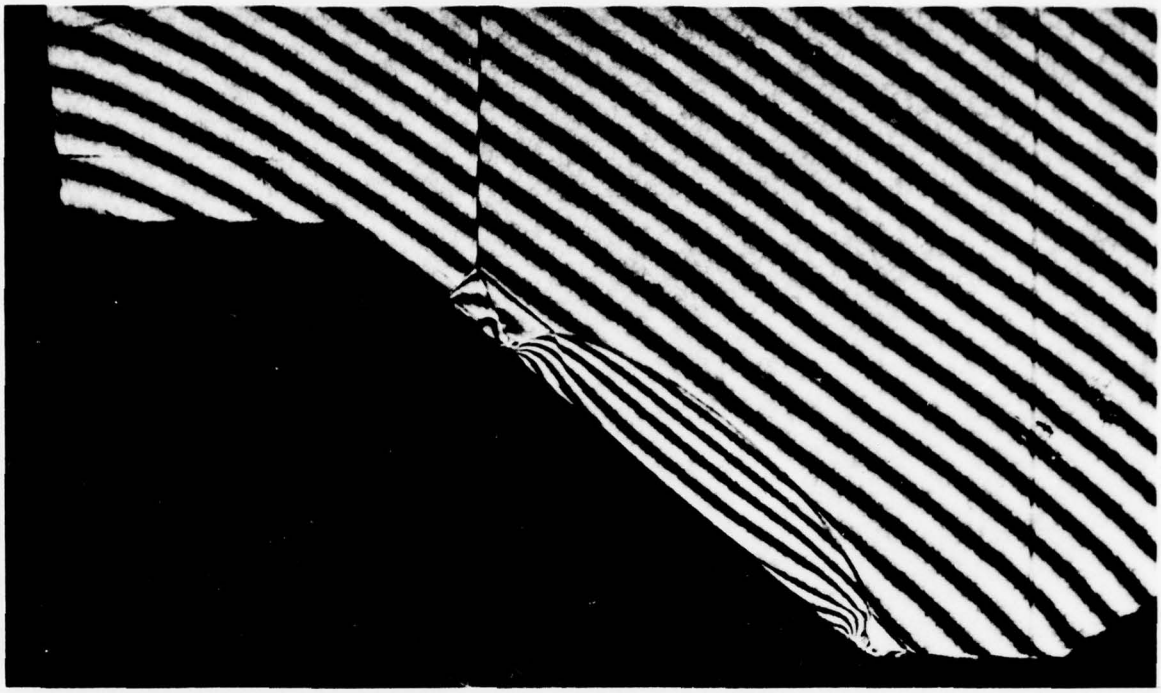

N44

N45

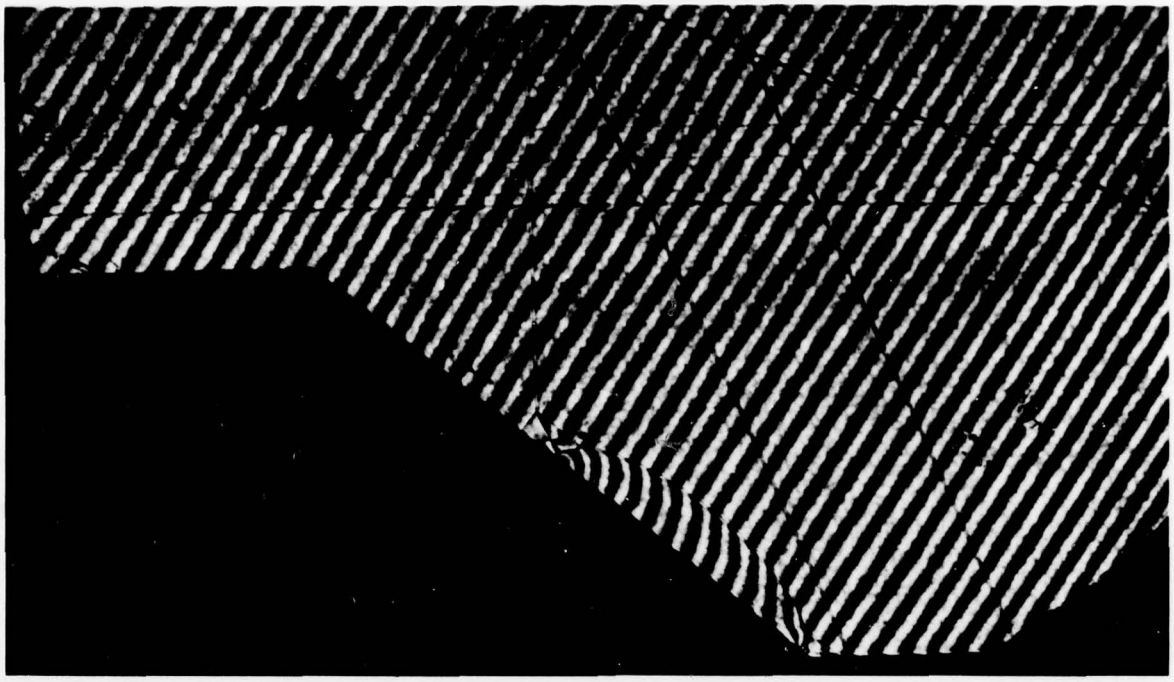

N46

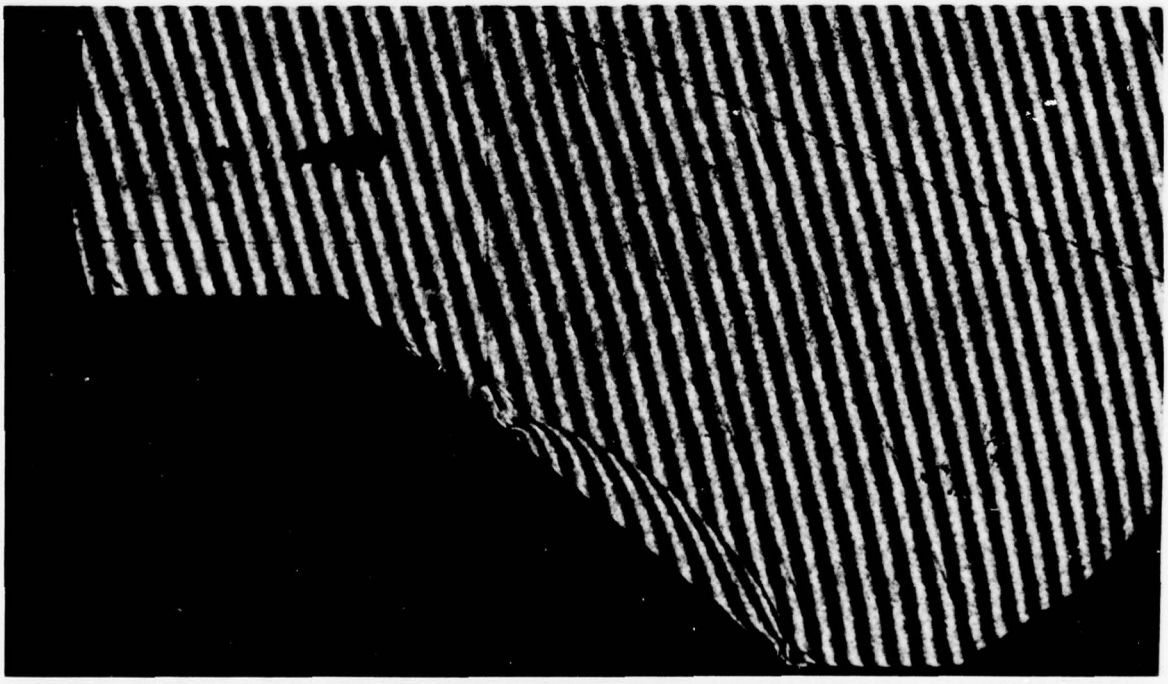

N47

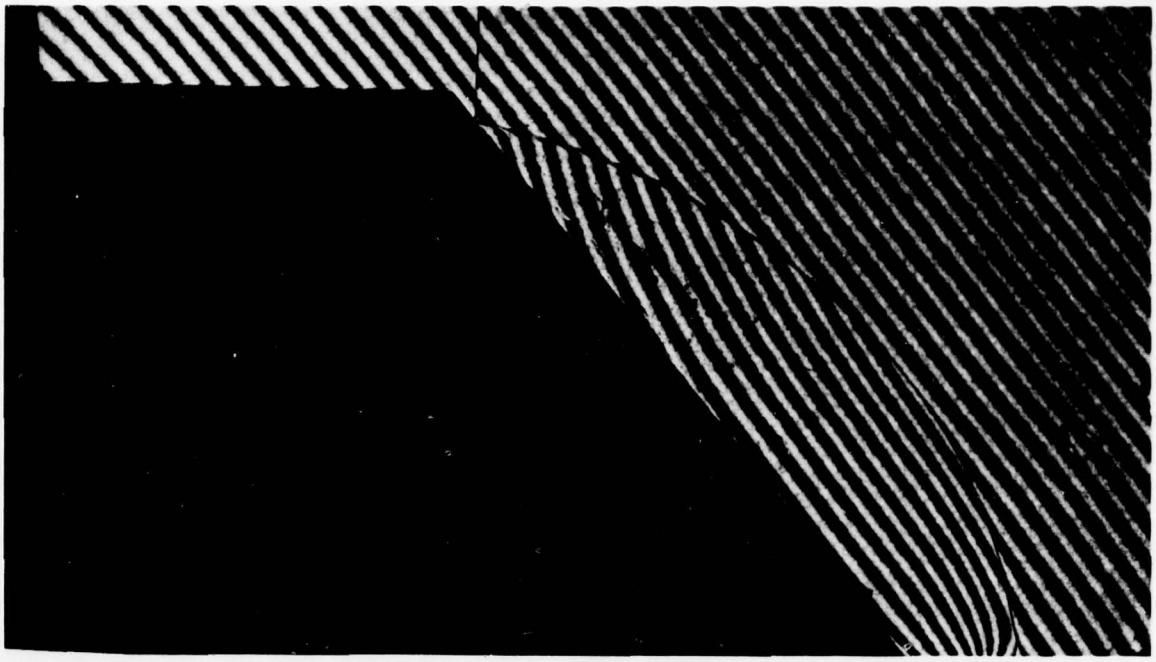

N48

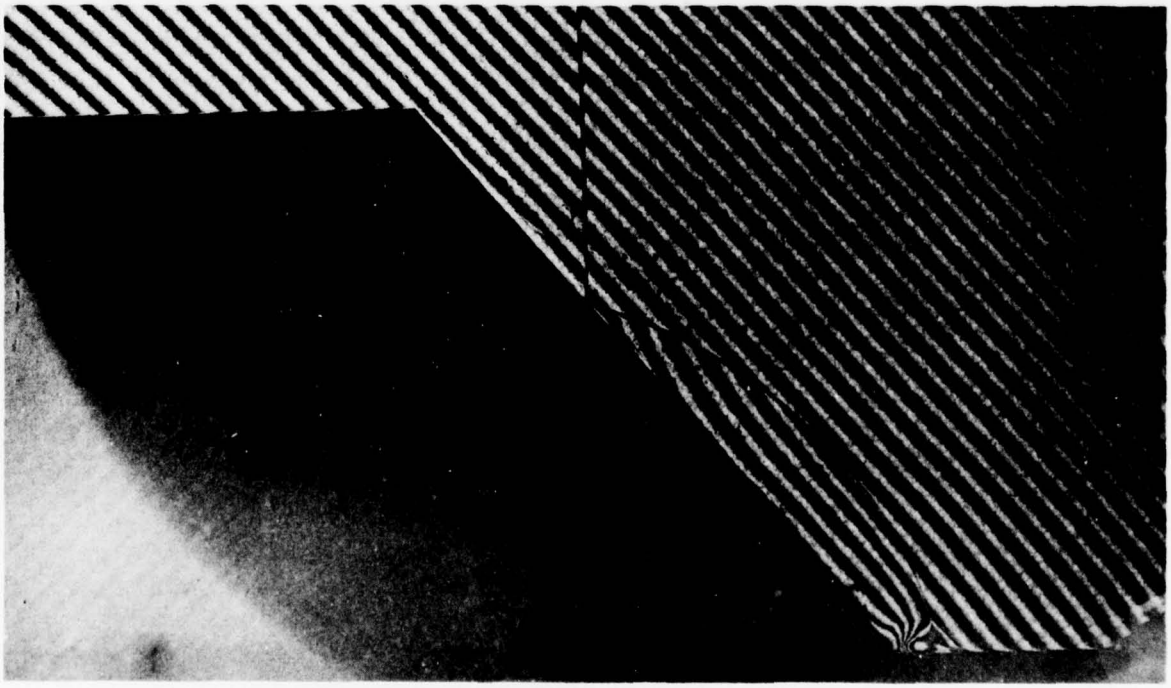

N49

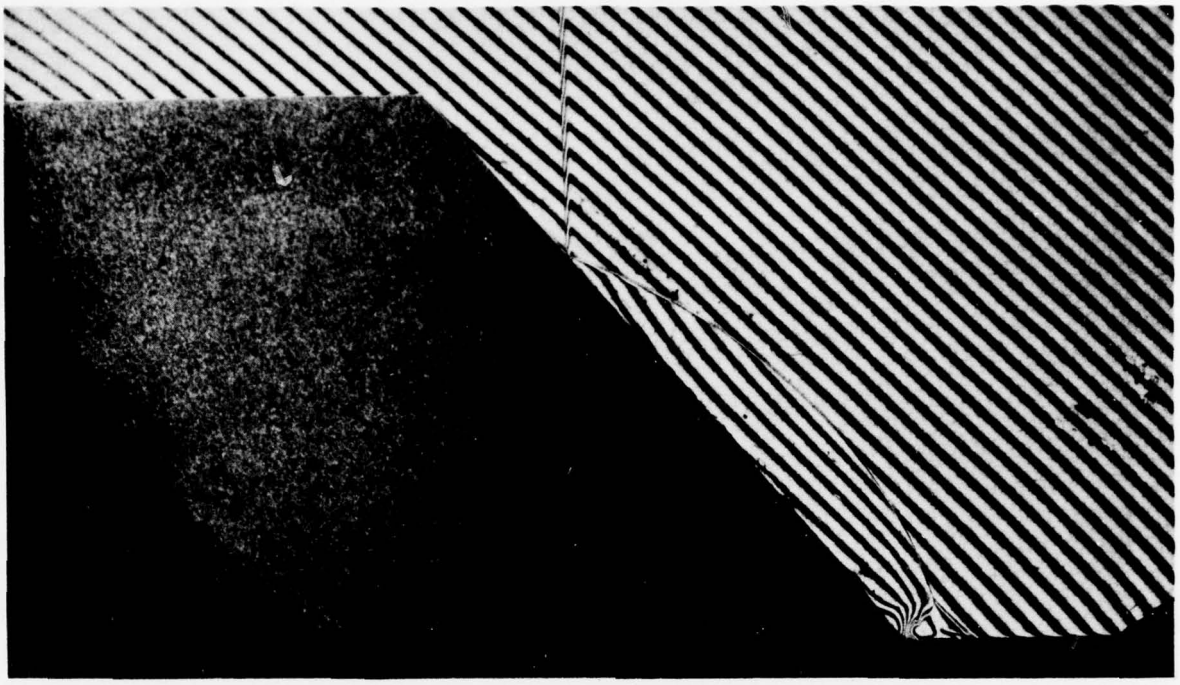

N50

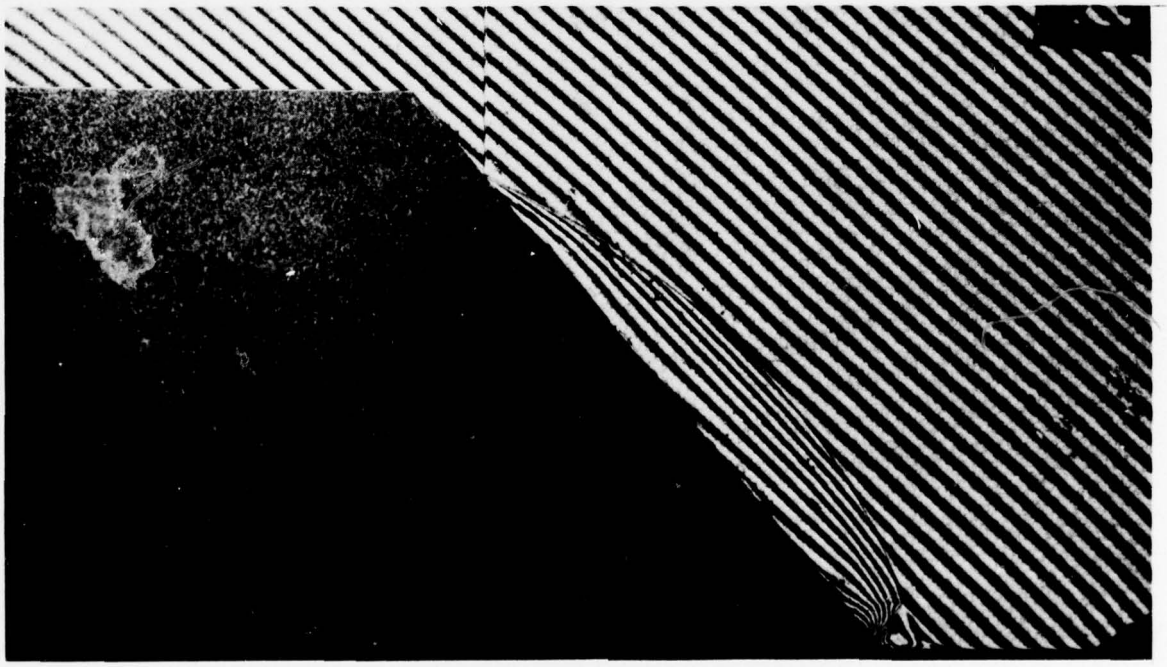

N51

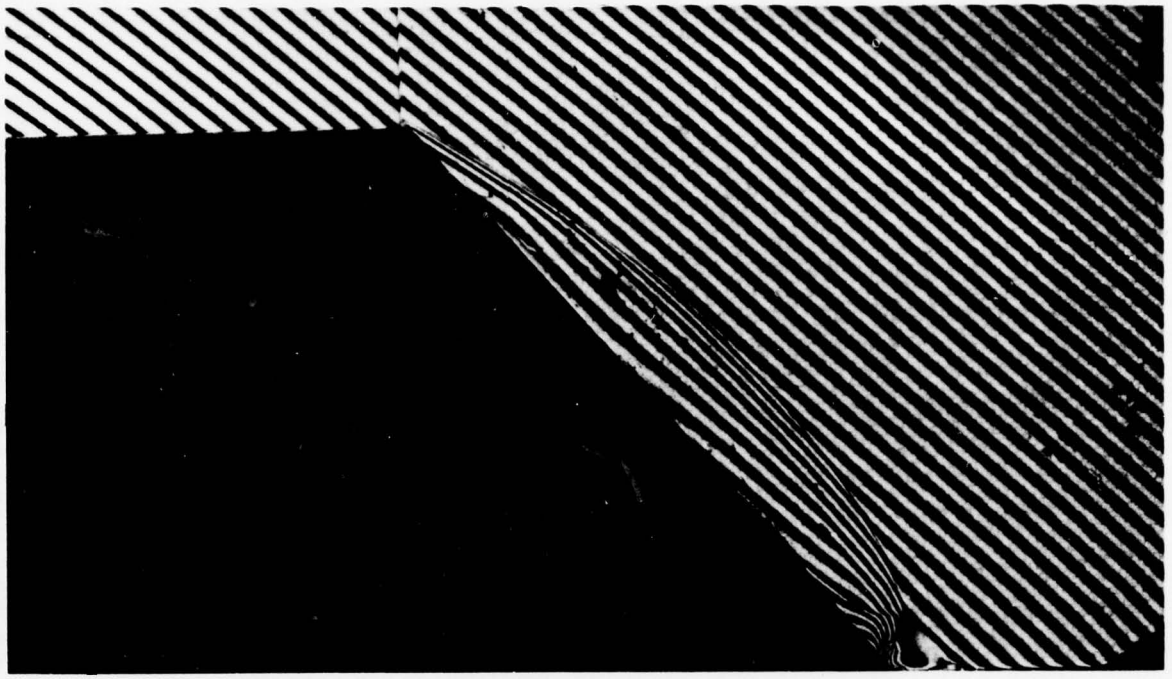

N52

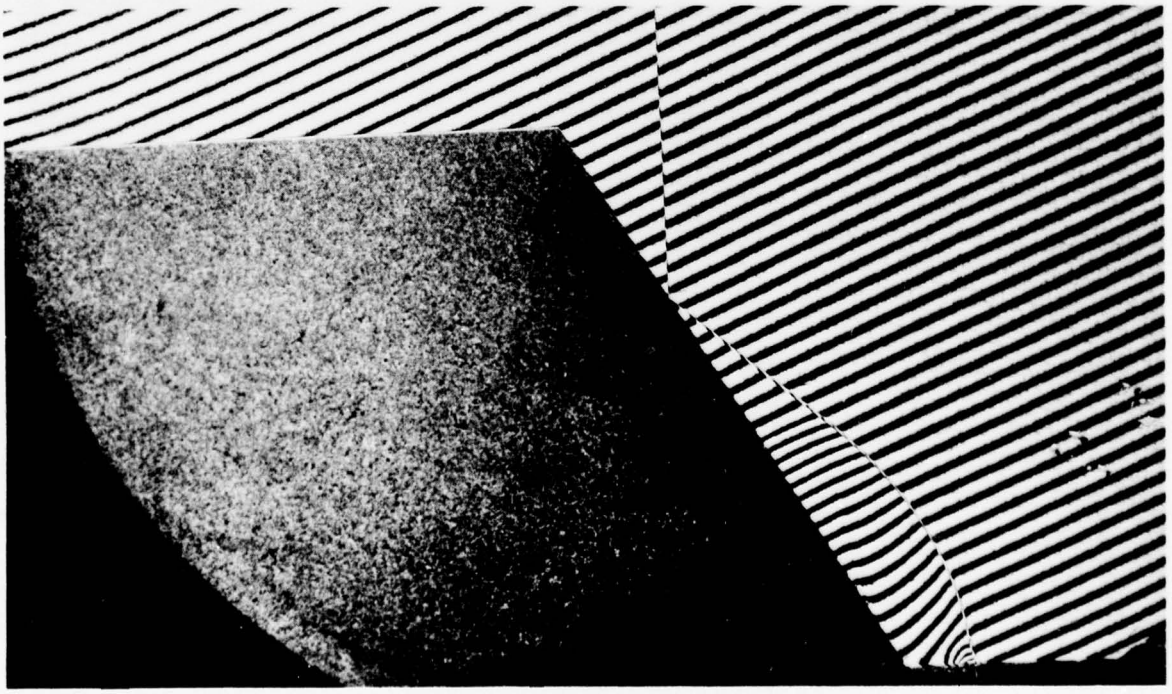

N53

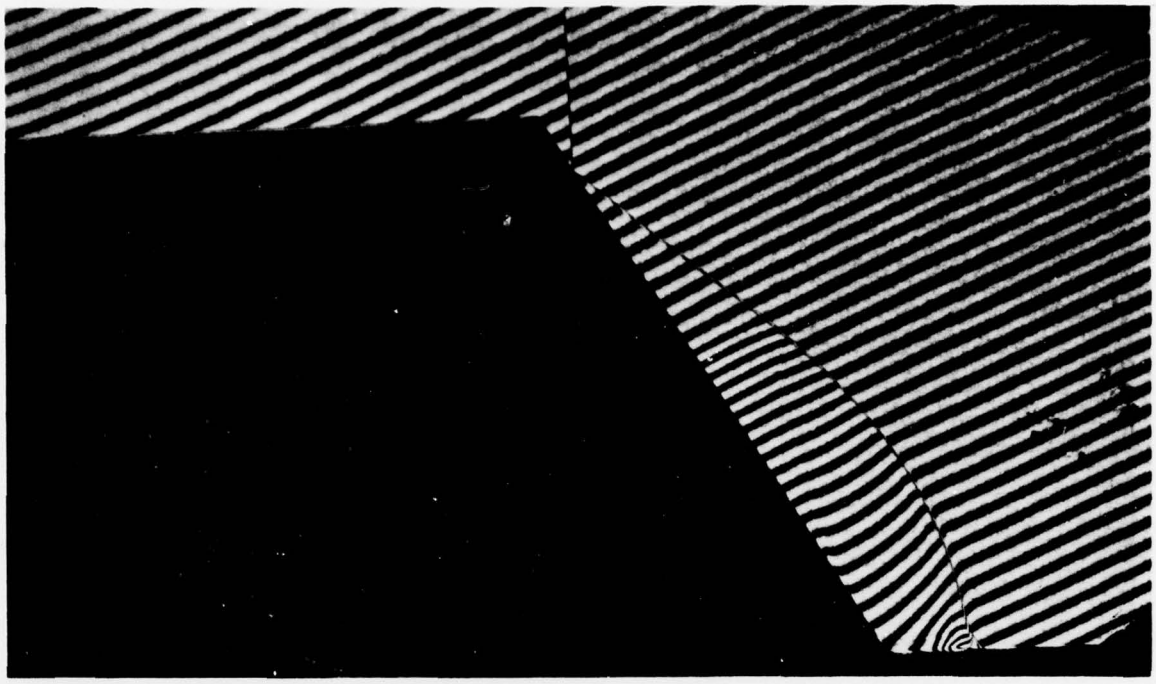

N54

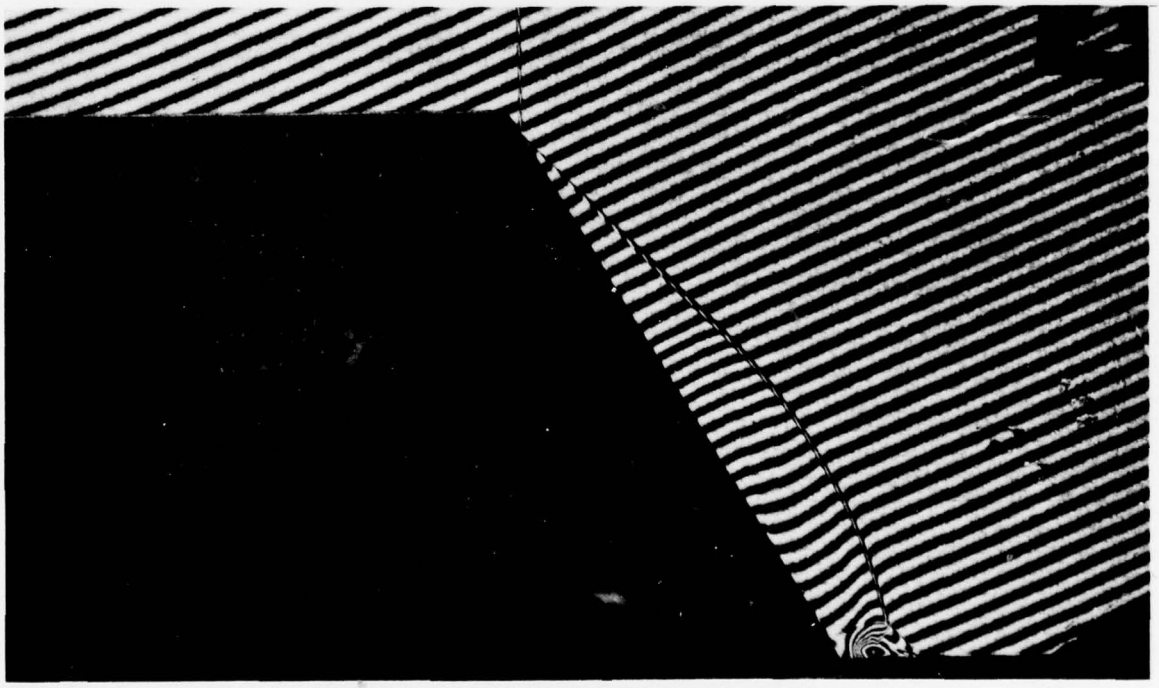

N55

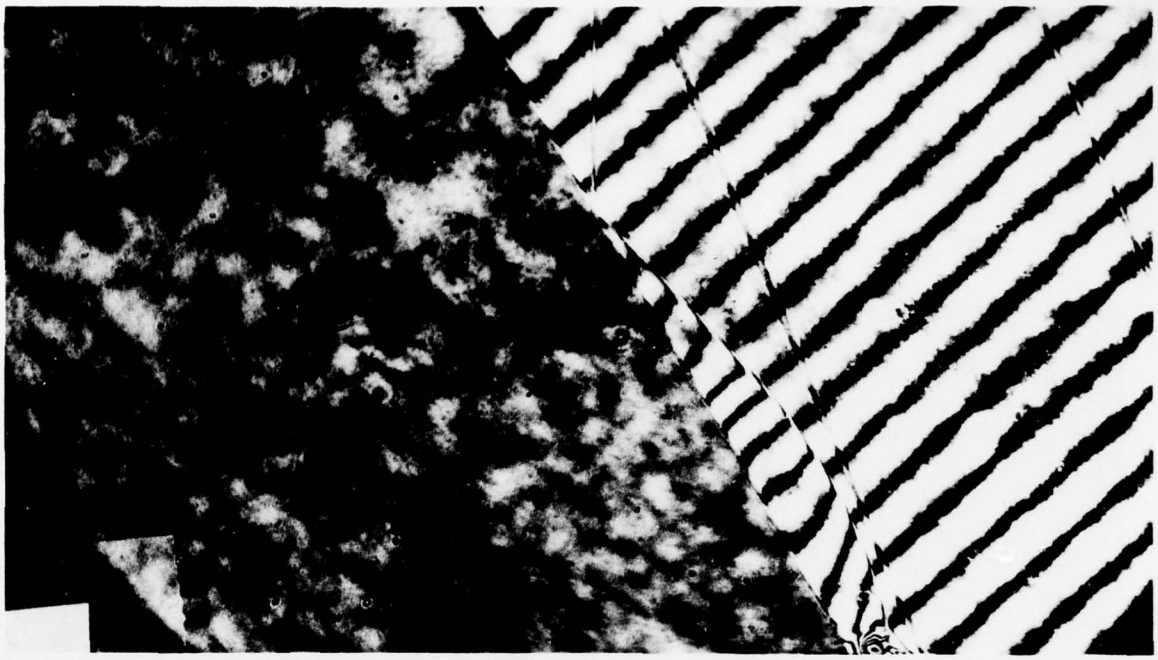

N56

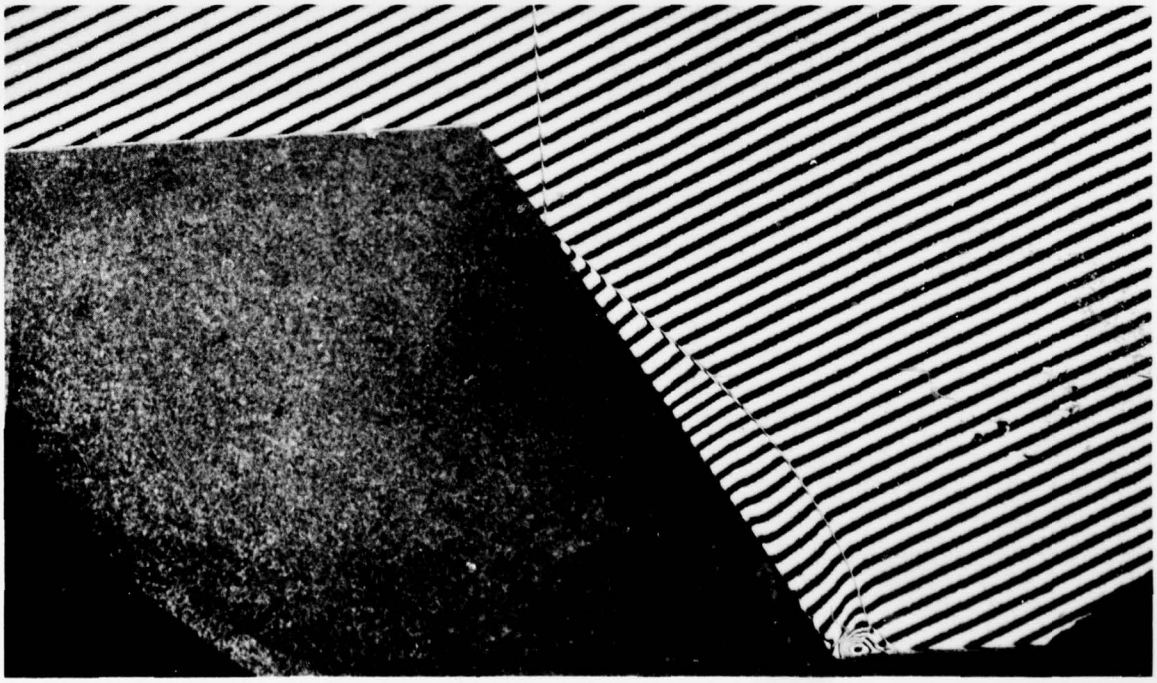

N57

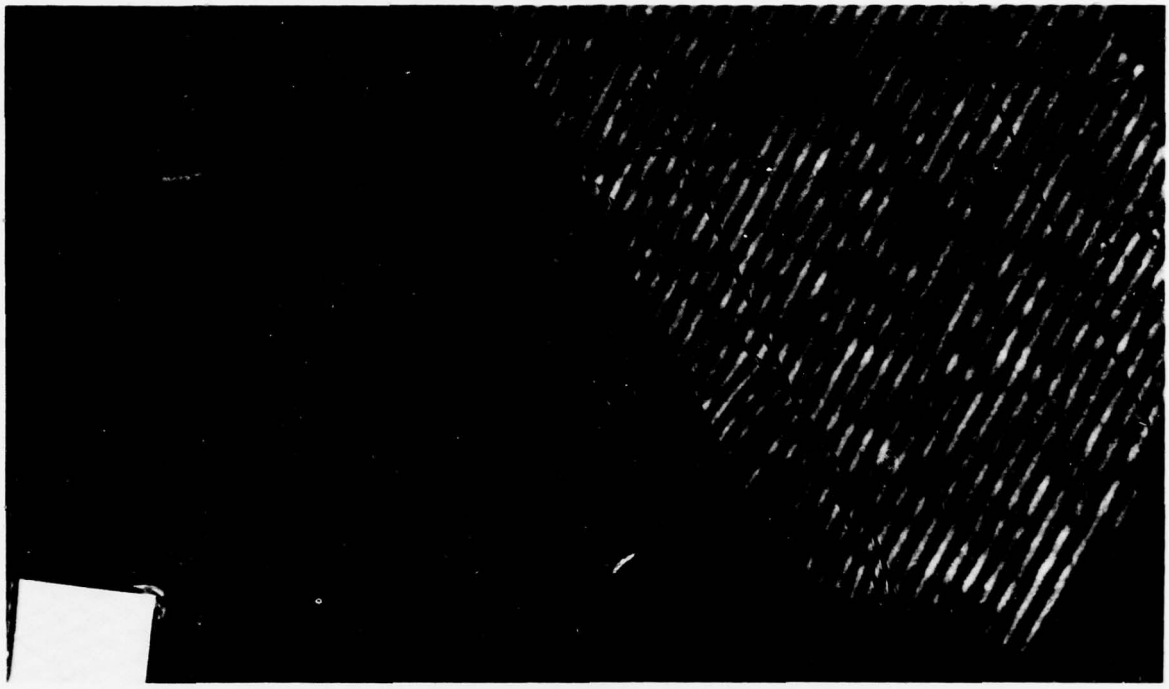

N58

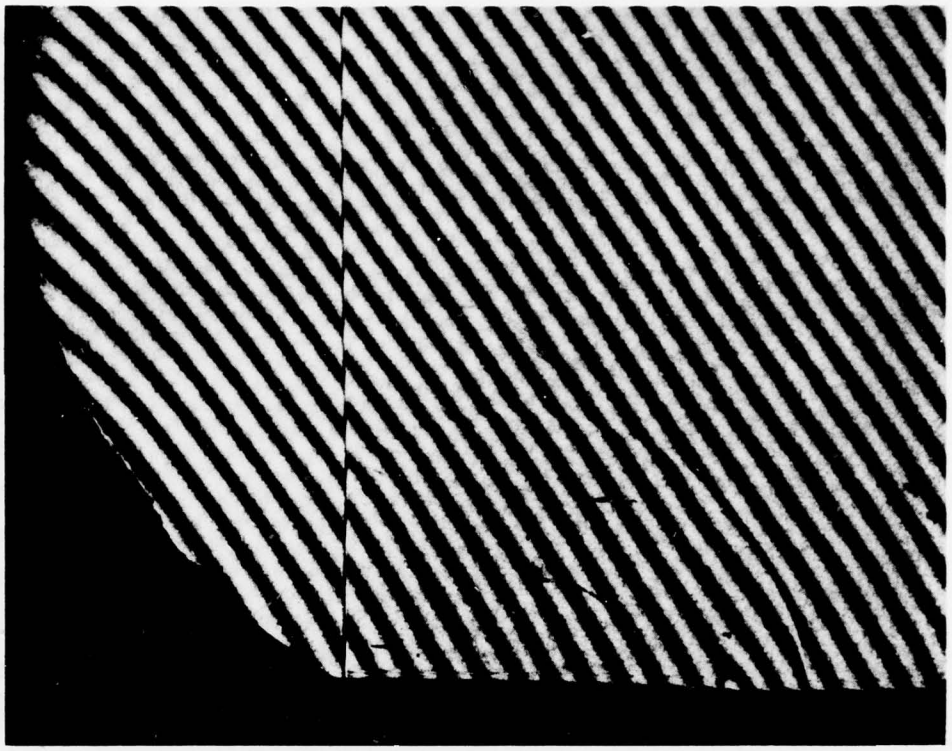

A1

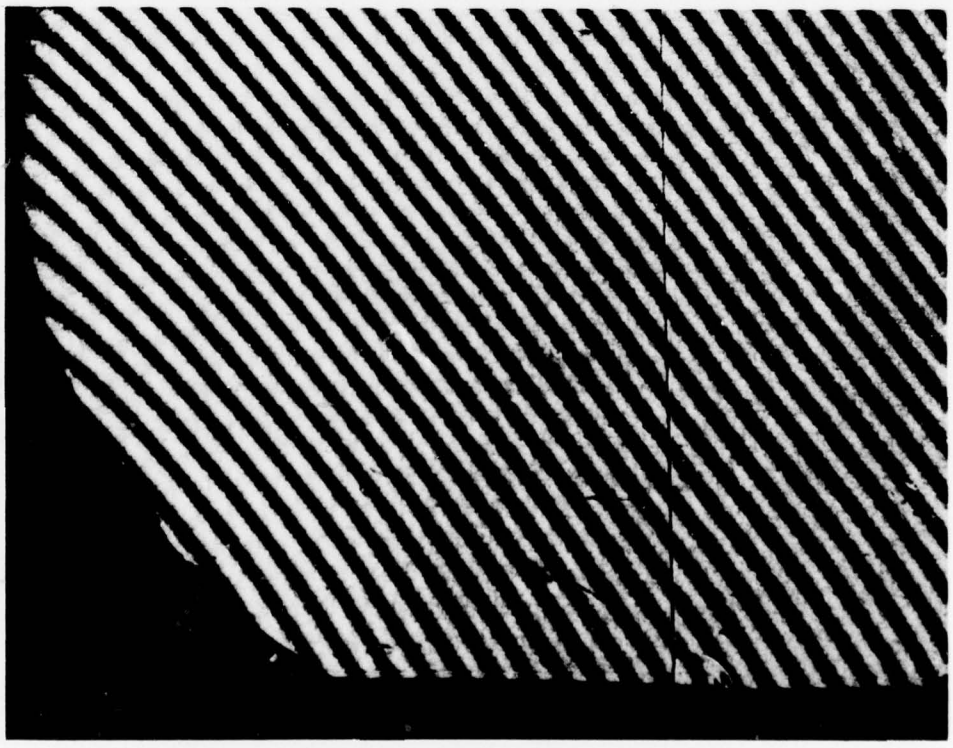

A2

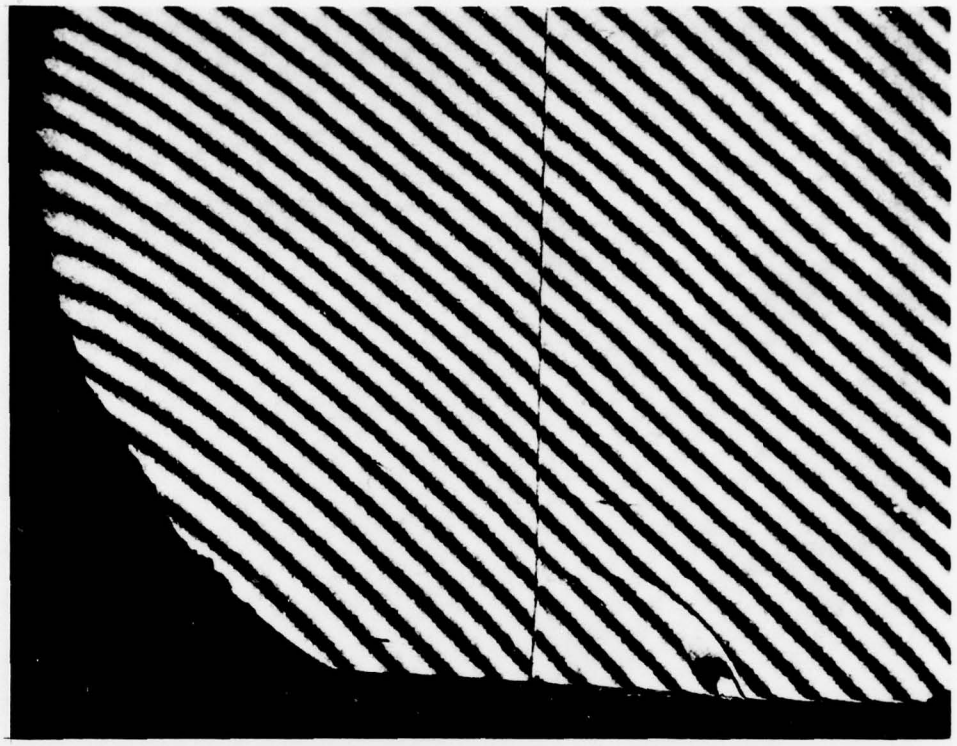

A3

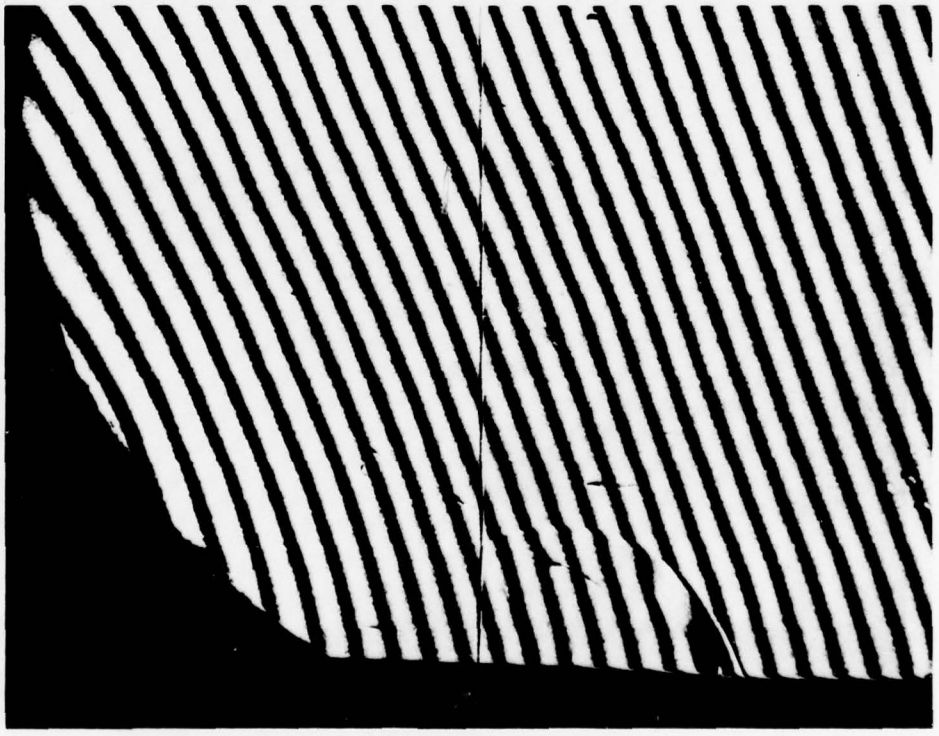

A4

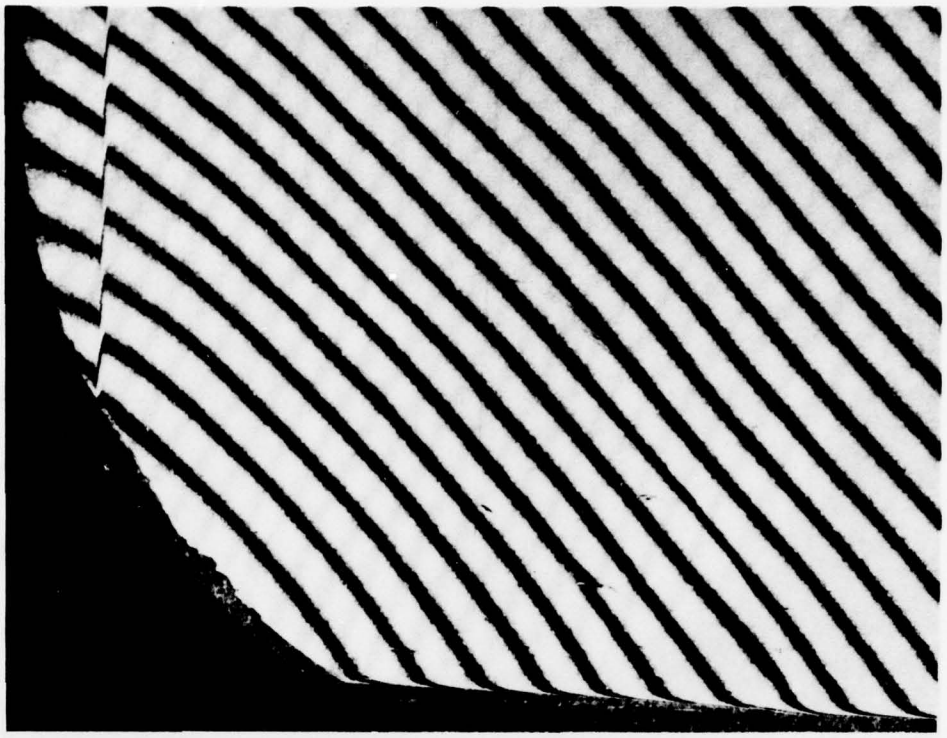

A5

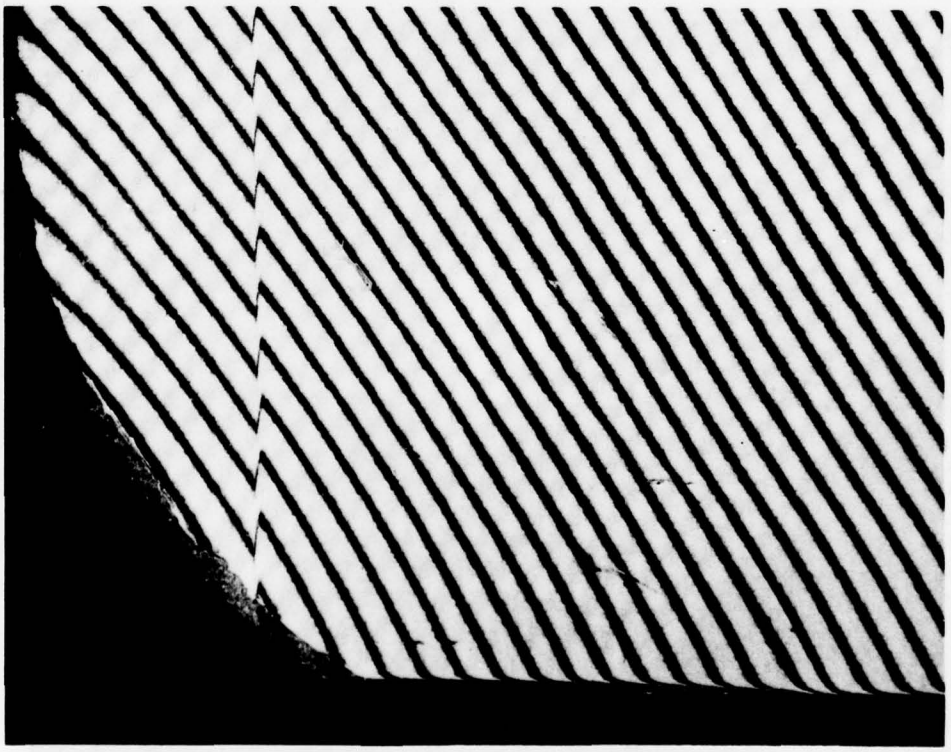

A6

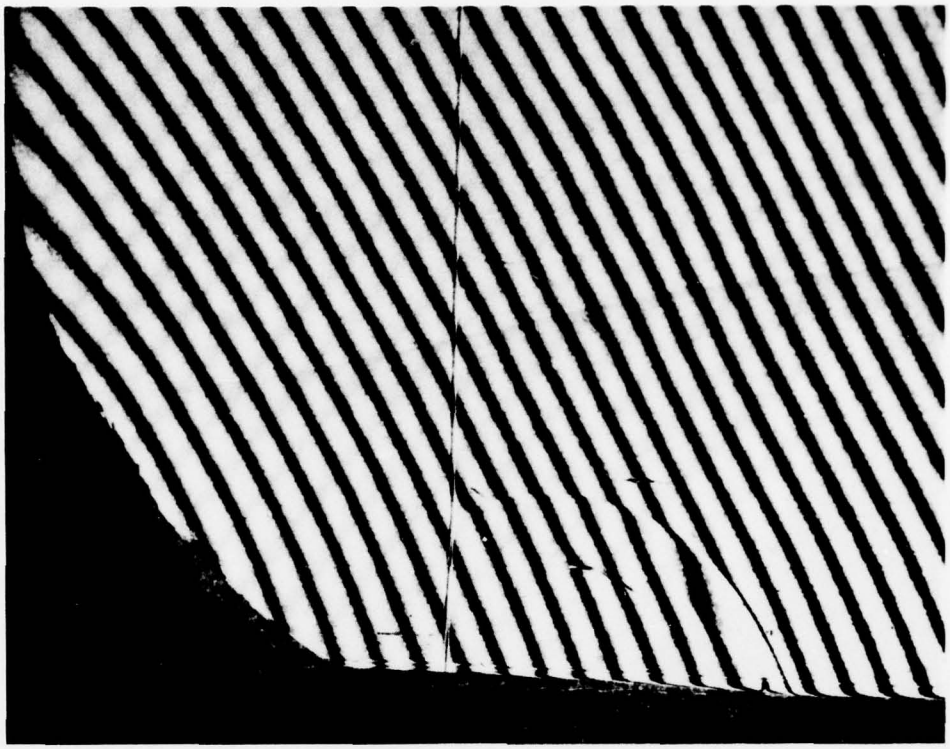

A7

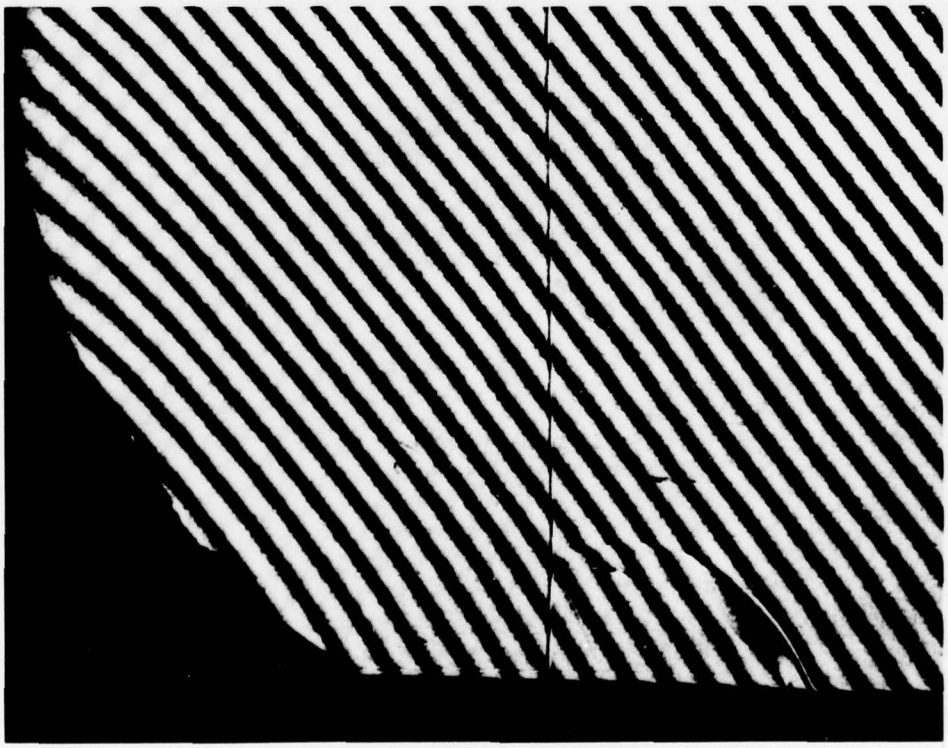

A8

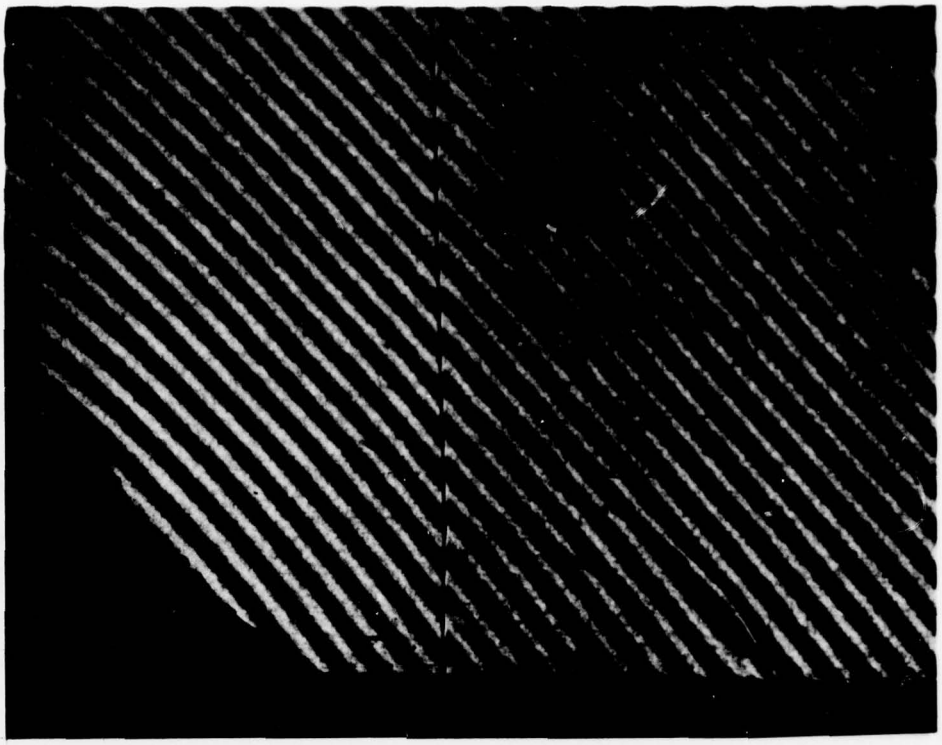

A9

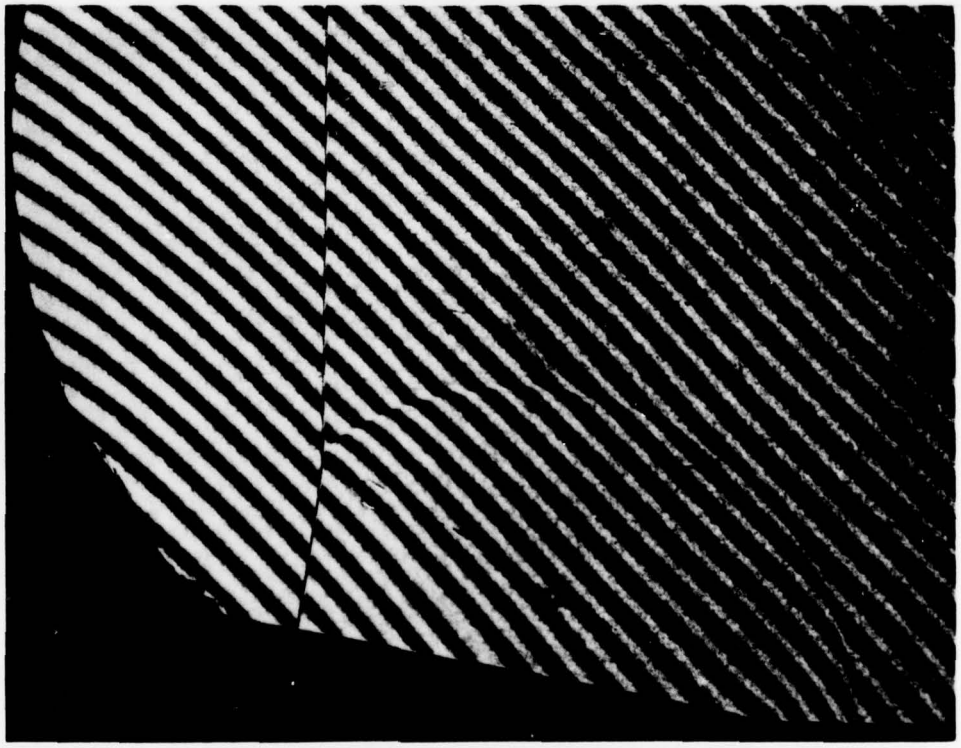

A10

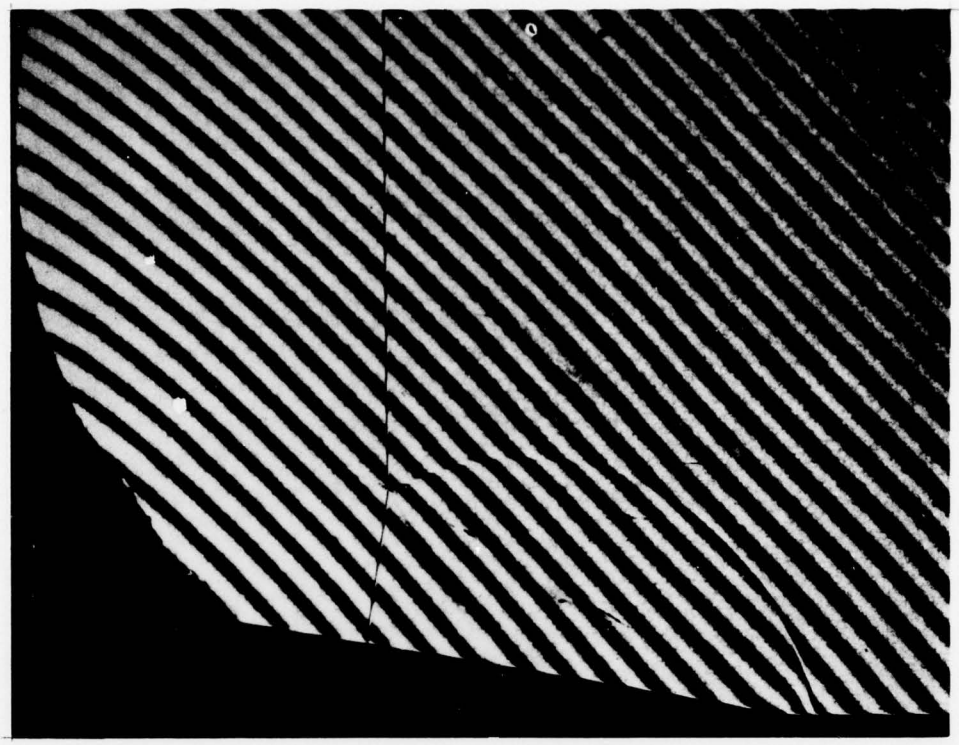

A11

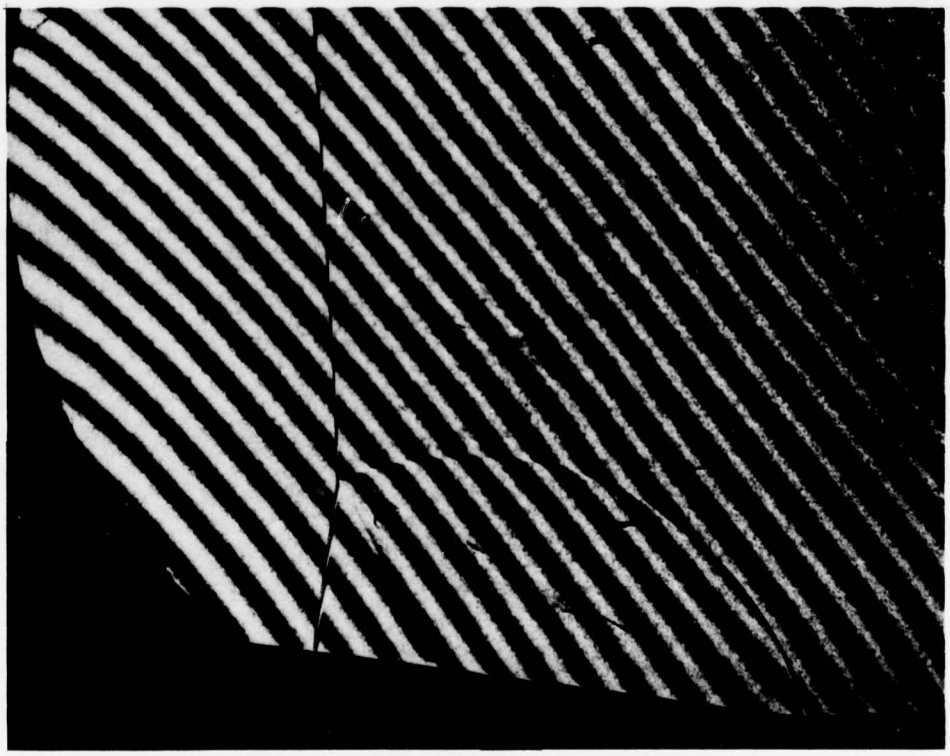

A12

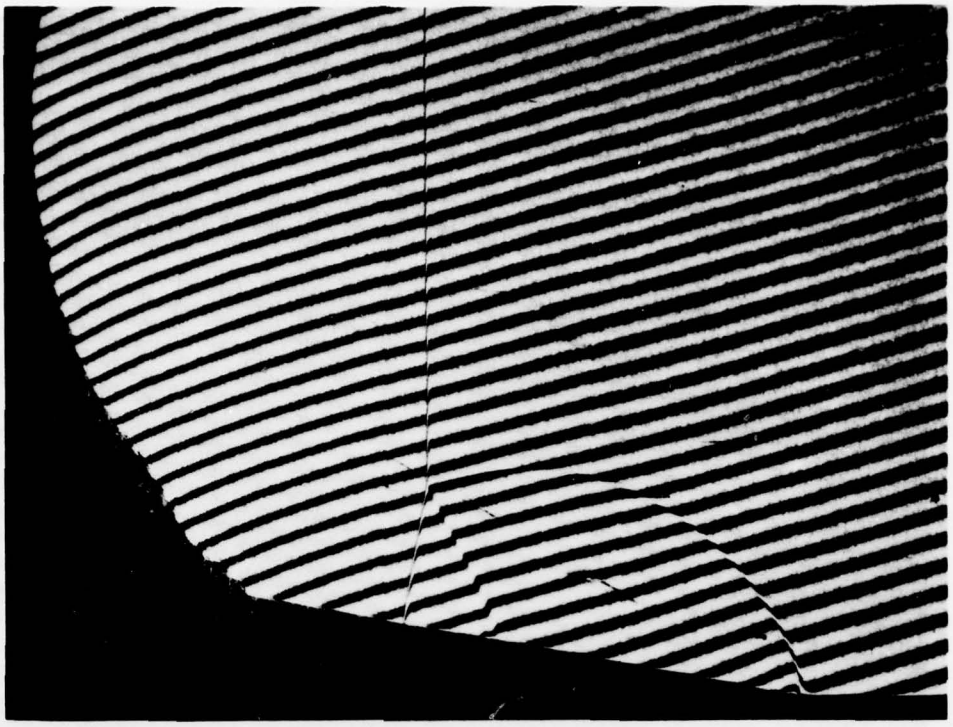

A13

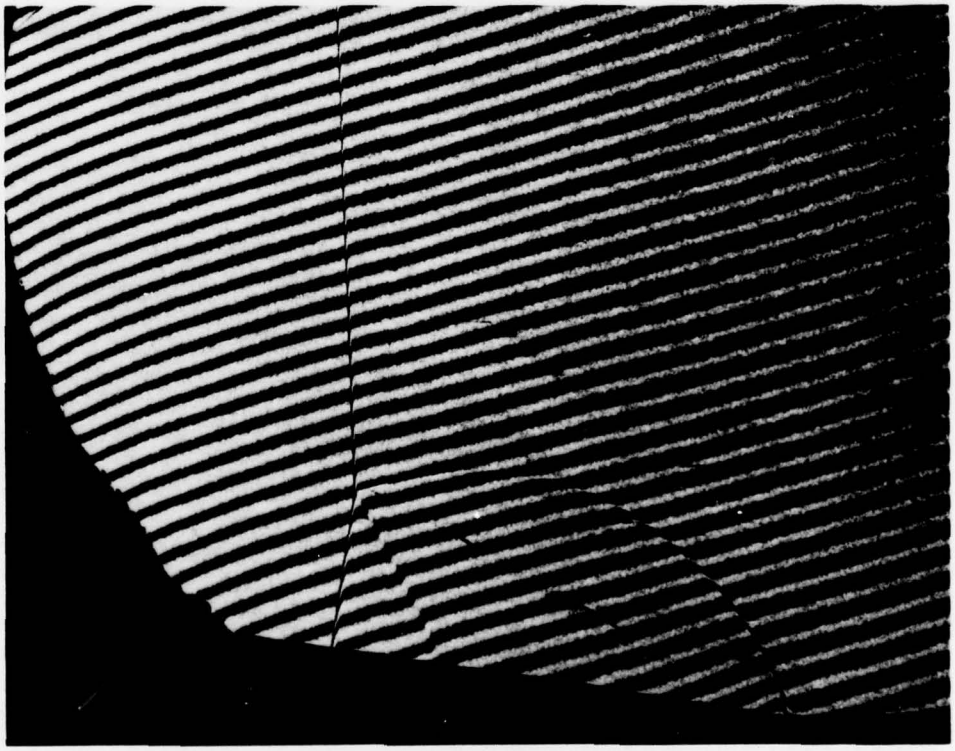

A14

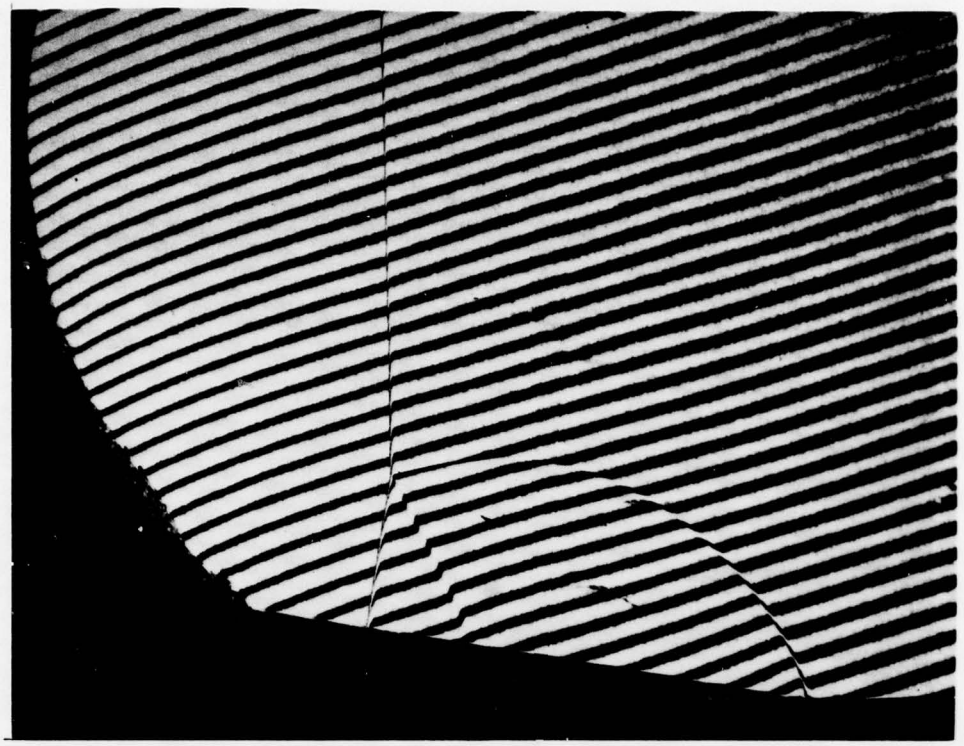

A15

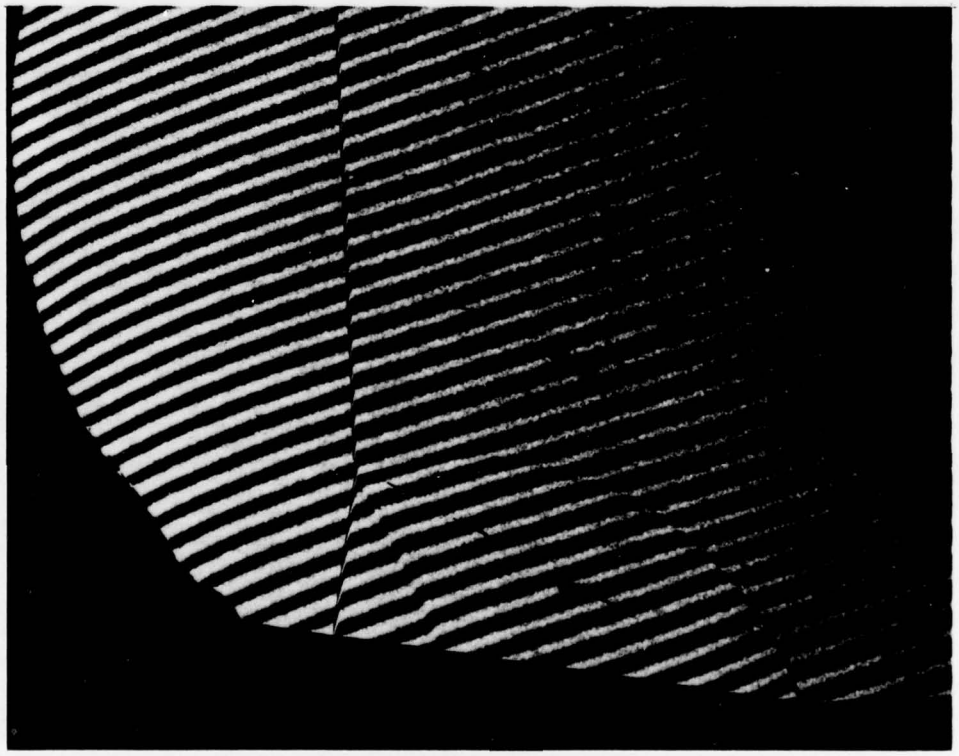

A16

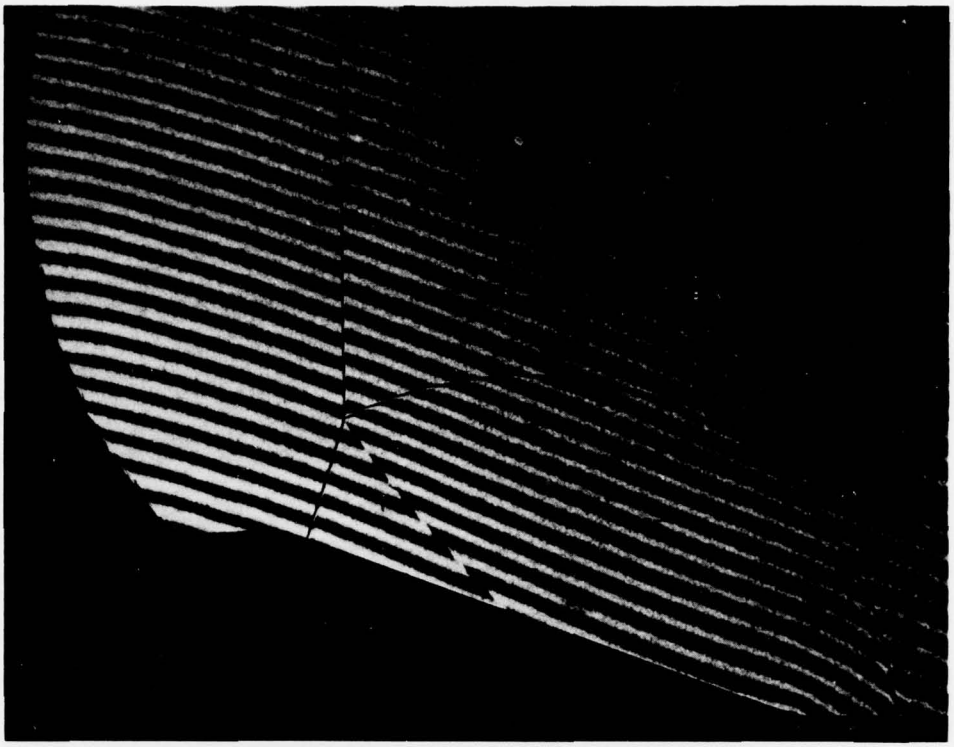

A17

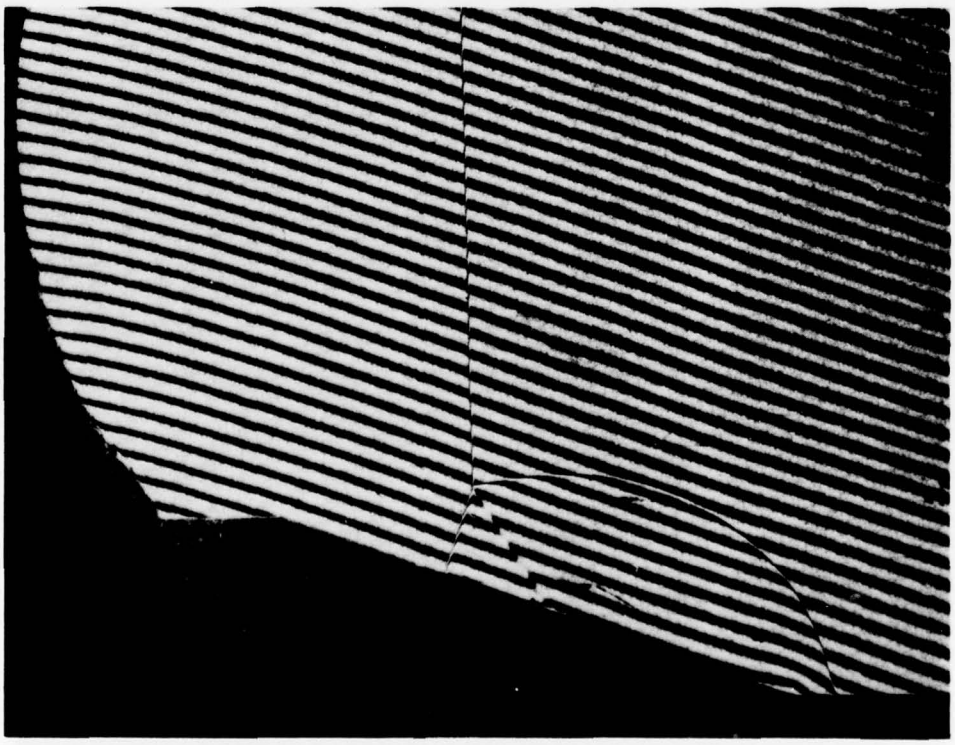

A18

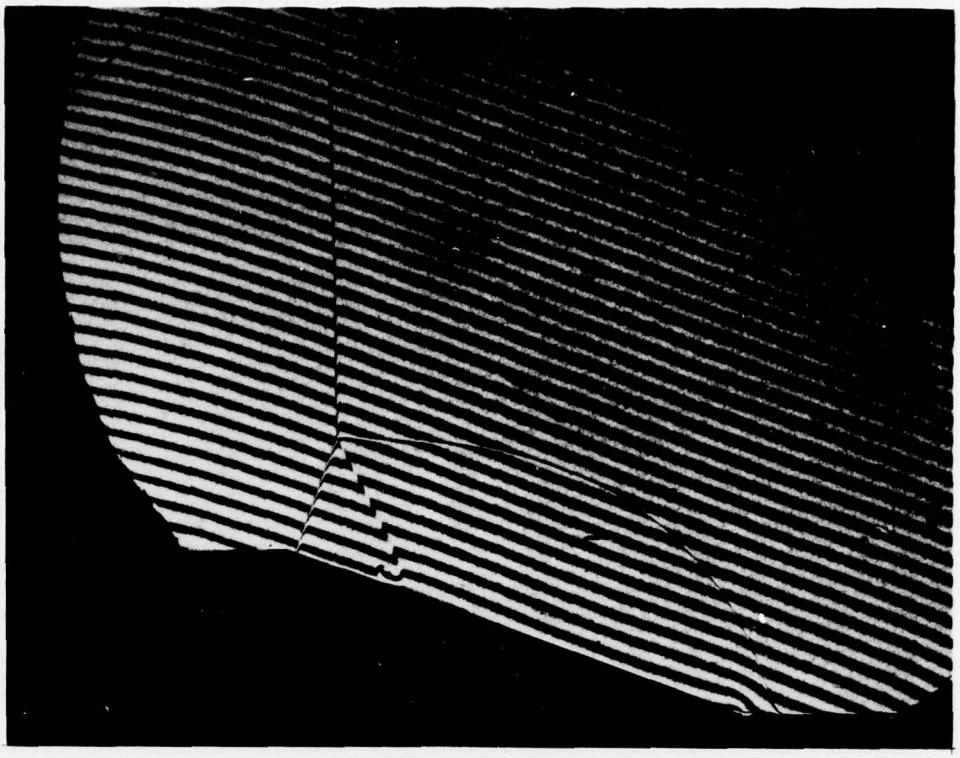

A19

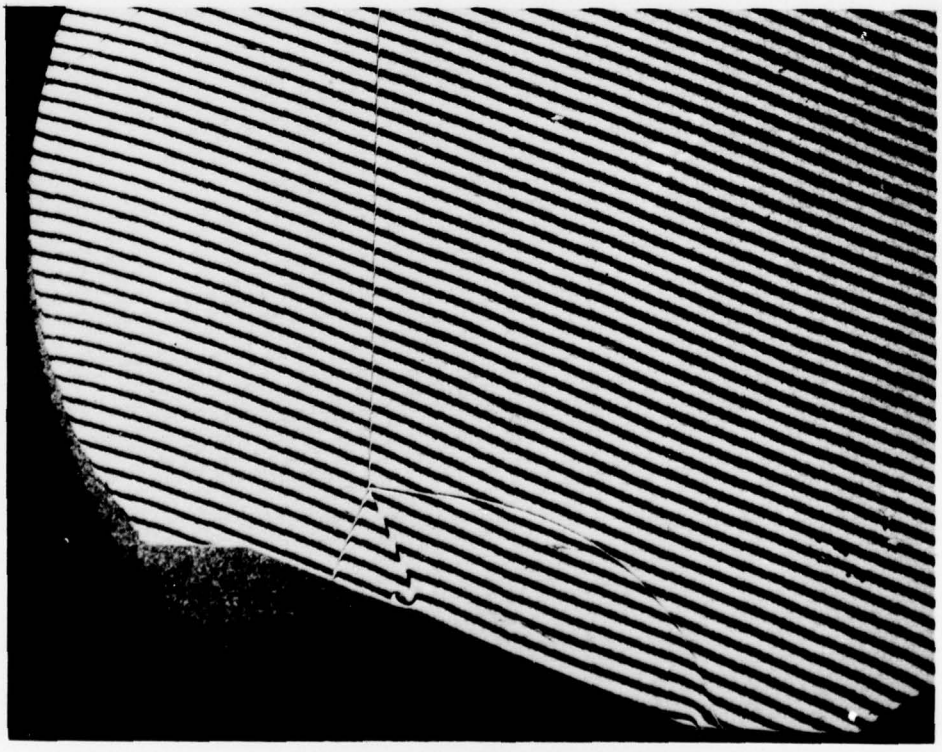

A20

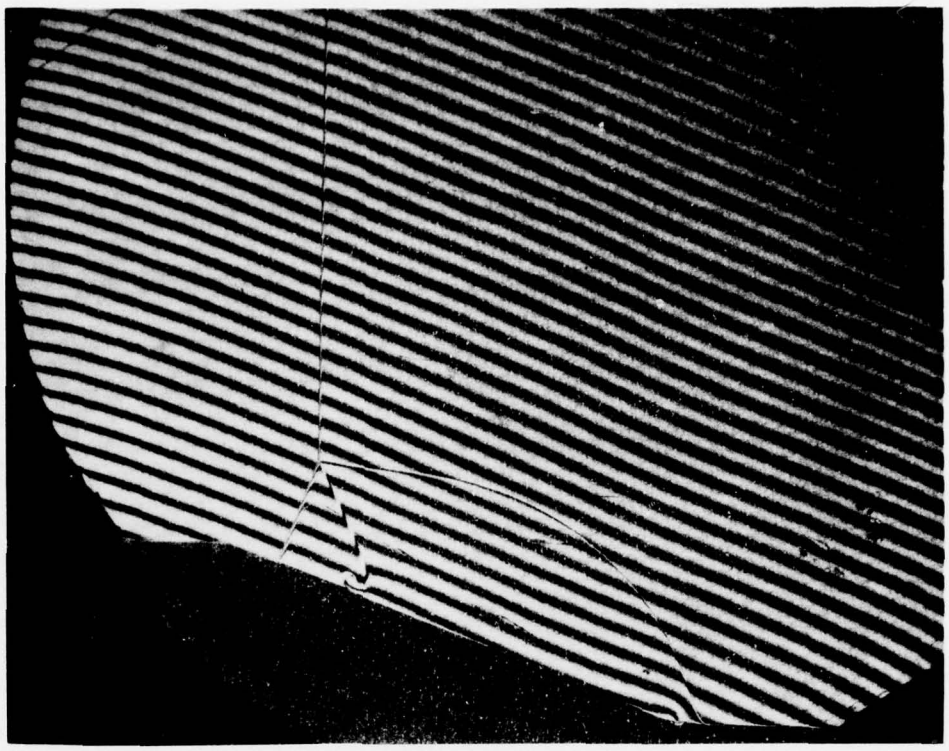

A21

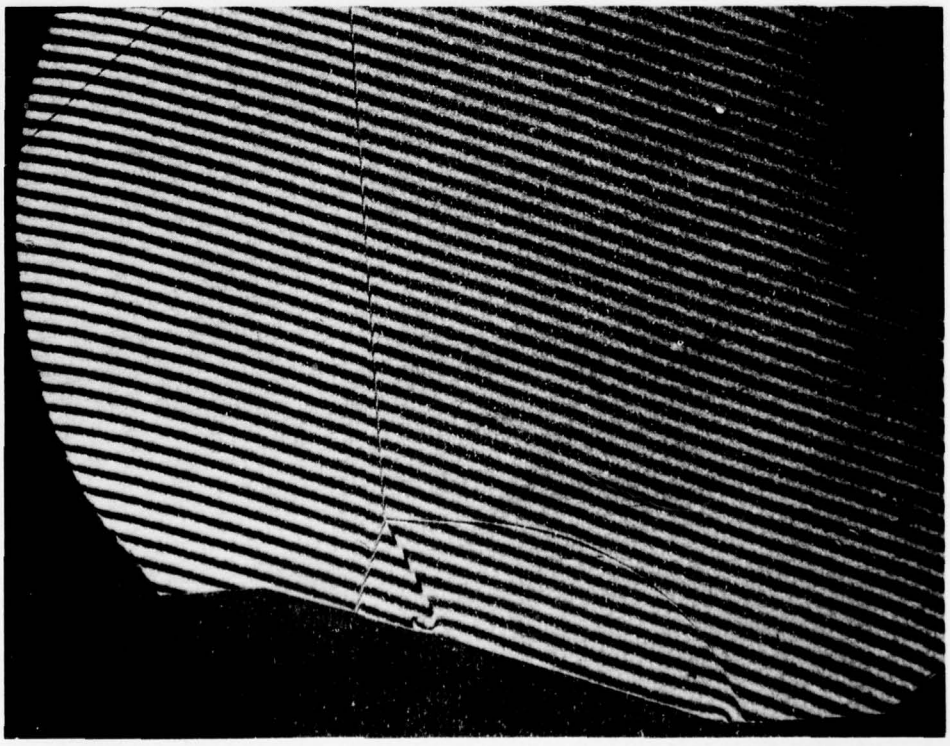

A22

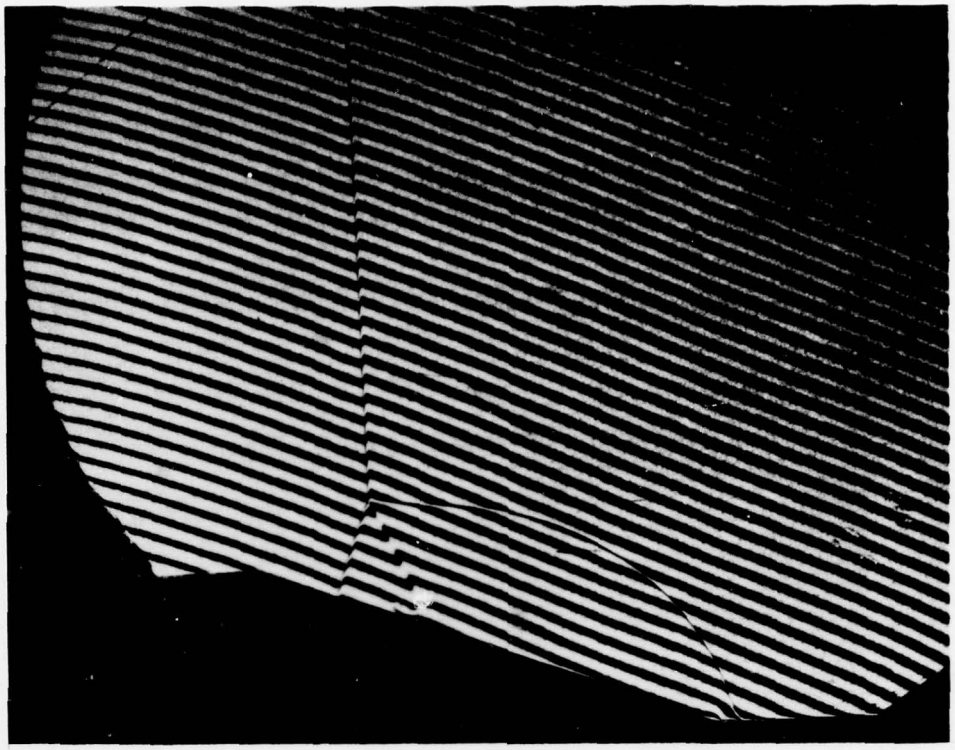

A23

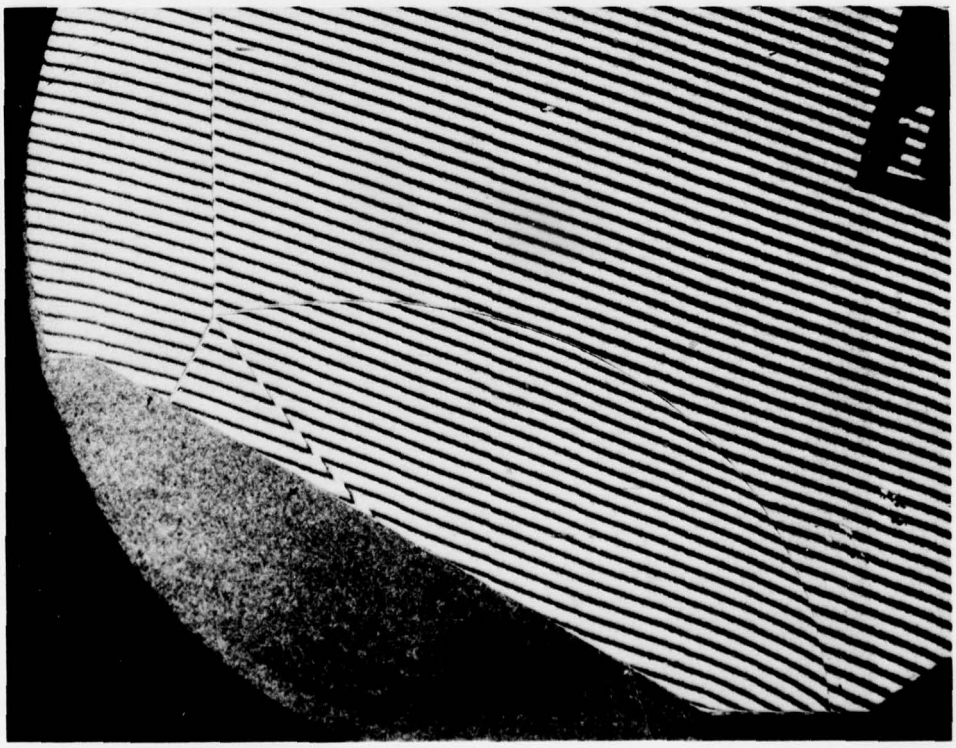

A24

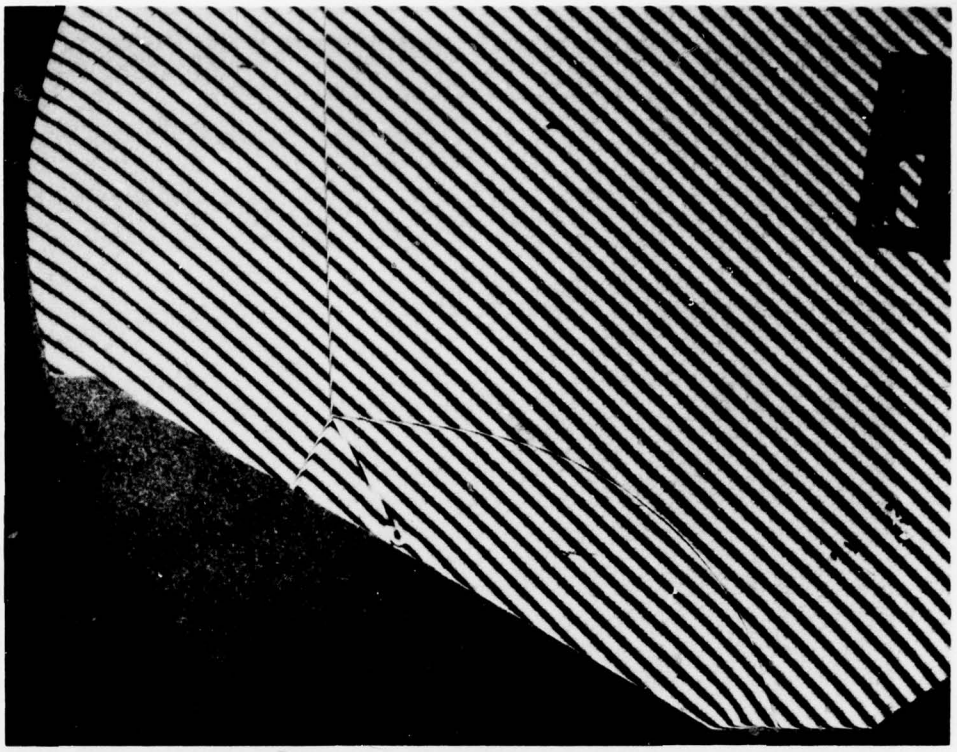

A25

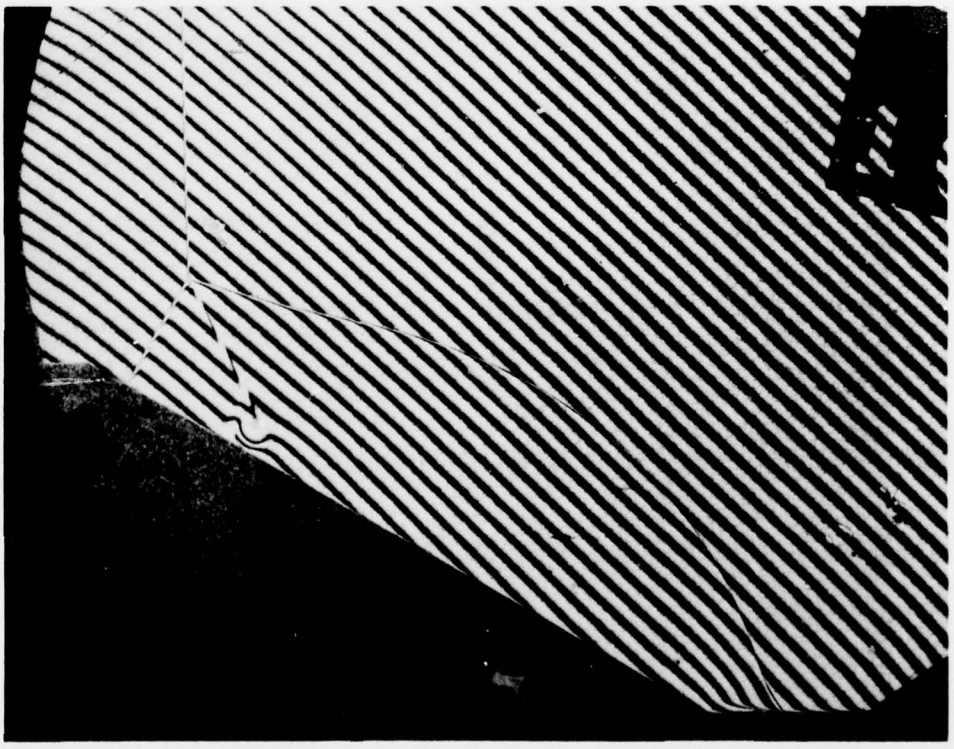

A26

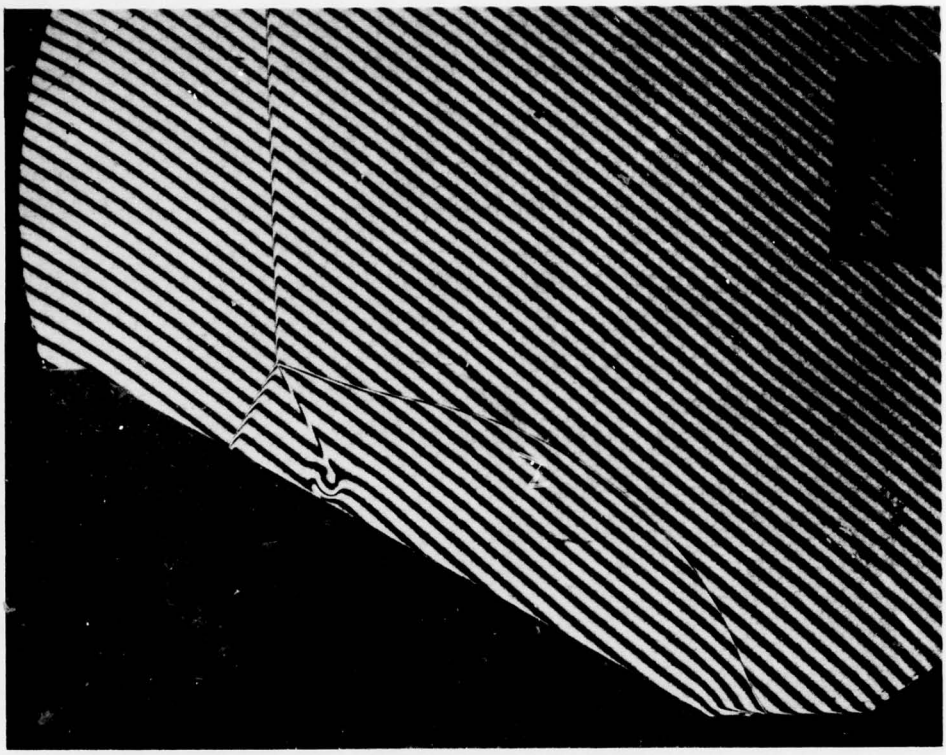

A27

A28

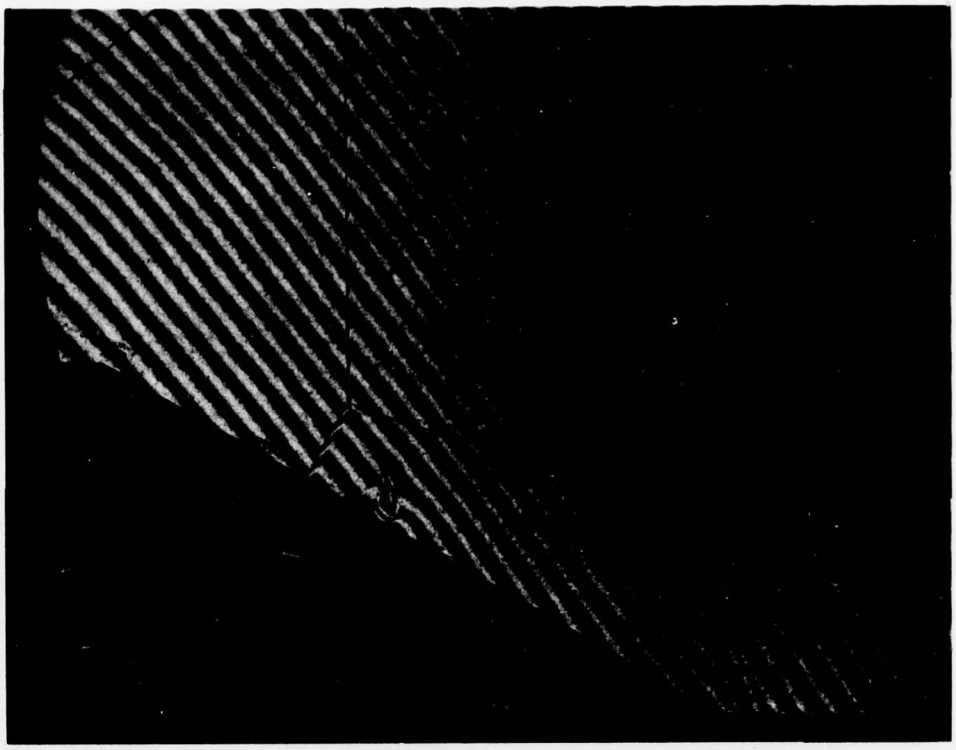

A29

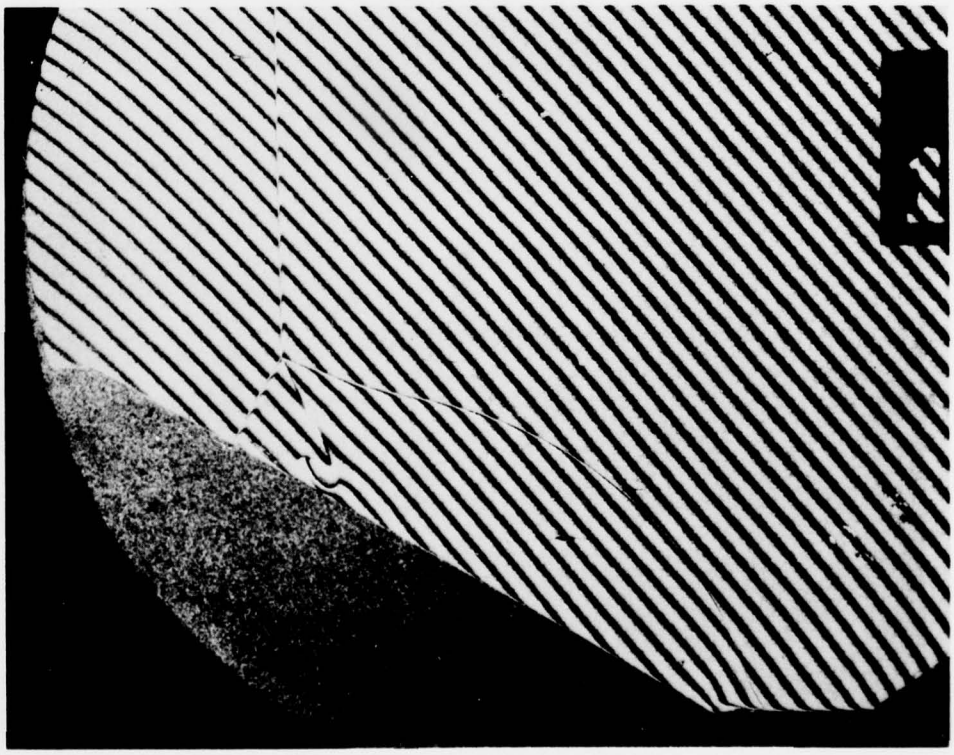

A30

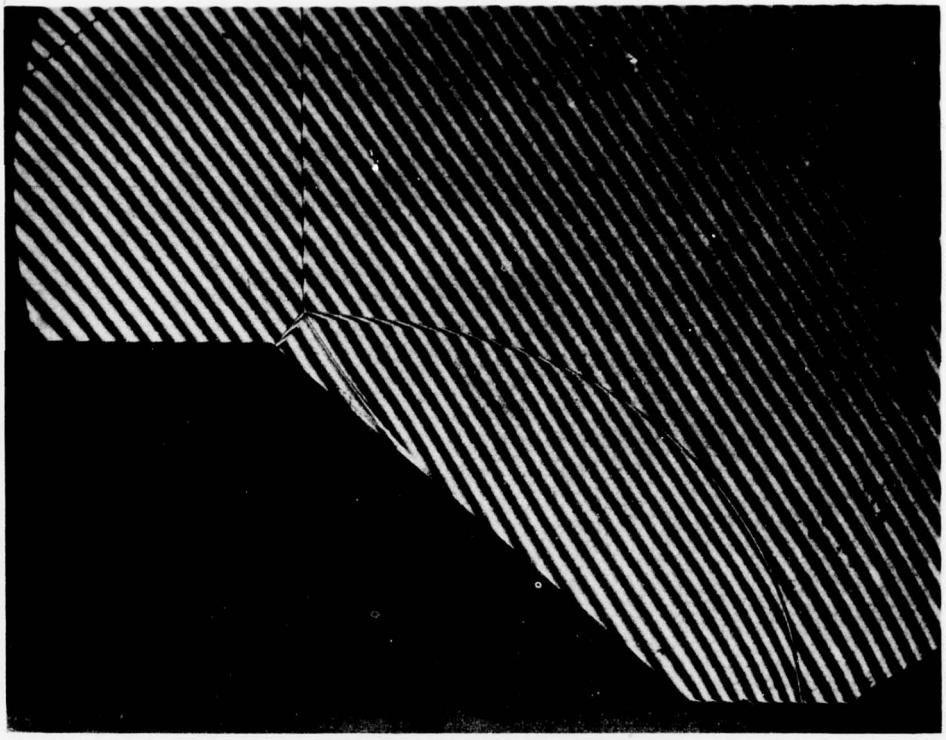

A31

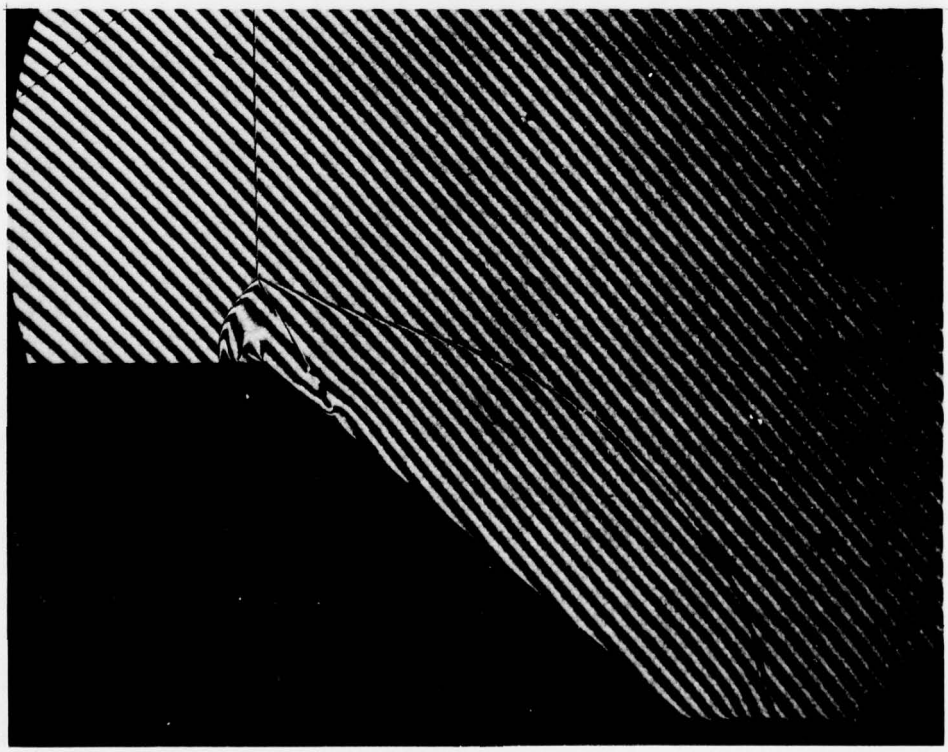

A32

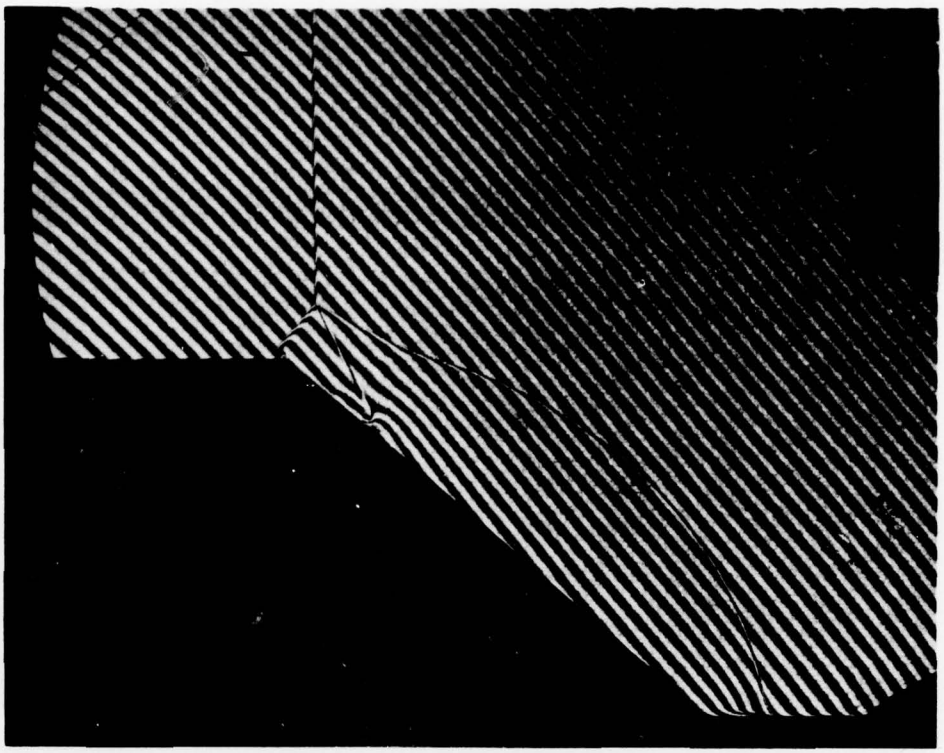

A33

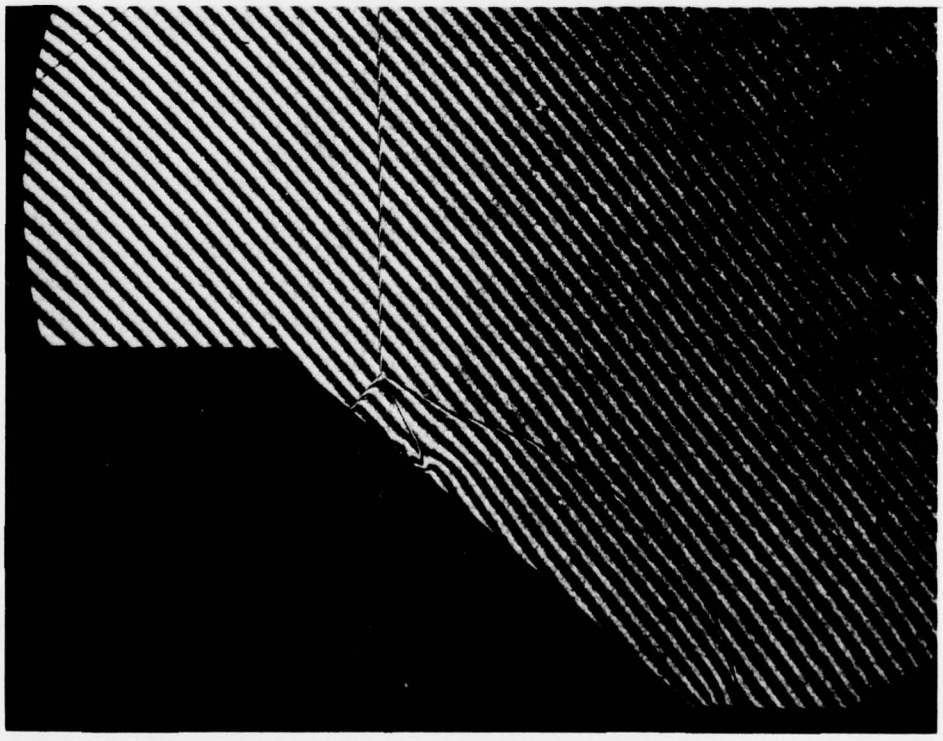

A34

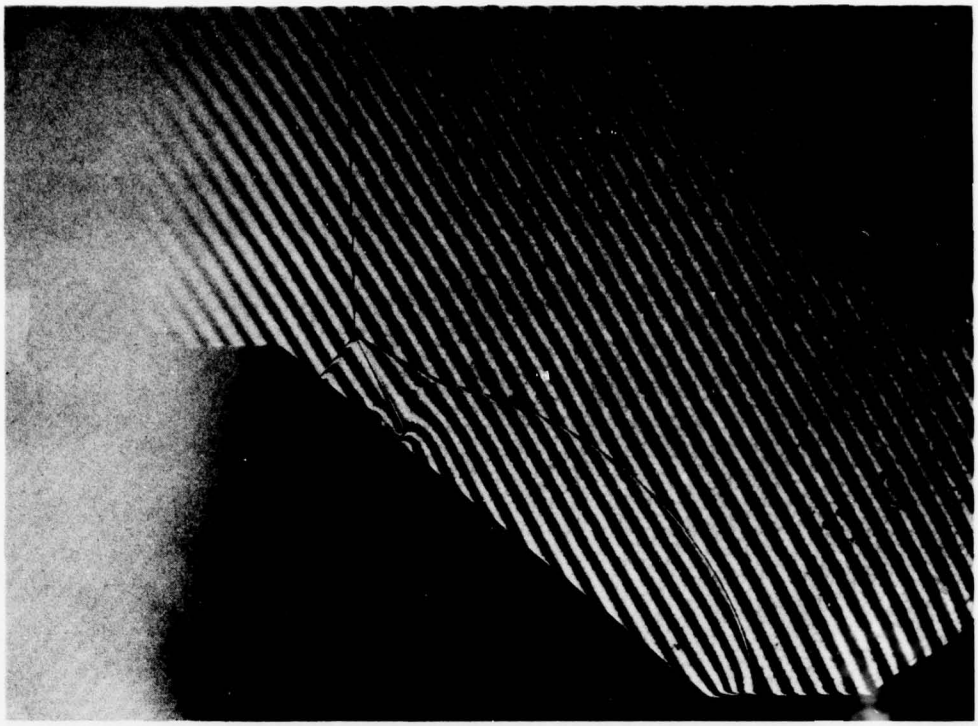

A35

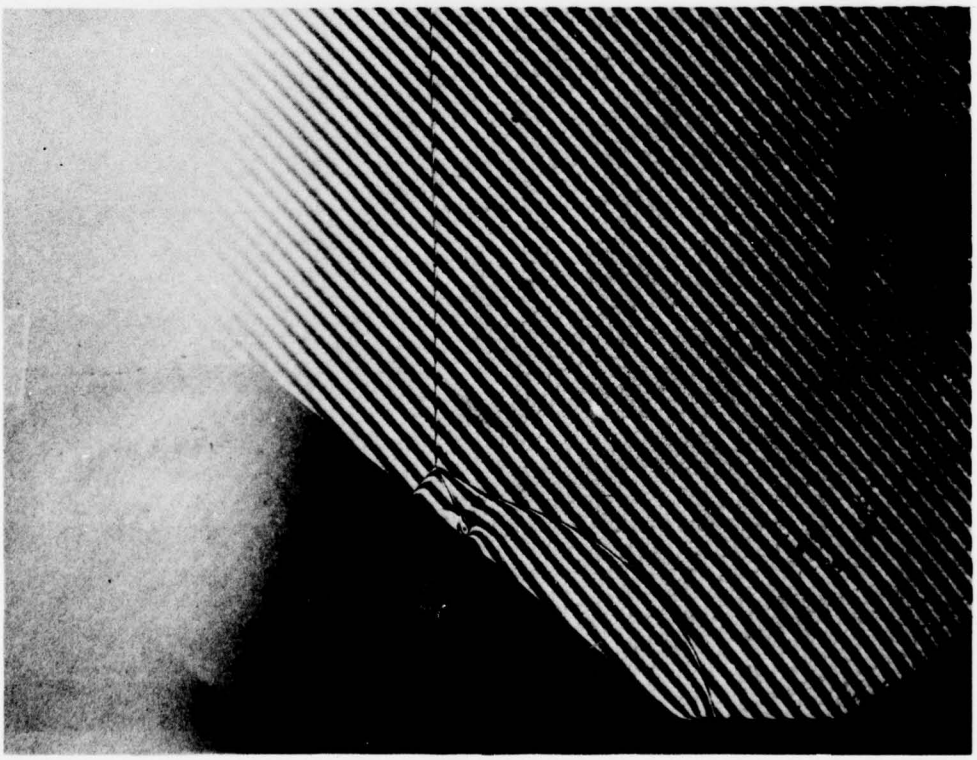

A36

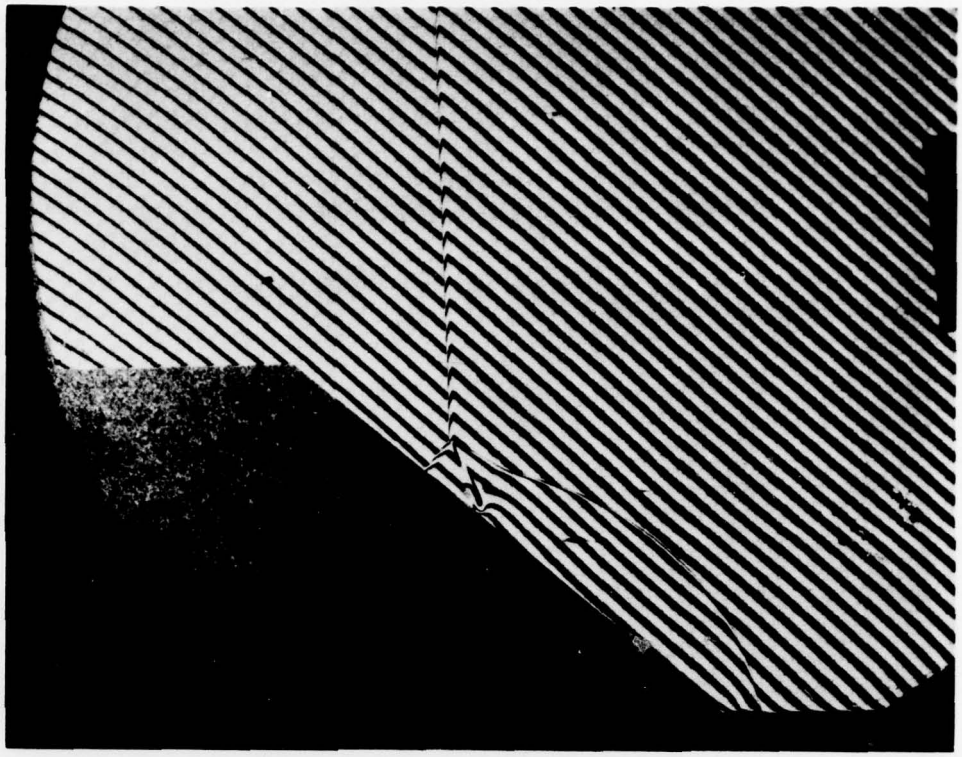

A37

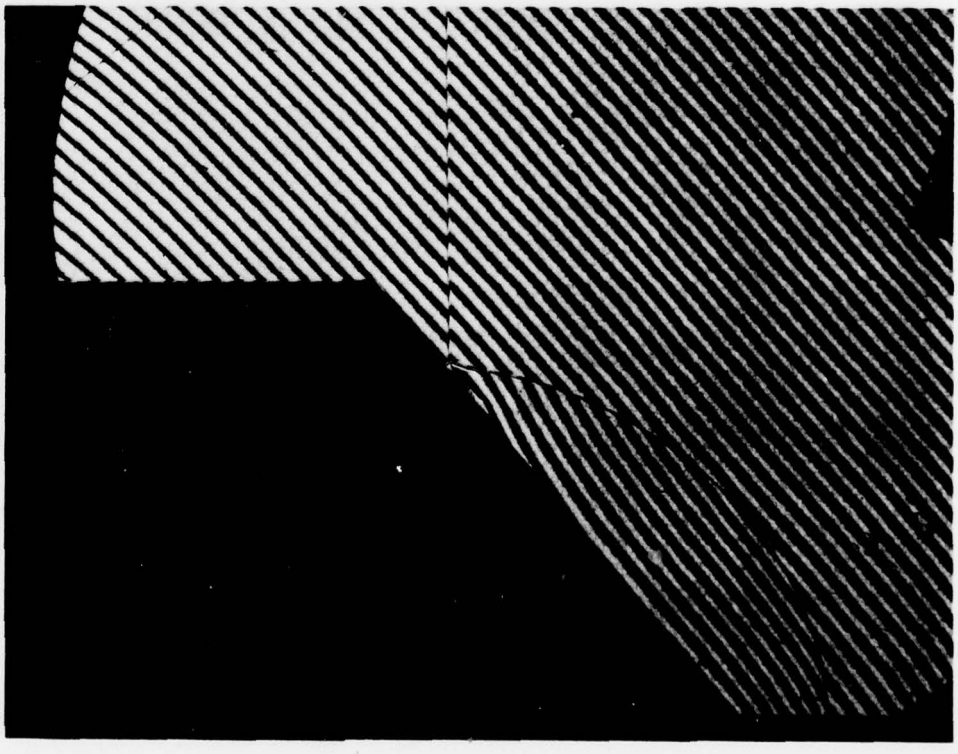

A38

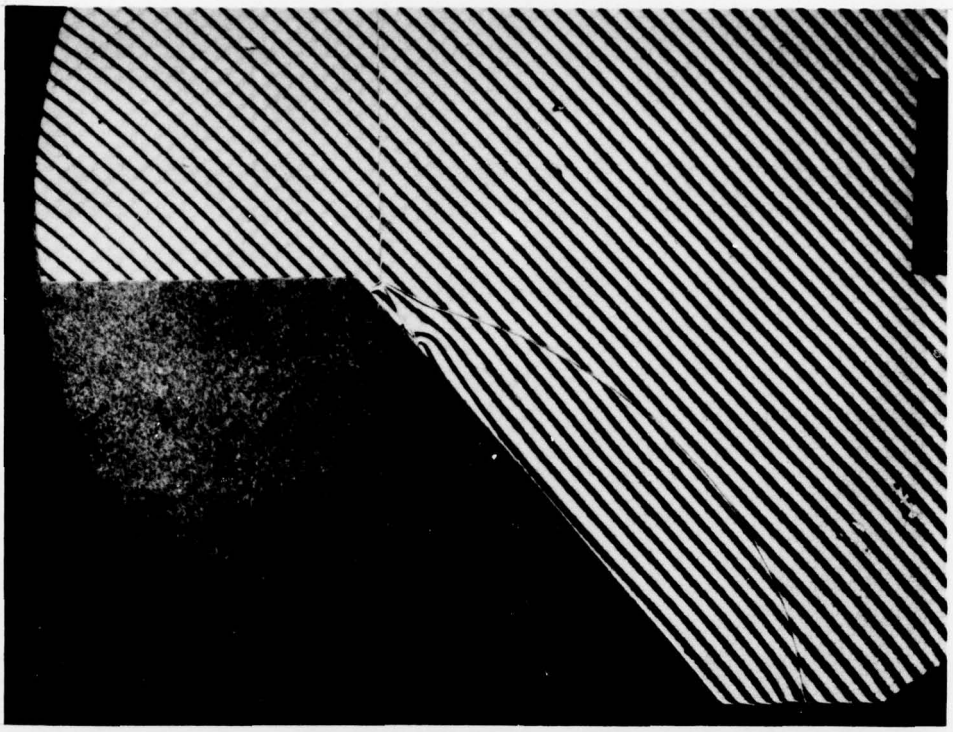

A39

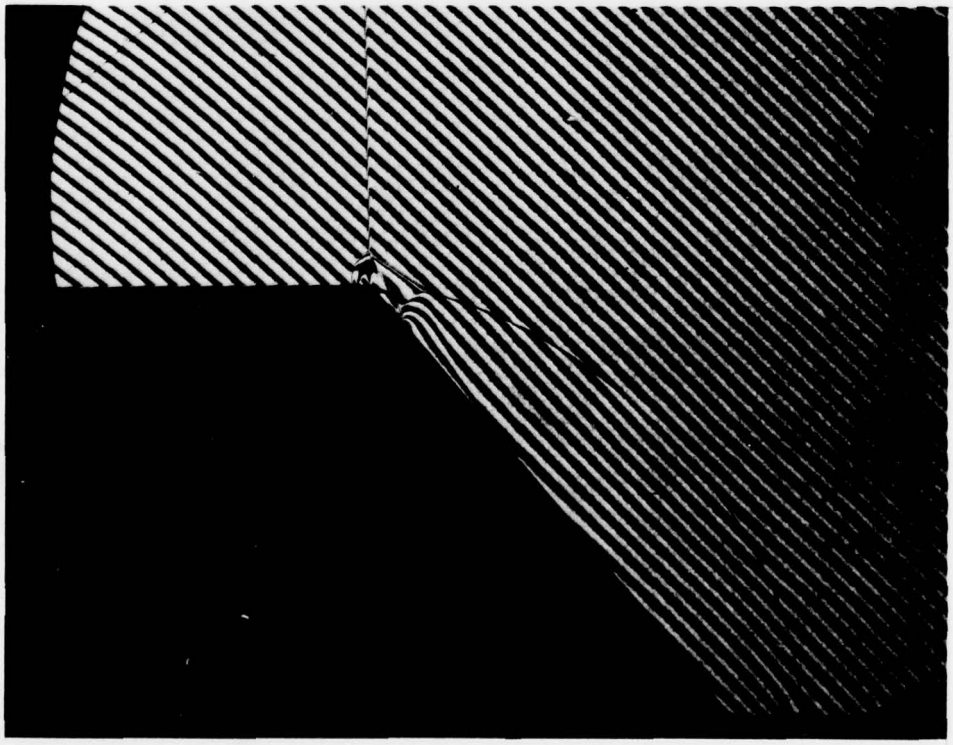

A40

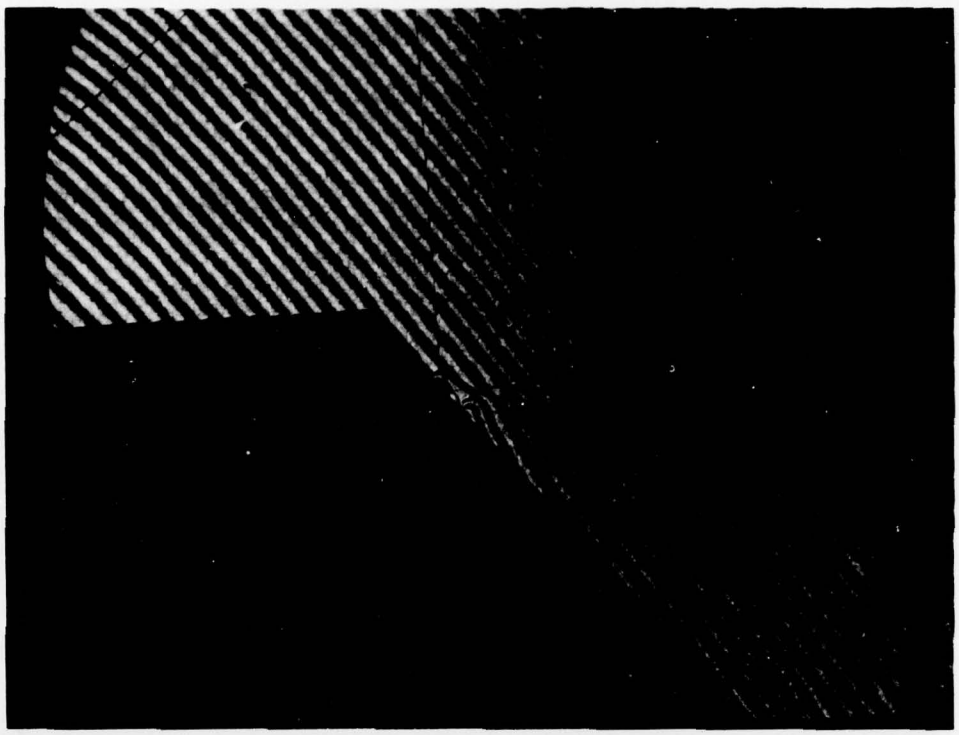

A41

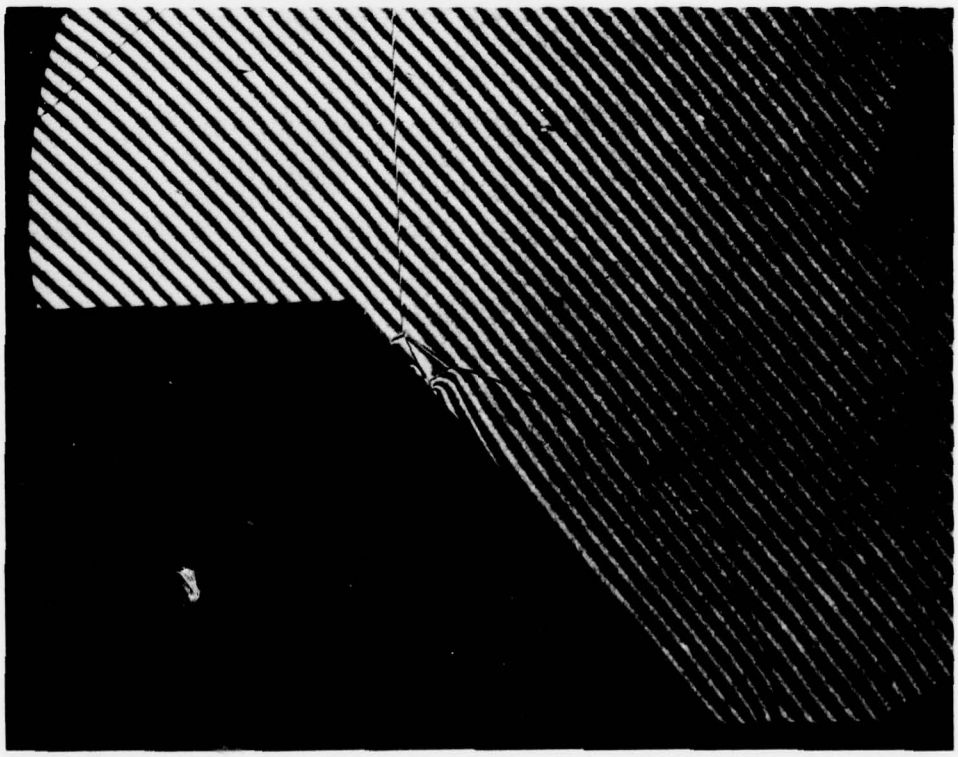

A42

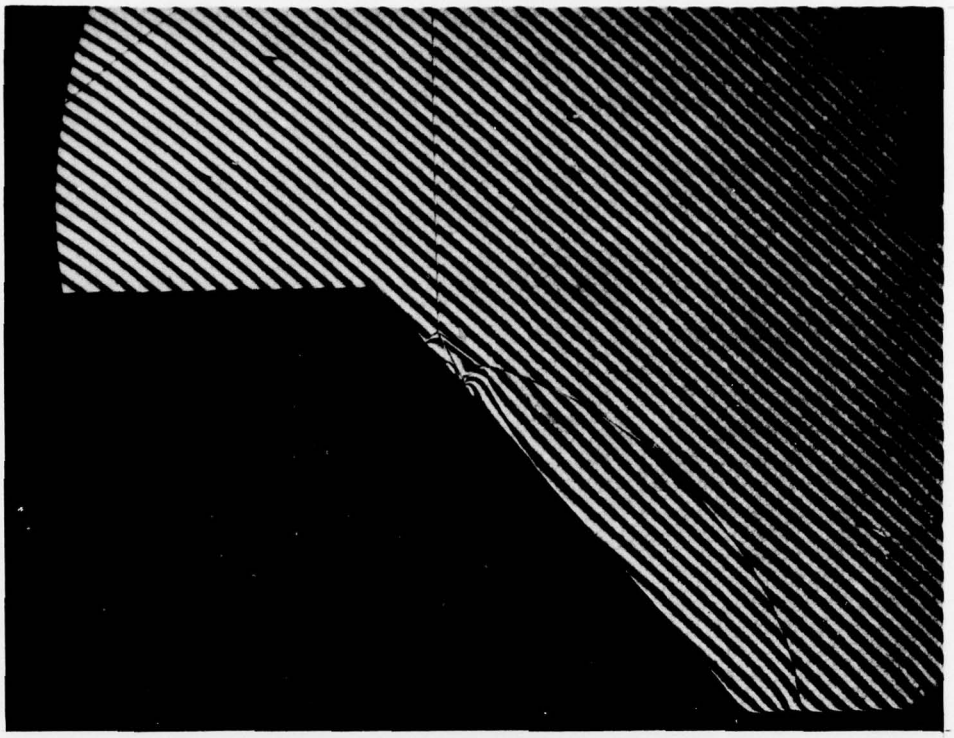

A43

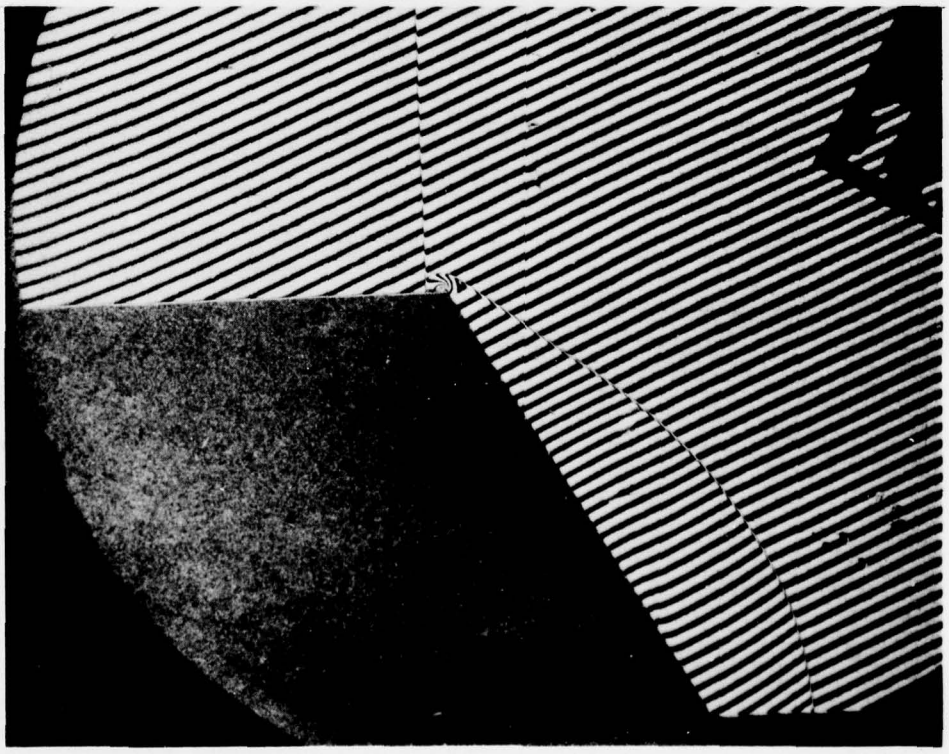

A44

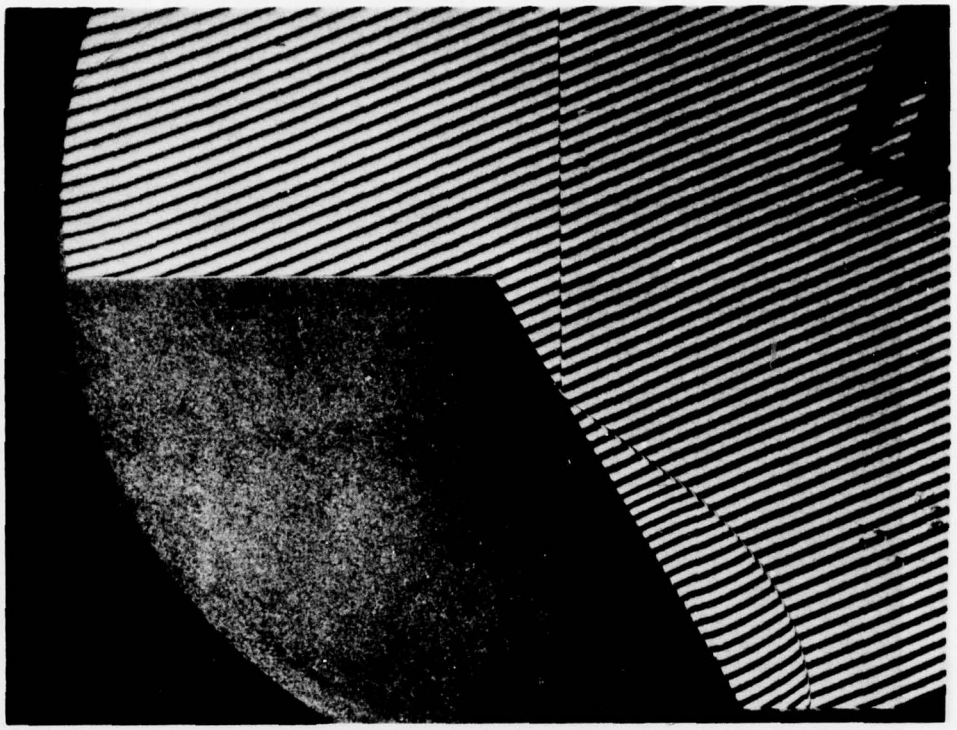

A45

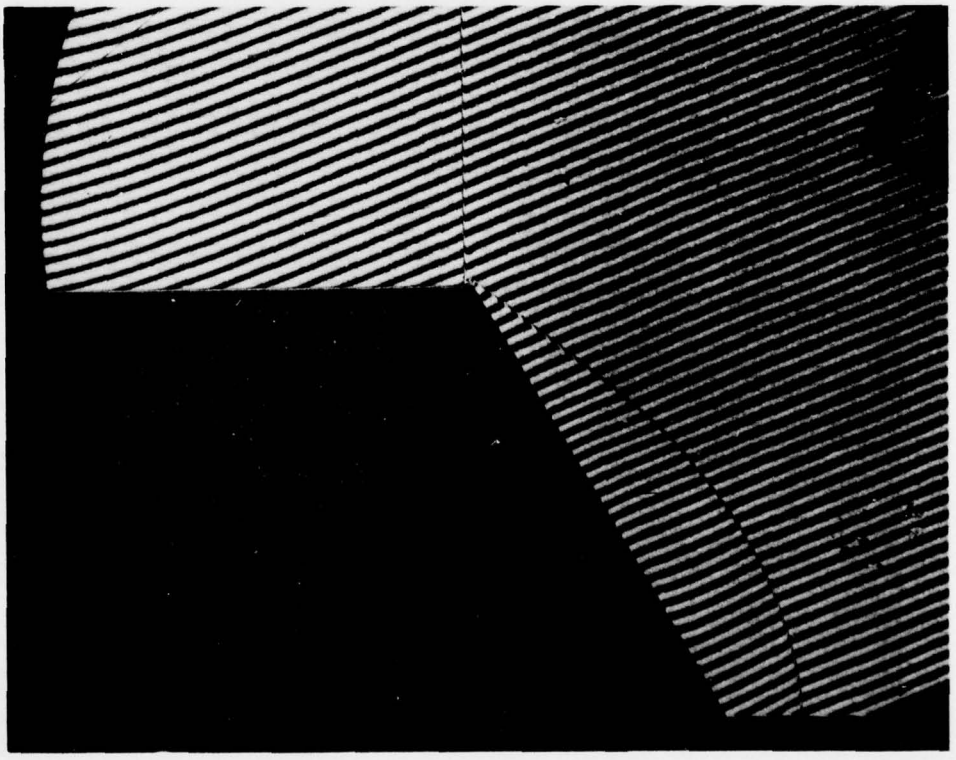

A46

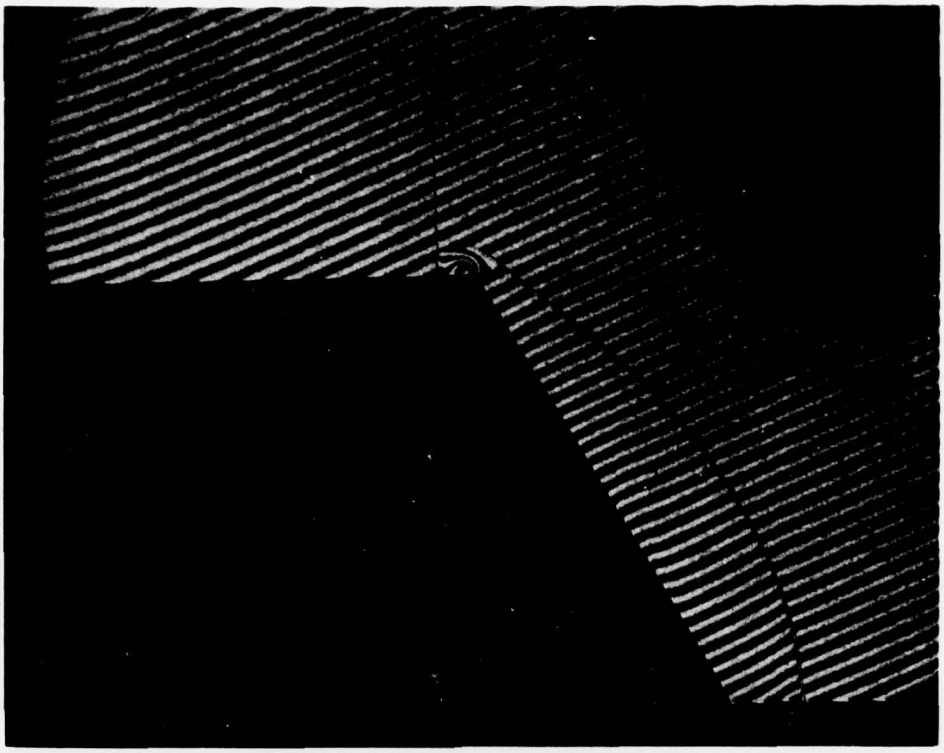

A47

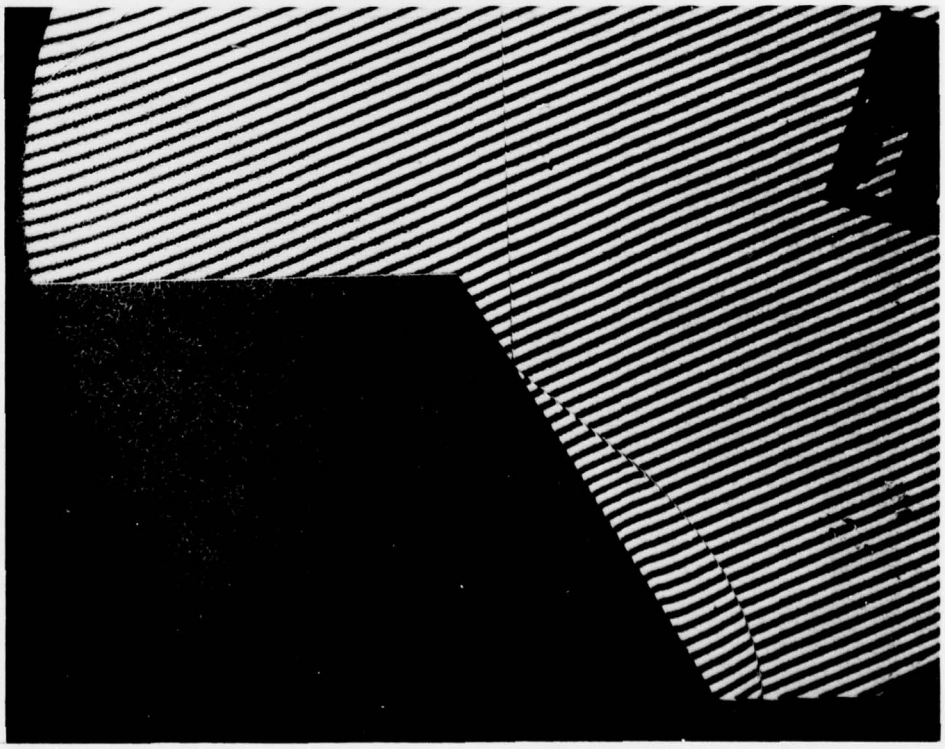

A48

UTIAS REPORT NO. 237

Institute for Aerospace Studies, University of Toronto (UTIAS)
4925 Dufferin Street, Downsview, Ontario, Canada, M3H 5T6

NONSTATIONARY OBLIQUE-SHOCK-WAVE REFLECTIONS IN NITROGEN AND ARGON: EXPERIMENTAL RESULTS

Ben-Dor, G. Approx. 80 pages 112 figures 2 tables

1. Nonstationary oblique shock-wave reflections 2. Shock tube flows 3. Interferometry

I. Ben-Dor, G. II. UTIAS Report No. 237

The interferograms of a detailed study on the reflection of nonstationary oblique shock-waves using a 23 cm dia field of view Mach-Zehnder interferometer and the UTIAS 10 cm x 18 cm Hypervelocity Shock Tube are presented in this separate report.

The investigated incident shock-wave Mach number and compression corner angle ranges were $1 \leq M_s \leq 8$ and $2° \leq \theta_w \leq 60°$, respectively for both argon and nitrogen at an initial pressure $P_o \approx 15$ torr and temperature $T_o \approx 300$ K. The initial conditions, i.e., M_s, θ_w, P_o and T_o as well as the accuracy with which they were measured are given. A brief theoretical review underlying major findings of the above mentioned study is also presented.

Available copies of this report are limited. Return this card to UTIAS, if you require a copy.

UTIAS REPORT NO. 237

Institute for Aerospace Studies, University of Toronto (UTIAS)
4925 Dufferin Street, Downsview, Ontario, Canada, M3H 5T6

NONSTATIONARY OBLIQUE-SHOCK-WAVE REFLECTIONS IN NITROGEN AND ARGON: EXPERIMENTAL RESULTS

Ben-Dor, G. Approx. 80 pages 112 figures 2 tables

1. Nonstationary oblique shock-wave reflections 2. Shock tube flows 3. Interferometry

I. Ben-Dor, G. II. UTIAS Report No. 237

The interferograms of a detailed study on the reflection of nonstationary oblique shock-waves using a 23 cm dia field of view Mach-Zehnder interferometer and the UTIAS 10 cm x 18 cm Hypervelocity Shock Tube are presented in this separate report.

The investigated incident shock-wave Mach number and compression corner angle ranges were $1 \leq M_s \leq 8$ and $2° \leq \theta_w \leq 60°$, respectively for both argon and nitrogen at an initial pressure $P_o \approx 15$ torr and temperature $T_o \approx 300$ K. The initial conditions, i.e., M_s, θ_w, P_o and T_o as well as the accuracy with which they were measured are given. A brief theoretical review underlying major findings of the above mentioned study is also presented.

Available copies of this report are limited. Return this card to UTIAS, if you require a copy.

UTIAS REPORT NO. 237

Institute for Aerospace Studies, University of Toronto (UTIAS)
4925 Dufferin Street, Downsview, Ontario, Canada, M3H 5T6

NONSTATIONARY OBLIQUE-SHOCK-WAVE REFLECTIONS IN NITROGEN AND ARGON: EXPERIMENTAL RESULTS

Ben-Dor, G. Approx. 80 pages 112 figures 2 tables

1. Nonstationary oblique shock-wave reflections 2. Shock tube flows 3. Interferometry

I. Ben-Dor, G. II. UTIAS Report No. 237

The interferograms of a detailed study on the reflection of nonstationary oblique shock-waves using a 23 cm dia field of view Mach-Zehnder interferometer and the UTIAS 10 cm x 18 cm Hypervelocity Shock Tube are presented in this separate report.

The investigated incident shock-wave Mach number and compression corner angle ranges were $1 \leq M_s \leq 8$ and $2° \leq \theta_w \leq 60°$, respectively for both argon and nitrogen at an initial pressure $P_o \approx 15$ torr and temperature $T_o \approx 300$ K. The initial conditions, i.e., M_s, θ_w, P_o and T_o as well as the accuracy with which they were measured are given. A brief theoretical review underlying major findings of the above mentioned study is also presented.

Available copies of this report are limited. Return this card to UTIAS, if you require a copy.

UTIAS REPORT NO. 237

Institute for Aerospace Studies, University of Toronto (UTIAS)
4925 Dufferin Street, Downsview, Ontario, Canada, M3H 5T6

NONSTATIONARY OBLIQUE-SHOCK-WAVE REFLECTIONS IN NITROGEN AND ARGON: EXPERIMENTAL RESULTS

Ben-Dor, G. Approx. 80 pages 112 figures 2 tables

1. Nonstationary oblique shock-wave reflections 2. Shock tube flows 3. Interferometry

I. Ben-Dor, G. II. UTIAS Report No. 237

The interferograms of a detailed study on the reflection of nonstationary oblique shock-waves using a 23 cm dia field of view Mach-Zehnder interferometer and the UTIAS 10 cm x 18 cm Hypervelocity Shock Tube are presented in this separate report.

The investigated incident shock-wave Mach number and compression corner angle ranges were $1 \leq M_s \leq 8$ and $2° \leq \theta_w \leq 60°$, respectively for both argon and nitrogen at an initial pressure $P_o \approx 15$ torr and temperature $T_o \approx 300$ K. The initial conditions, i.e., M_s, θ_w, P_o and T_o as well as the accuracy with which they were measured are given. A brief theoretical review underlying major findings of the above mentioned study is also presented.

Available copies of this report are limited. Return this card to UTIAS, if you require a copy.